STUDY INTO GRID INTEGRATION OF VARIABLE RENEWABLE ENERGY IN ETHIOPIAN POWER SYSTEM

A dissertation submitted to the Graduate School of Electrical and Computer Engineering in partial fulfilment of the requirements for the Degree of Doctor of Philosophy (PhD) in Electrical Engineering (Electrical Power Engineering).

By:

Kena Likassa Nefabas

June 2024

Addis Ababa University

Addis Ababa University

School of Graduate Studies

Addis Ababa Institute of Technology

School of Electrical and Computer Engineering

STUDY INTO GRID INTEGRATION OF VARIABLE RENEWABLE ENERGY IN ETHIOPIAN POWER SYSTEM

Doctoral dissertation of:

Kena Likassa Nefabas

kena0912@gmail.com

Supervisor:

Dr. Mengesha Mamo, *School of Electrical and Computer Engineering, Addis Ababa University*

Co-supervisor:

Prof. Lennart Söder, *Department of Electric Power & Energy Systems, Royal Institute of Technology*

To the loving memory of my mother.

Yaadannoo jaalala haadha kootiif.

Acknowledgments

First and foremost, I want to express my gratitude to my Almighty God for his blessings throughout this research work. He gave me the knowledge and courage I needed to get through a challenging period and successfully finish the study.

I owe sincere thanks to my supervisors, Dr. Mengesha Mamo and Prof. Lennart Söder for their guidance, support and encouragement. Without their support, this work would never have come to fruition. I have learned much from their unique perspectives and useful critiques on this research. I look forward to the opportunity to work with you again.

I am deeply grateful to the staff of Ethiopian Electric Power for their invaluable support in gathering the data that significantly enhanced my research.

Next, I would like thank the faculty members of Division of Electrical Power and Energy at KTH. I am especially thankful to Mikael Amelin and Jon Ouloson for their generous assistance and collaboration throughout my time at KTH. The supportive and professional connections within the research community in this division have fostered an exceptional research atmosphere, allowing me to develop as a research student. Undoubtedly, this experience will leave a lasting impact on me.

I would also like to thank the staff members of Power Chair, School of Electrical and Computer Engineering, Addis Ababa University, for their invaluable insights and feedback throughout the various stages of my work. I would also like to extend my thanks to Dr. Mengesha Mamo, the Principal Investigator of the Ethio-Sweden capacity-building project, for his exceptional leadership and unwavering support on top of advising me. Furthermore, I would like to acknowledge the management and administrative staff of the school, as well as the Addis Ababa Institute of Technology, for their efficient project management and handling of financial matters related to this research.

I would like to express my gratitude to the Swedish International Development Cooperation Agency (SIDA) for funding my research work. This support was provided as part of Addis Ababa University's research, training, and capacity building program.

Last but by no means the least, many thanks and lots of love to my wife Sannaayit (aka Simbookoo) for her support, love, encouragement, patience, and understanding throughout all the ups and downs of my Ph.D. work. And, yes, I should acknowledge my cute kids, Heeraan (aka

Basheekoo) and Naafileet (aka Giiftiikoo) for always making me optimistic and motivated to go forward.

AAU, AAiT, 2024

Kena Likassa Nefabas

Abstract

Energy has been a crucial factor for the survival of mankind since early primitive societies began to make fire from timber wood. Since then, there have been significant revolutions in using energy sources from fossil fuels such as coal and gasoline and the development of energy conversion technologies such as electric energy generators up to the more recent use of renewable energy sources (REs). The uneven distribution of fossil fuels in the world, the growing economic and social need for energy, the difficulty of tackling climate change, advances in energy technology, rising oil prices and the emergence of low-carbon societies have all contributed to the recent revolution towards renewable energy sources.

However, REs especially variable renewable energies (VREs) such as wind and solar energy, pose an additional challenge for electric grid operators due to their inherent variability and unpredictability nature. Because of these characteristics of VREs, the grid integration of VREs can potentially jeopardize the reliability of the power grid.

Countries need to conduct grid integration studies to overcome the challenges of integrating VREs. In this regard, utilities are increasingly relying on the traditional grid integration model, which ignores the various operational characteristics of VREs. Accordingly, it is important for the grid integration study to either develop new models or modify existing models to study the characteristics of VREs in the power sector. In developing countries, especially in Ethiopia, there is currently little research of this kind due to the slow development of VREs.

Thus, this dissertation deals with the study of grid integration of VREs into the power system of Ethiopia according to local as well as global needs. The specific objectives are to assess the variability of existing VREs, simulate wind energy production for grid integration studies, estimate the maximum integration of VREs, and assess the difficulty of integrating them into the grid. To achieve these goals, the following four specific objectives are defined and briefed: **To assess the variability of existing wind power in the grid of Ethiopia.** This objective is pursued to evaluate and assess the magnitude and frequency of variability of individual and aggregate wind power in the Ethiopian power grid. A step-change and correlation are used to examine the variability of wind power generation. The results indicates that variability of Ethiopian wind power is significant. This huge variability is due to the small installed capacity. However, this variability does not have much influence on system operation because of the smaller magnitude of the wind compared with system

size.

Modeling Ethiopian wind power production for grid integration study using ERA5 reanalysis data is the second specific objective. The objective of this particular purpose is to produce wind power time series considering the various factors affecting wind power production including wake effect, diurnal and seasonal bias, and the loss in upcoming wind speed. The modeling was performed using wind speed data from ERA5 of the European Center for Medium-Range Weather Forecasts (ECMWF) and wind farm data from Ethiopian Electric Power (EEP). Moreover, the model has used spatial statistical down-scaling and interpolation to obtain the required result. The outcomes show that the model result and the measurements agree well, with a low root mean square error. This means that this model can be extended to other regions of the country to predict future wind power generation and to show the potential areas for simulating wind power generation for planning and operating wind turbines using ERA5 data.

The third specific aim is to estimate a maximum variable renewable energy integration with a goal of 100% renewable energy and a high share of hydropower under different scenarios . This particular objective aims to determine the maximum integration of wind and solar PV into the power grid of Ethiopia. The current national VRE integration plan for the year 2030 is analyzed using the model along with eight alternative scenarios that consider dry years and annual variations in VRE for minimum load shedding and VRE curtailment. GenX, a modified version of capacity expansion planning, has been used for this work. The findings showed that Ethiopia could integrate more VRE into the grid than EEP had anticipated.

The fourth specific objective is to study the challenges of system balancing and curtailment of wind power in Ethiopia grid under different scenarios. In addition to analyzing the challenge of system operation with wind, developing an hourly dispatch model and simulation of the Ethiopia power grid is the specific aim of this work. This model will be useful in analyzing future wind power curtailment and system balancing issues. The developed model was used to analyze the grid for the year 2030 under different scenarios and verified using historical data. With an annual wind energy share of 14.5%, 17.8%, and 25.2%, the study analyzed the impact of transmission capacity, regulation reserve needed, and daily minimum hydropower production. The result showed that the curtailment was less than 0.2%, 1.1%, and 9.8% for each wind share respectively.

The cost of wind energy is also directly related to the extent of curtailment and the capacity of

transmission lines. A better balance between production and consumption and fewer wind power curtailments is the result of a reduction in the minimum electricity production from hydropower and full utilization of transmission lines to neighboring countries.

Keywords: Balancing, Curtailment, Ethiopia, Grid integration study, Model, PV, Uncertainty, Wind, VRE, Variability

Table of Contents

List of Figures

List of Tables

List of Abbreviations

CRGE	Climate Resilient Green Economy
EEP	Ethiopian Electric Power
LCOE	Levelized cost of energy
G.C	Gregorian calendar
NREL	National Renewable Energy Laboratory
RE	Renewable energy
SDG	Sustainable Development Goal
VRE	Variable renewable energy
MWh	Mega watt hour
GW	Giga watt
GHG	Greenhouse gas
PV	Photovoltaic
IEA	International Energy Agency
CO2	Carbon dioxide
WTG	Wind Turbine Generators
ECMWF	European Centre for Medium-Range Weather Forecasts
NMSA	National Meteorological Services Agency
TWh	Tera watt hour
NASA	National Aeronautics and Space Administration
MERRA	Modern Era Retrospective Analysis for Research and Applications
GWA	Global Wind Atlas
RMSE	Root Mean Square Error
RMSD	Root Mean Square Difference
MAE	Mean Absolute Error
GEP	Generation Expansion Planning
MILP	Mixed Integer Linear Programming
CO2	Carbon Dioxide
NEA	Nuclear Energy Agency

Indices and Sets

$t \in \mathscr{T}$ t denotes time step in hour and $\mathscr{T}$ is the set of hours in the planning horizon.

$g \in \mathscr{G}$ g denotes a technology and $\mathscr{G}$ is the set of available technologies.

$l \in \mathscr{L}$ l denotes a transmission line and $\mathscr{L}$ is the set of available transmission lines.

F_g^Q set of upstream hydropower plants for downstream plants g (discharge).

F_g^S set of upstream hydropower plants for downstream plants g (spillage).

τ_g^q time delay for the discharged water of upstream power plants to reach the downstream power plant g.

τ_g^s time delay for the spilled water of upstream power plant to reach the downstream power plant g.

$\mathscr{VRE} \in \mathscr{G}$ $\mathscr{VRE}$ is the subset of Variable Renewable Energy (wind ($\mathscr{W}$) and Photovoltaic ($\mathscr{PV}$)) resources.

$\mathscr{H} \in \mathscr{G}$ $\mathscr{H}$ is set of hydropower generators.

$\mathscr{MR} \in \mathscr{G}$ $\mathscr{MR}$ is a set of must-run generators (biomass and geothermal).

Variables

cap_g^{new} new installed capacity of technology g [MW].

cap_g^{tot} total installed capacity of technology g [MW].

$p_{g,t}$ hourly generation of technology g during time t [MWh].

$s_{g,t}$ spillage capacity of reservoir hydropower plant g for time t [MWh].

$m_{g,t}$ storage capacity of hydropower of plant g for time t [MWh].

Λ_t non-served energy or shed load during time t [MWh].

$f_{g,t}$ frequency regulation contribution for reserve from hydropower plant g during time t [MWh].

$r_{g,t}$ balancing reserve from hydropower of plant g during time t [MWh].

w_t^{curt} curtailed wind during time t [MWh].

pv_t^{curt} curtailed PV during time t [MWh].

$exp_{l,t}$ power flow over line l for time t from Ethiopia to neighboring countries [MWh].

Parameters

D_t electricity demand during time t [MWh].

c^{ns} cost of non-served energy/demand curtailment [$/MWh].

cap_g^{exist} existing Installed capacity of technology g [MW].

x_{reg}^{load} frequency regulation reserve requirement as a fraction of forecasted demand in each time step[%].

x_{reg}^{vre} frequency regulation reserve requirement as a fraction of variable renewable energy generation in each time step[%].

x_{blc}^{vre} operating (balancing) reserve requirement as a fraction of forecasted variable renewable energy generation in each time step[%].

x_{blc}^{load} operating (balancing) reserve requirement as a fraction of forecasted demand in each time step[%].

c^{curt} cost of wind and pv curtailment [$/MWh].

$\rho_{g,t}^{max}$ maximum available generation per unit of installed capacity during time step t for technology g [%].

ρ_{g}^{min} minimum stable power output per unit of installed capacity for technology g [%].

m_{g}^{max} maximum storage capacity of hydrpower plant g [MWh].

δ_{g}^{up} maximum ramp-up rate per time step as a percentage of installed capacity of hydropower plant g [%/hr].

δ_{g}^{down} maximum ramp-down rate per time step as a percentage of installed capacity of hydropower plant g [%/hr].

Q_{i}^{avg} average inflow of water to each reservoir per hour [MWh].

exp_{l}^{max} maximum power flow on line l from Ethiopia to neighboring countries [MW].

Chapter 1

Introduction

1.1 Background

Since the beginning of civilization, when a fire was first produced by burning timber wood, energy has been a vital component of human survival and has undergone several revolutions. The first revolution in the energy sector took place in the 1780s when coal was thought to account for the biggest proportion of the main energy mix. This was because human civilization was growing faster and faster, which stimulated the coal industry's growth and led to coal overtaking wood for the first time. The second revolution occurred in 1886 when the internal combustion engine was developed, sparking interest in oil and gas as reliable energy sources to replace coal. Currently, these energy resources are more widely used than coal as the world's major energy source [3].

Because of the uneven distribution of fossil fuels around the world, the rising need for energy for both social and economic purposes, the difficulty of addressing climate change, the advancement of energy technology, the rising oil prices, and the emergence of low-carbon societies, the third revolution from traditional fossil fuels to environmentally friendly renewable energy sources has become indispensable [4].

Solar and wind energy are among the renewable energy resources used for thousands of years in various applications. However, due to technological, social, and economic reasons, they have been dominated by other sources for most of this time [5]. However, there has been a resurgence of interest in wind energy, particularly since the rise in oil prices in the early 1970s. This time, however, the focus has been on the electrical energy provided by wind power rather than the mechanical energy.

Additionally, there are numerous reasons in the energy industry to focus on renewable energy, particularly variable renewable energies (VRE). The United Nations Conference on Sustainable Development Goals (SDGs), held in Rio de Janeiro, Brazil, in 2012, contributed significantly to increase the percentage of renewable energy. Launched in 2015, the SDGs include 17 goals that will lead the world until 2030. The aims include "Goal 7: Ensure access to affordable, reliable, sustainable and modern energy for all." In particular, sub-goal 2 of Goal 7 stipulates that a significant increase in the share of renewable energy in the global energy mix should be achieved by 2030.

Moreover, environmental concerns, the desire for energy security, and the declining levelized cost of electricity (LCOE) of VRE were other motivators. The zero fuel costs and the comparatively low variable costs of VRE technologies are responsible for the falling electricity production costs. Therefore, LCOE is often used as an informative measure to compare the general competitiveness of different production technologies [6].

Furthermore, as analysis from [7]shows, the energy sector is now responsible for around 75% of greenhouse gas (GHG) emissions and is crucial to mitigating the most serious cause of climate change. To reduce the impact of greenhouse gas emissions from the energy industry, increasing the proportion of environmentally friendly renewable energy is essential. Consequently, the need to increase renewable energy is primarily due to environmental concerns. The use of renewable energy sources, particularly variable energy sources such as wind power and photovoltaics (PV), is crucial to decarbonizing the energy industry. Therefore, efforts are being made to integrate VRE into the network to achieve this goal [7].

However, the grid integration of VRE could threaten the reliability of the power system or the achievement of decarbonization goals due to their inherent variability and uncertainty. Therefore, several countries have begun grid integration studies to assess the influence of VRE on their respective power system [8, 9, 10].

As per the National Renewable Energy Laboratory (NREL), a grid integration study is defined as the analysis of the technical and/or economic influence of accomplishing significant levels of VRE in the power grid [11]. On the other hand, as per the International Energy Agency (IEA), a grid integration study is defined as the simulation of a future electricity grid with wind and PV penetration varying between 5% and greater than 50% of the annual electrical energy supply. In general, the study aims to assess the potential influence of wind and PV energy on power system

operations and planning.

Grid integration studies are classified into three categories based on the topics most important to a particular electricity system [11]. The first is capacity expansion planning, which focuses on minimizing production and investment costs to optimally mix different power sources. The second option is to simulate the production costs. The goal of this type of grid integration study is to reduce operating costs for the best possible use of different power sources. It is also known as unit commitment. The third is power system analysis, which focuses more on the dynamics of the power system. Thus, this dissertation aimed to apply the first two grid integration studies for the Ethiopian power system.

1.2 Problem statement

VRE is one of the incredibly cleanest and most environmentally friendly energy resources available on today's electrical grids. However, it poses a challenge for network operators due to its inherent variability and uncertainty as well as location specificity. This means that these features pose additional challenges for smooth and cost-effective integration [11, 12, 13, 14, 15, 16, 17, 18]. However, the level of challenges varies based on the power system profile for the same VRE penetration levels [19].

Among the most difficult issues with VRE integration is system balance. The basic principle of any power grid operation is that total production, including line losses, must always match total demand. This is called system balancing. However, in a power grid with high VRE penetration, grid operators face a significant challenge in balancing production and demand. A significant amount of VRE will increase the rate of change and frequency of the system's existing variability [20]. Article [21] identified when the balancing challenge worsens (acid test for power system). These problems occur when the minimum power demand increases to peak as VRE production decreases to minimum, and when high power demand decreases to minimum while low VRE power increases to peak.

In addition, the unpredictability of the resource represents a significant barrier to system planning and unit commitment with significant VRE integration. Inaccurate forecasts require a high reserve, which creates additional costs for the network operator.

Moreover, most VRE resources are located far from the load center, which may cause trans-

mission line congestion when transmitting power to the load center. For these reasons, investments in new and existing transmission lines for solar and wind energy are required. The known cause of limitation in VRE production is transmission congestion, among other factors such as excessive supply during off-peak periods, electricity market mechanisms and policies, grid flexibility and stability, and interconnection problems. The restriction brought on by transmission bottlenecks forces the use of costly generators in place of less expensive VRE production. In addition, the construction of a long-distance transmission line takes longer time than the construction of VRE power plants. This limits the transfer of available energy to the load center. Ethiopia's solar and wind power potential is located in the northeast, east, and southeast, whereas the country's load is concentrated in the center.

Furthermore, several research studies have focused on ways to improve wind turbines so that they can support the grid with reactive power during a voltage dip. However, most wind generators are induction generators, which by definition consume reactive power. As a result, it lacks the importance that synchronous machines have in terms of reactive power provision. Therefore, as solar and wind power penetration increases, the other power plant would be shut down because of low efficiency (e.g.Aba Samuel dam of Ethiopia) and high emission of CO2. Another reason is that hydropower is also used for other purposes, such as irrigation. For this reason, the area where the old power plant was closed does not have enough reactive power supply, resulting in unstable voltage and reducing the transmission capacity of the available lines [22].

Overall system inertia is reduced when VRE-generated power is injected into the grid, and this has a significant impact on smaller isolated systems. For example, most wind turbine control systems disconnect the mechanical system from the electrical system during the fault, thereby reducing the wind turbine's support to the inertia of the grid. Any network that integrates significant VRE will have a significant inertia problem. Furthermore, replacing traditional generators with inverter-based wind turbines reduces the inertia of the existing power system contained in the rotational masses of synchronously connected generators, resulting in low-inertia power systems. Due to the enormous kinetic energy stored in rotating masses, synchronous generators respond instantly to frequency changes, but wind turbine generators (WTG) connected to a converter cannot give the same response because of converter limitations [23, 24]. This shows that a low inertia in the system leads to a lower ability of the system to dampen disturbances and the frequency falls to the low point more quickly.

The huge penetration of wind energy increases the difficulty of energy system planning in addition to the aforementioned challenges. Traditional and widely used energy system planning and simulation modeling tools are utilized to design optimal production portfolios over the entire planning horizon, with cost minimization as the main target. Due to VRE's limited dispatchability, demand management regulates non-critical loads to increase system elasticity, energy storage smooths fluctuations, transmission networks balance production and demand, and dispatchable power plants must rapidly supplement production at low wind speeds. Therefore, the planning tools need to be updated taking into account the practical constraints and available flexible solutions to achieve the economics and technology of VRE.

Despite Ethiopia's huge potential of VRE, the installed capacity is very low [1]. Over the next ten years, the government plans to integrate more VRE. Referring to the third pillar of Ethiopia's 2011 Climate Resilient Green Economy (CRGE) strategy, 15-20% of energy supply is expected to come from non-hydroelectric renewable resources by 2030 [25]. However, there is no trend in the country to explore grid integration of variable renewable energy to plan for any challenges the resource may pose. Furthermore, in Ethiopia, the challenge of integrating VRE into the network could be particularly significant due to the very weak network that prevents high penetration. To address these issues, the goal of this dissertation was to look into how much VRE might be integrated into Ethiopia's electrical grid and to study the balancing challenge of the resource.

Moreover, Ethiopian Electric Power as a power utility company is responsible to properly forecasting future demand and is accordingly required to identify and plan the available energy resources, with the best possible optimal investment decision. In the past EEP has been preparing power system expansion master plan updates. In May 2019, EEP did the load forecast and the generation expansion plan was updated for the horizon years of 2019-2030.

Studies on grid integration of variable renewable energy (VRE) has not been carried out in Ethiopia. It posses a series of challenges such as wind power generation modeling, wind power curtailment and system balancing due to its variability and unpredictability. This thesis addresses the problems of grid integration of VRE in Ethiopian Power System. The specific problems considered are assessment of wind power variability in Ethiopia, wind power generation modeling, estimation of maximum variable renewable energy integration and analysis of challenges of wind power curtailment and system balancing.

1.3 Objectives of the research

Grid integration studies are crucial to ensure a smooth transition to highly renewable energy systems. Realistic VRE power production and corresponding time series, other power plant data, and transmission data are key elements of any grid integration study. To conduct a good grid integration study in the Ethiopian power system, the following main objectives and specific objectives were defined in this dissertation.

The main objective of this dissertation is to study grid integration of VRE into the Ethiopian power system for the year 2030 G.C. This main objective is achieved through the following specific questions.

The research questions are:

Objective 1: To assess the variability of existing wind power in the Ethiopian power grid (**Paper-I**).

This is chosen to answer the following research questions.

- How does the variability of existing wind power in the Ethiopian power grid look like ?
- How high is the ramping rate of wind power in terms of magnitude ?
- How high is the influence of existing wind power in the Ethiopian power grid ?

Objective 2: To model production of Ethiopian wind power time series for grid integration study using ERA5 reanalysis data (**Paper-II**).

This is chosen to answer the following research questions.

- How to generate wind power time series using meteorological data for grid integration study?
- How do the parameters affect the wind power production time series?
- To check the applicability of reanalysis wind speed data for Ethiopia.
- To prepare wind power production time series for grid integration study.

Objective 3: To estimate the maximum variable renewable energy integration with 100% renewable goal and a high share of hydropower under different scenarios (**Paper-III, accepted for publication**).

This is chosen to answer the following research questions.

- How much VRE can be reliably integrated to Ethiopian grid in the year 2030 ?
- What are the technical impacts of VRE on the grid ?
- How much energy can be exported to the neighboring countries ?

Objective 4: Analysis of the wind power curtailment and system balancing challenges in the power grid of Ethiopia under different scenarios (**Paper-IV**).
This is chosen to answer the following research questions.

- What is the reason for wind curtailment in Ethiopia grid ?
- How much wind will be curtailed ?
- What are the balancing challenges ?
- How to balance wind fluctuations ?
- What are the influences of deploying significant amounts of wind power ?

1.4 Scope of the research

The study focuses on the grid integration study of VRE in the power grid of Ethiopia. The study aims to examine the challenges and possible remedies related to integrating significant variable renewable energy production into the power system. In addition, the potential VRE carrying capacity of the power grid is determined.

The study includes assessing the variability of wind energy, modeling wind energy production for a grid integration study, estimating the maximum amount of VRE to be integrated into the grid, and finally the study will be finalized with examining the challenges of integrating significant VRE into the Ethiopian grid.

1.5 Significance and contribution of the research

In developing countries, energy is the primary need for economic growth and community service. Developing good knowledge and skills in grid integration and operation of VRE-based electrical energy is one of the ways to meet energy needs.

Therefore, this dissertation will contribute to providing research-based knowledge and skills in modeling VRE production, operation of the power system under different VRE penetration levels, and its balancing during the ramp and uncertainty. This can be achieved through a grid integration study of VRE for the Ethiopian power system. It is extremely helpful for Ethiopian Electricity Utility (EEP), Ethiopian Electricity Utility (EEU), and research communities.

The contribution of the authors during this PhD study period is summarized below. And this dissertation is also based on the contribution of the authors which are published and accepted for publication and summarized as follows.

I. K. Likassa, M. Mamo and L. Söder, Assessment of Wind Power Variability in Ethiopian Power System, 2021 IEEE PES/IAS PowerAfrica, Nairobi, Kenya, 2021, pp. 1-5, doi: 10.1109/PowerAfrica52236.2021.9543094.

II. Nefabas KL, Söder L, Mamo M, Olauson J. Modeling of Ethiopian Wind Power Production Using ERA5 Reanalysis Data.
Energies. 2021; 14(9):2573. https://doi.org/10.3390/en14092573

III. Nefabas KL, Mamo M, Söder L. Analysis of System Balancing and Wind Power Curtailment Challenges in the Ethiopian Power System under Different Scenarios.
Sustainability. 2023; 15(14):11400. https://doi.org/10.3390/su151411400

Kena Likassa is the principal author of Papers I-III and conducted all the modeling and analysis of these papers. Prof. Lennart Söder and Dr. Mengesha Mamo are the supervisors who contributed to the discussions, reviewing, and editing of all four papers.

1.6 Dissertation outline

This dissertation has the following outline which is categorized into seven chapters.

Chapter 1 discusses overall introduction including objectives, problem statements and contribution of the authors.

Chapter 2 discusses grid integration study and its different types of classification. Furthermore, it is also followed by the discussion of different types of grid integration models and the selection of an appropriate model for this dissertation. Also, this chapter presents an overview of the Ethiopian power sector and energy policies.

Chapter 3 addresses **specific objective one**. It evaluates the wind power variability of the Ethiopian power system. This work starts with a review of different wind power variability assessment methods and the selection of the appropriate method for this study. Finally, it discusses how ramping characteristics of existing Ethiopian wind power and discussion of the result.

Chapter 4 addresses the **specific objective two**. It developed a model for wind power production time series for Ethiopia using a reanalysis of wind speed which is complete in time and space. It starts with methods of wind power modeling and the selection of different parameters for the model. Finally, it comes with results and a discussion of wind power modeling in the Ethiopian power grid.

Chapter 5 addresses the **specific objective three**. This part has adapted the existing model for the Ethiopian power grid to estimate the maximum capacity of VRE to be integrated. It starts with reviewing of literature regarding the grid integration study of VRE and obtaining the way forward. Next, this objective is addressed by adapting the existing model known as GenX and finally, it came up with results and discussion.

Chapter 6 addresses the **specific objective four**. Generally, this part evaluates the challenges of power system balancing under different wind power penetration levels. It also evaluates the curtailment level of VRE. This objective is addressed by developing a model and used it to simulate power system operation. Finally, it comes with a discussion of the result.

Chapter 7 gives the overall conclusion of the dissertation and possible future works.

Chapter 2

Grid Integration Study and Ethiopian Power Sector

2.1 Introduction

Various countries around the globe are setting ambitious targets to increase the share of REs to meet their domestic energy needs [18, 26, 10, 27]. However, renewable energy sources such as wind and solar increase variability and uncertainty and pose a challenge for power system planners and operators. Significant penetration of these resources into the power system needs further evolution of power grid planning and operations [18, 11, 12, 13, 14, 15, 16, 17]. To plan for this change, utilities can conduct a grid integration study. A grid integration study is an analytical framework for evaluating a power grid with large amounts of VRE [11]. It is also defined as a thorough study of the challenges and possible remedies related to the integration of VRE into the system [11].

Overview of Ethiopian power sector has also been discussed. Currently, Ethiopian power grid consists of hydropower, wind,biomass and geothermal energy sources.

2.2 Ethiopian power sector overview

Ethiopia is a landlocked country in the Horn of Africa that is very large and diverse. Its territory is 1.1 million square kilometers and its population was estimated at over 110 million in 2015, of which 81 percent lived in rural areas. After Nigeria, it is the second most populous country in Africa. Ethiopia has made significant changes in promoting social, economic, and human de-

velopment over the past decade. With an average annual growth rate of around 10% since 2004, Ethiopia's economy is one of the fastest growing in the region. The Government of Ethiopia (GoE) has set a long-term goal of becoming a lower-middle-income country by 2025.

Ethiopian energy resources

Significant changes in the Ethiopian power system are expected in the coming years due to increasing electricity demand, development of generation and transmission projects, promotion of exports to neighboring countries, and other factors. It also has numerous renewable energy sources such as biomass, solar energy, geothermal energy, wind power, and hydroelectric power [28]. Although the country has enormous potential, it has one of the lowest clean energy access rates in the globe and depends predominantly on biomass energy for domestic use [29]. The Ethiopian Ministry of Water, Irrigation and Electricity produced a report in 2017 stating that while access to the electricity grid is estimated at 56%, residential connectivity is only about 25% [30].

45 GW of hydropower, more than 7 GW of geothermal power, 1350 GW of wind power, and 5.5 kWh/m2/day of solar power are the identified potential of these resources, as indicated in Table 2.1 [1]. In addition, Ethiopia has large quantities of wood, coal, oil shale, natural gas, and agricultural waste. The following section discusses each of these energy sources.

Table 2.1: Ethiopian energy resources [1].

Resource	Unit	Exploitable Reserve	Exploited Percent
Hydropower	GW	45	< 5
Wind power	GW	1350	< 1
Solar/day	kWh/m2	5.5	< 1
Geothermal	GW	7	< 1
Wood	Million tons	1120	50
Agricultural waste	Million tons	15 - 20	30
Natural gas	Billions m^3	113	0
Coal	Million tons	300	0
Oil shale	Million tons	253	0

Hydropower The major renewable energy resource that can help the country transition to greener energy resources is hydropower. Given this, the Ethiopian government has recognized hydropower as an economically viable and environmentally friendly alternative. It has an abundance of lakes, rivers, and water resources, accounting for 20% of Africa's total technological potential. Because

of this potential, the country is often referred to as the powerhouse of Africa. But so far it has only exploited less than 10% of its potential [31, 32].

Ethiopia has twelve major river basins, eight of which were selected for their potential to provide hydropower (see figure 2.1) [28, 33]. Around 300 hydroelectric power plants with a combined technical electricity potential of 159,300 GWh/year were identified in these eight river basins. 102 of these possible sites (more than 60%) are large-scale, while the remaining sites (less than 40%) are small-scale [34]. In 2018, 4.5 GW of electricity production capacity came from fifteen (15) hydroelectric power plants, approximately equivalent to more than 94% of the country's total capacity, making hydropower the primary energy source [32].

Moreover, the country has initiated the development of numerous extensive hydropower initiatives. These include the 2160 MW Gilgel Gibe-IV (Koysha) hydropower project and the massive 5150 MW Great Ethiopian Renaissance Dam (GERD) situated on the Abbay (Blue River) which when completed will be the largest dam in Africa and the sixth largest in the world. To provide an overview of the current and projected hydropower plants by the year 2030, please refer to Table 2.2.

The cascading of hydropower plants is a common practice in Ethiopia. As a result, it is crucial to take into account the timing and volume of water that flows from the upstream to the downstream power plant when operating these cascaded plants. The diagram in Figure 2.2 illustrates the arrangement of the cascaded hydropower plants, while Table 2.3 provides information on the time intervals between each power plant.

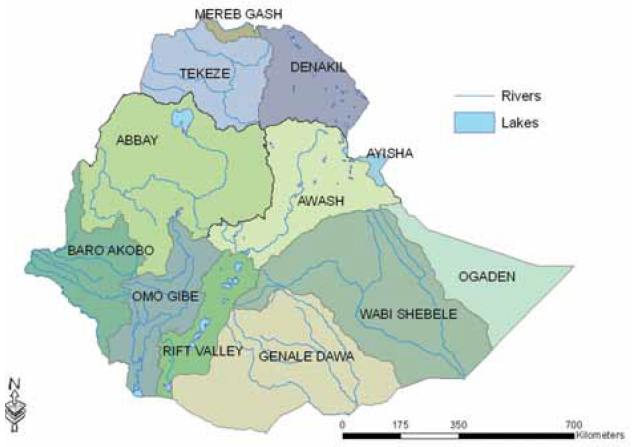

Figure 2.1: Map of Ethiopian major river basins.

Table 2.2: Existing and candidate hydropower plants.

Name of hydropower plant	Installed capacity [MW]	Commission year	status	Average annual generating capacity [MWh]
Koka	43	1960	Existing	133470
Awash2	32	1966	Existing	183480
Awash3	32	1971	Existing	184220
Gilgel gibe2	420	2010	Existing	2030170
Tisabay1	11	1964/2000	Existing	1700
Tisabay2	67	2001	Existing	10100
Koisha	2160	2022	Existing	6460000
Tana Beles	460	2010	Existing	2748740
Fincha	128	1974	Existing	614670
Genale Dawa 3	254	2018	Existing	1690560
Gilgel gibe1	210	2004	Existing	882130
Gilgel gibe3	1870	2010	Existing	5348270
Melkawakena	153	1988/2014	Existing	555490
Amertineshe	97	2013	Existing	245000
Tekeze	300	2009	Existing	1399480
GERD	5150	2024	UC	14684100
Baro1	166	2023	candidate	651710
Baro2	507	2023	candidate	1573186
Birbir	467	2023	candidate	2716650
Dabus	304	2023	candidate	2626082
Geba1	214	2023	candidate	951970
Geba2	157	2023	candidate	753490
Genale5	100	2023	candidate	572990
Genale6	246	2023	candidate	1528460
Genji	214	2023	candidate	814100
Halele	96	2024	candidate	449770
Karadobi	1600	2029	candidate	7830780
Tams	1700	2025	candidate	5714000
Warabesa	340	2024	candidate	224885
Yeda1	162	2023	candidate	627110
Yeda2	118	2023	candidate	460450
Total				64667213

Wind power Ethiopia has a remarkably large potential for wind energy production. The eastern and northeastern regions of Ethiopia, located near the regional state of Tigray, are two of the most promising wind-rich regions in the country. These lie along the most important East African Rift Valley. Wind speeds in these regions are between 7 and 9 m/s, which is ideal for generating wind power. A report on Ethiopian electricity states that the country has a total exploitable wind power potential of about 1350 GW [31].

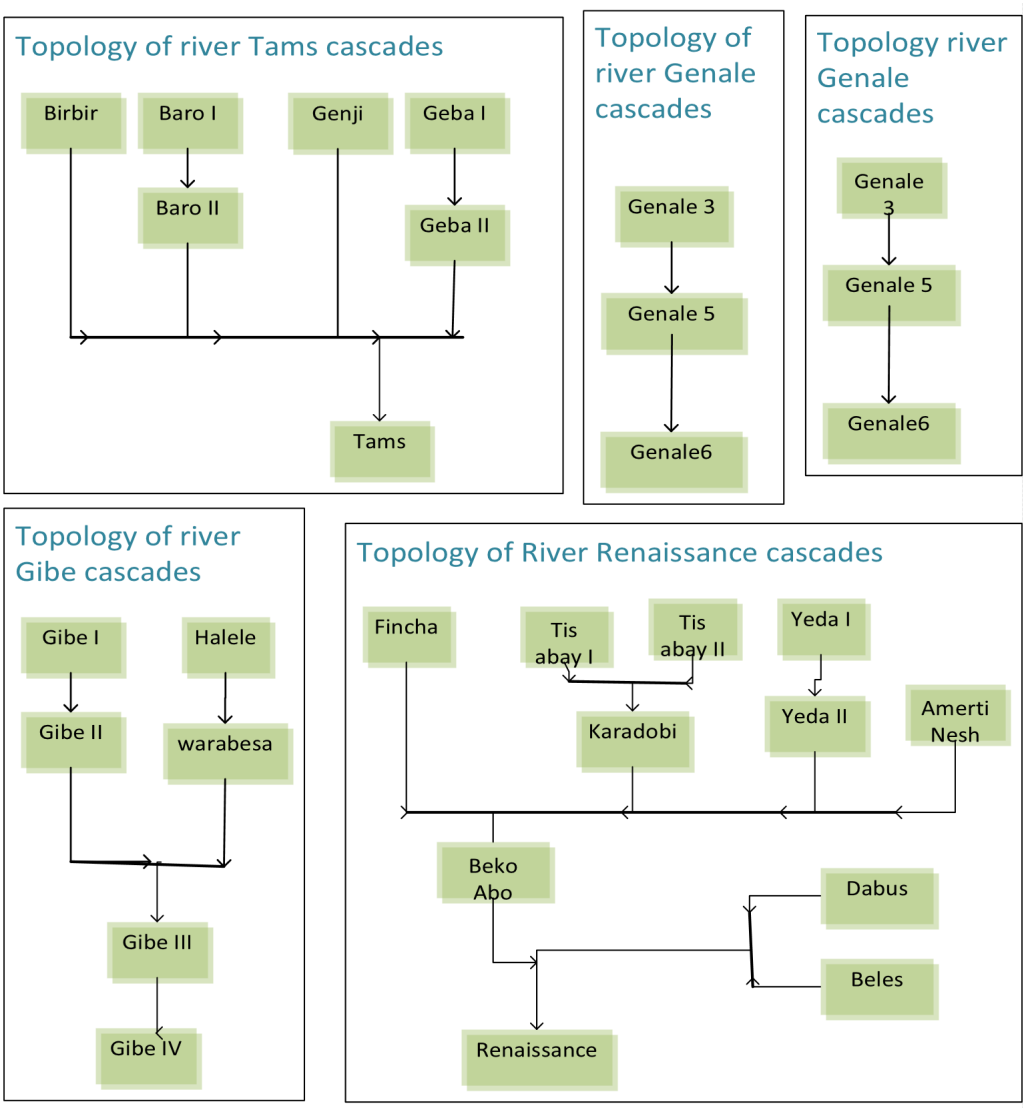

Figure 2.2: Cascaded diagram of hydropower plants in Ethiopia.

Although this energy system has enormous potential, the development of wind farms in the country is still in its infancy. As shown in Figure 2.3, currently , 324 MW of installed capacity in the Ashegoda, Adama-I, and Adama-II wind farms have been completed and connected to the grid [34]. Table 2.4 lists the current and planned wind turbines with their corresponding electricity production capacities. Because of the natural cycle of high availability of wind energy during the dry season, when hydroelectric storage contains little water and low availability of wind energy during the rainy season when storage quickly fills with water, wind power will play a crucial complementary role with hydropower framework of the Ethiopian energy system. This increases system reliability even in dry times and makes wind power an essential part of the grid energy mix [35].

Table 2.3: Hydropower plants distance and transit time [1].

Plant Name	Distance (miles)	Transit Time (Hours)
Koka - Awash 2	15	8
Awash 2 - Awash 3	2	0.4
Genale 3 - Genale 5	50	10
Genale 5 - Genale 6	20	4
Gibe 1 - Gibe 2	5	1
Gibe 2 - Gibe 3	75	19
WarabasHalel - Gibe 3	120	40
Gibe 3 - Koysha	110	55
Baro - Tams	25	8
Sor - Tams	70	23
Birbir - Tams	25	8
Geba - Tams	40	23
TS Abay - Karadobi	250	125
Yeda - Beko Abo	100	50
Neshe - Beko Abo	100	50
Fincha - Beko Abo	100	20
Karadobi - Beko Abo	75	38
Beko Abo - Mendaya	75	38
Mendaya - GERD	75	38
Beles - GERD	170	57
Dabus - GERD	60	30

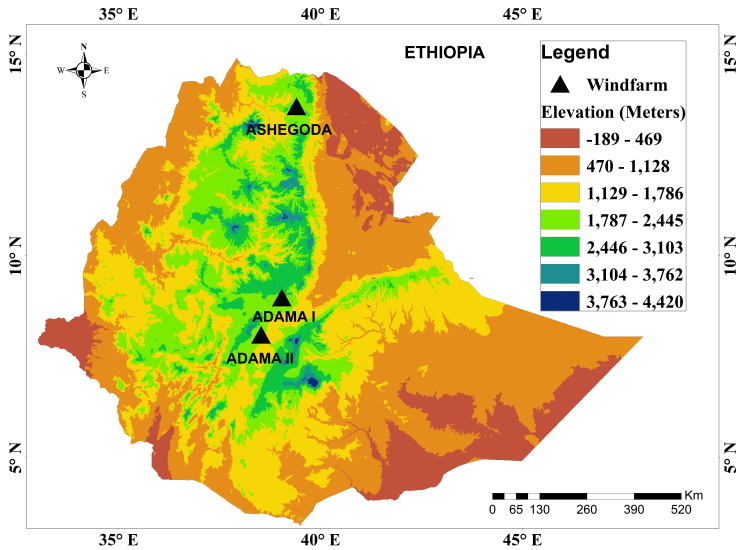

Figure 2.3: Ethiopian existing wind farms' geographical location.

Solar power The largest theoretical solar power potential of over 200,000 TWh/year was found in East Africa. It is estimated that the country's annual average radiation intensity is about 50.5

Table 2.4: Existing and candidate wind power plants.

Name of wind power plant	Installed capacity [MW]	Commission year	status	Average annual generating capacity [MWh]
Ashegoda	120	2011	Existing	368
Adama-I	51	2012	Existing	156
Adama-II	153	2016	Existing	469
Ayisha-I	120	2021	UC	368
Asela-I	100	2022	UC	307
Asela-II (Iteya)	150	2023	Finance secured	460
Ayisha-IA	150	2022	Committed	460
Ayisha-IB	150	2023	Committed	460
Ayisha-III	300	2024	Committed	460
Ayisha-IIIB	150	2023	Committed	460
Debre Birhan	125	2023	Committed	383
Deday	125	2025	candidate	383
Sure	150	2025	candidate	460
Tulu Guled	100	2025	candidate	307
Dire Dawa	150	2025	candidate	460
Gode	150	2025	candidate	460
Idabo	100	2025	candidate	460
Adigala	150	2025	candidate	307
Mekele	150	2025	candidate	460
Ashegoda	150	2025	candidate	460
Adigala	150	2025	candidate	460
Gode	150	2026	candidate	460
KebriBeyah	150	2026	candidate	460
Idabo	150	2026	candidate	460
May Mekdan	150	2026	candidate	460
Mega	150	2026	candidate	460
Assosa Bambasi	150	2026	candidate	460
Sela Dingay	100	2026	candidate	307

kWh/m2/day [36, 37]. The country's most populous highlands in the north, center, and west have comparatively lower solar resources, whereas the Rift Valley regions and western and eastern lowlands have significant annual average irradiance (above 6 kWh/m2/day) [38]. Despite the abundance of solar energy sources in the country, only about 14 MW of solar PV has been used in rural areas for water heating, telecommunications services, lighting, and water pumping [32]. Ethiopia's committed and planned solar power plants are shown in Table 2.5.

Geothermal Geological surveys of the Ethiopian Rift Valley show significant geothermal development potential in this area and the assessment confirms that all development sites together

Table 2.5: Existing and candidate solar power plants.

Name of Solar power plant	Installed capacity [MW]	Commission year	status	Average annual generating capacity [MWh]
Gad I	125	2022	Committed	274
Dicheto	51	2012	Committed	274
Mekele	100	2023	Committed	219
Humera	100	2023	Committed	219
Welenchiti	150	2023	Committed	329
Gad II	125	2023	Committed	274
Metema	100	2023	Committed	219
Weranfo	150	2023	Committed	329
Metehara	100	2022	Committed	219
Worota	100	2025	candidate	219
Meki	100	2025	candidate	219
Yirgalem	100	2025	candidate	219
Melkasedi	100	2025	candidate	219
Meshenti	100	2025	candidate	219

could support geothermal development with an installed capacity of 5,000 to 7,000 MW. At most sites, extensive further exploration is required to confirm the availability and quality of geothermal resources at a particular location.

The only geothermal plant currently operating in Ethiopia is Aluto Langano, which was commissioned as a pilot project in 1999. It was renovated in 2007 with an installed capacity of 7.3 MW. The new Aluto Langano-II project with an installed capacity of 70 MW is under development and is considered a completed project [39]. The latter project is currently scheduled to go into operation in 2027. Two other sites, Corbetti and Tulu Moye, have recently signed development agreements and are considered binding projects [39]. The list of all existing and planned geothermal power plants can be found in Table 2.6.

Biomass Among developing countries in sub-Saharan Africa, Ethiopia has significant household energy consumption. The main means of meeting this consumption is the excessive burning of biomass [40, 41].

Around 83.2 % of Ethiopians, according to World Bank data from 2010, reside in rural areas where access to modern energy services is limited. In these areas, the majority of Ethiopians primarily based on traditional biomass energy sources like wood, cow dung, and agricultural residues for cooking and heating. Even though electricity supply is widespread in urban areas, the major-

Table 2.6: Existing and planned geothermal power plants.

Geothermal plant	Installed capacity [MW]	Commission year	status	Average annual generating capacity [MWh]
Aluto Langano-I	7.3	1997	Existing	20
Tulu Moye-I (IPP)	50	2026	Drilling	394
Tulu Moye-II (IPP)	100	2027	Committed	798
Corbeti-I (IPP)	50	2027	Committed	394
Corbeti-II (IPP)	100	2028	Committed	788
Aluto Langano-II (EPC)	70	2027	candidate	552
Tendaho Alalobad-I (EPC)	100	2029	candidate	788
Shashemene (IPP)	100	2028	candidate	788
Dofan (IPP)	100	2030	candidate	788
Dugna Fango (IPP)	100	2029	candidate	788
Boku (IPP)	100	2030	candidate	788
Fentale (IPP)	50	2030	candidate	394

ity of applications come from traditional biomass energy input. Half of urban households rely on traditional biomass for cooking, and virtually all in rural areas (except 0.2% of households use kerosene and 1.2% charcoal) [42].

2.3 Ethiopian energy policies and strategies

Policy is a key tool to orient a country towards the efficient use of its energy resources for socio-economic growth. In developing countries like Ethiopia, an energy policy is therefore essential. For this reason, the country has developed an energy policy since 1994, which is explained below.

The national energy policy, 1994 In March 1994, when Ethiopia was in a transitional government, the first national energy policy was launched. Addressing the problem of energy supply and usage was the objective of this policy[43]. Energy efficiency, the shift to modern energy services for the household sector, and the development of hydropower resources for the electricity sector were given top priority in this policy. It does not, however, address the electrification of rural areas, nor does the energy supply process follow a thorough needs assessment. In the 1994 National Energy Policy, which should be amended, the researchers identified the following shortcomings [43, 44, 45, 46]:

- To save foreign currency, the 1994 energy policy said nothing about the development and promotion of modern fuels such as biofuels.
- In addition, modern technologies such as flexifuel vehicles, electric trains, hybrid, and electric cars, which could reduce the country's dependence on foreign fuels and carbon emissions, have been ignored.
- To build a green economy, policies must also be in accordance with the recently launched Climate Resilient Green Economy (CRGE) strategy.
- To deal with inter-regional power connections to be a source of foreign currency and also play a crucial role in geopolitical stability.

The Ethiopian Ministry of Water, Irrigation, and Energy thus prepared a draft of a national energy policy in 2013 to fill those gaps and place a focus on the development and application of all renewable energy sources.

The National Energy Policy (2nd draft), 2013

Ensuring the availability, affordability, accessibility, security, and dependability of energy services is the primary goal of the updated national energy policy, which aims to support the country's rapid and sustainable social and economic development and transformation. The following broad objectives are the target of energy policy [43, 47]:

- Enhance the energy supply's security and dependability and be a hub for renewable energy in the area.
- Enhance access to affordable modern energy.
- Promote efficient, clean, and appropriate energy technologies and energy-saving measures.
- Establish robust energy institutions and improve the governance of the energy sector.
- Ensuring ecological and social security as well as the sustainability of energy supply and use.
- Enhance energy sector financing.

2.4 Grid integration study

Grid integration studies vary based on the characteristics of each power system [18, 26, 10, 27]. Each investigation aims to address problems that are important to a particular energy system. Therefore, one or more of the following three methods are used to model the power system in a grid integration study: capacity expansion planning [10, 27, 48], production cost simulation [18, 26, 27] and power flow [27]. While many grid integration studies focus on only one or two of the three types of methods, the best ones use all the three.

Articles [18, 26] have conducted grid integration studies for the power systems in the Philippines and India, respectively. The investigations only consider the production cost simulation of the system using the PLEXOS® model. Additional research [10] conducted the grid integration study for the electrical system connection between the United States and Quebec in Canada. The study used PLEXOS® and ReEDS models to simulate system production costs and capacity expansion planning. In addition, the study [27] used all three methods - capacity expansion, production costs, and power flow analysis - to analyze the European electrical system technically and economically.

However, the choice of which type of grid integration study or a combination of grid integration analyses to use can be made based on the policy-relevant issues that best match a country's priorities. For instance, capacity expansion planning that focuses on expanding production and transmission may be most beneficial as the country determines the best energy supply mix to achieve long-term policy objectives. On the other hand, production cost analysis could provide the most useful framework for energy system planners and operators to prioritize short and medium-term actions. If a grid operator expresses concerns about the potential reliability risks that significant variable RE scenarios could pose to the power system, power flow modeling may be the most appropriate approach.

Selecting the right models is an essential first step in conducting the grid integration study. Depending on the objective of the study, several types of models can be selected for capacity expansion, production cost, and power flow assessments.

Grid integration studies can utilize commercially available and open-source grid integration models customized to a specific place. Yet, traditional platforms are not designed to capture the different temporal, stochastic, and spatial properties of wind and solar energy [49]. For this reason, most grid integration study researchers are using a grid integration model to study significantly

variable renewable energy scenarios that have three basic options. These are:

- Apply power grid-specific data, policies, economic conditions, and operating practices to existing grid integration models that specifically address the unique features of weather-dependent wind and solar energy.
- Adapting existing power grid-specific grid integration models that include important system features to capture variable RE characteristics and issues.
- Building a new model that fully captures the unique features of wind and solar energy resources, takes into account the details of each energy system, and answers the key questions of the grid integration study.

In general, thousands of grid integration models were developed depending on the characteristics of each power grid to explore possible combinations of power production units. Various scientists have classified planning models according to different criteria. The author [50] has divided planning models based on two criteria. The first criterion is associated with the scope of the model, i.e. its sectoral, geographical, and temporal coverage. Therefore, the planning models are divided into four categories: energy system planning models, energy economic models, integrated assessment models, and power system planning models. The second criterion concerned the approach used, which can be broadly divided into four categories: commutable general equilibrium models, optimization models, equilibrium models, system dynamics models, and agent-based models. According to [51], planning models have been classified according to their intended use (Power System Analysis Tools, Operation Decision Support, Investment Decision Support, Scenario), methodology (simulation models, optimization models and equilibrium), and approach (top-bottom or bottom-up). In addition, according to [52], planning models were classified based on nine criteria. Purpose, model structure, analytical approach, methodology, mathematical approach, and data requirements.

In addition, the planning models were classified according to whether they were open-access or commercial models. Therefore, author [53] has categorized the planning model based on accessibility. Switch and GenX are two examples of open-access power system planning models. To address the characteristics of intermittent renewable energy, in this study, we also introduced additional criteria to categorize the power system planning model based on its configurability and

availability of additional short-term constraints. The configurability of the model shows how flexible the model is in accepting user-defined constraints and goals. GenX is an open-source model with high adaptability for determining the capacity of electrical resources.

GenX is a bottom-up, adaptable, open-planning model for optimizing power systems. The model in question is a constrained linear or mixed-integer linear optimization model that determines the portfolio of investments and operational decisions related to electricity production, storage, transmission, and demand-side resources to meet electricity demand at the lowest possible cost in one or more future planning years. This process is subject to several operational constraints related to the energy system, resource availability constraints, and additional constraints imposed by environmental, market design, and political factors. Therefore, compared to the other tools described above, GenX is the most suitable for this dissertation.

Chapter 3

Assessment of Wind Power Variability in Ethiopian Power Grid

3.1 Introduction

The amount of electricity generated worldwide is growing regularly, with wind energy currently accounting for about 7.2% [54] of the total and is expected to increase shortly. According to the energy supply forecast for 2050, wind and solar PV will meet more than half of the world's electricity needs [7].

However, operating an electric grid with a significant level of wind is challenging due to its inherent unpredictability and variability. Difficulties in utilizing huge level of wind power in the electric grid include load tracking, requirements of balancing power, reserve requirements, reinforcement of transmission line, security of the grid, stability and quality of the grid [14, 19, 15]. Thus, to determine the level of difficulty that wind power poses to the power grid, it is essential to assess its variability.

3.2 Literature review

Numerous studies have examined the variability of wind power in their respective power system. Author [55] has studied hourly wind power variations in the Nordic countries. The author has identified that the variability of wind power can be reduced by increasing the distance between farms. The aggregated influence of load and wind power fluctuations on the operation of the

power grid was also noted by author [56]. According to this author, the difficulty of integrating wind power into the grid varies depending on the size and type of source.

Author [15] has examined several challenges associated with integrating wind power into the power grid. The difficulties in integrating wind power were divided into three categories: power system stability, power quality, and voltage regulation. The author also examined the various strategies to reduce the difficulties in wind grid integration.

The possible difficulties in integrating significant wind power into the power grid were mentioned in the study [16]. This author has identified several issues related to wind power integration, including social, economic, environmental, and technical impacts on power quality. The future fluctuations of wind power production in the Swedish electric grid were identified by the author [57]. This research focuses on how much future wind power will vary as capacity is increased.

Finally, the above studies assessed the existing level of wind power generation in each of their countries and predicted future fluctuations. Thus, the purpose of this article is to analyze the hourly variability of existing wind power generation time series in the Ethiopian power grid.

3.3 Data collection

Ethiopia now gets 94.7% of its electricity from hydropower, below 5.2% from wind power, and the rest from diesel and geothermal energy [58]. This article analyzes data from two years of the Ethiopian electricity system (2017–2018) to assess the fluctuations in wind power production. EEP provides the hourly wind power generation time series. Ethiopia has a total of 324 MW of wind power, of which 51 MW comes from Adama-I, 120 MW from Ashegoda, and 153 MW from Adama-II, as indicated in Table 2.1. Ethiopia's usable reserves and exploited quantity are also given in the same table.

The capacity factor has been used to express the data sets as a proportion of installed capacity so that they could be compared across different installed capacities and it is given by equation 3.1.

$$CF = \frac{P(MW)}{P_{inst}(MW)} * 100 \tag{3.1}$$

Where: CF is a capacity factor in percentage, P is an average power output in MW, P_{inst} is installed capacity of the farm in MW. Figure 2.3 indicates the locations of each existing wind farm. The

blue curve in Figure 3.1 illustrates the production duration curve, whereas the red line represents the production time series. The production duration curve shows the duration of time that a specific production exceeds. As stated otherwise, the duration curve shows the generation of all 8760 hours in the chosen year, arranged in descending order.

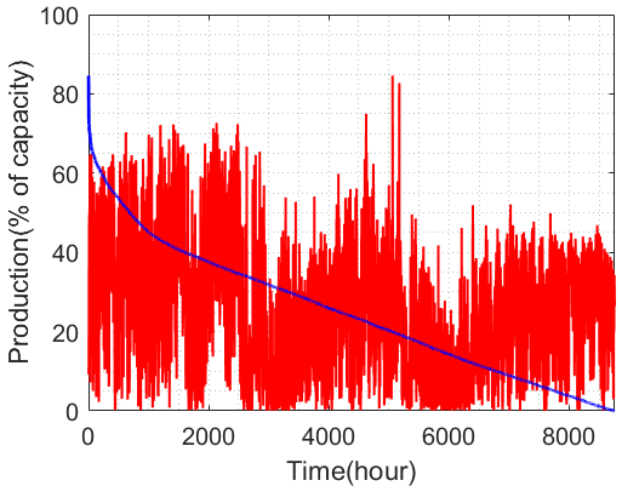

Figure 3.1: Ethiopian wind power generation time series and generation duration curve

3.4 Assessment of wind power variability

Step changes in hourly production or simulation of hourly generation time series can be used to find out the challenges that wind power poses to the electrical system [56]. This chapter attempted to use various techniques to determine the variability of wind power production time series. We attempted to use the step change and correlation between wind farms to evaluate the variability of the wind power generation time series in this study.

Another technique for determining variability in wind energy production is step change. It shows the fluctuations in wind power over short, medium, and long time intervals. In addition, it helps to represent the duration of low and high fluctuations in generation during a given time. This idea comes from the difference in power between one hour and the next. It is represented mathematically as given by equation 3.2.

$$\triangle_h P(t) = P(t) - P(t-h) \tag{3.2}$$

where:

t = (h+1,2,3...8760) in hour.

h is the length of step-change in hour.

The correlation coefficient can also be used to determine the degree to which two wind farms are correlated. Production variability experiences ups and downs simultaneously when the correlation between two wind farms reaches the peak value of 1. If it is close to the minimum value of -1, this indicates a tendency towards decreasing generation at one farm and increasing generation at another. However, if the value is close to zero, the two are not correlated and the production fluctuations at the two locations do not follow each other. The total production is more consistent and less volatile if the wind power is distributed over a larger region.

3.5 Simulation results and discussion

In this part, the results of assessing the variability of wind power generation in the Ethiopian electric grid using the described methodology are presented and discussed. The description of the analysis of the and their respective generation step change are given in the following section.

Table 3.1 illustrates the correlation of the farms. The result indicates that Adama-I and Adama-II have a strong correlation, as their correlation coefficients are close to 1. This indicates that the two farms are not able to balance variation by complementing each other. The power system operators in these wind farms must maintain a high reserve to ensure balance in the event of strong fluctuations. As Table 3.1 illustrates, there is an almost weak link between Adama-I and Ashegoda, between Adama-II and Ashegoda. This indicates that they can complement each other to some extent, as they rise and fall in opposite directions. The distance between the farms is usually the cause of high and low correlations. Adama-I and Adama-II are close to each other and therefore highly correlated. The Ashegoda wind farm is poorly correlated with the two wind farms because they are located 850 km apart.

The results of the hourly step change over an hour and four hours in wind power production, using equation 3.2 are evaluated. This helps to determine the extent to which production fluctuates on an hourly or multi-hourly basis.

Table 3.2 shows that the maximum up and down fluctuation of a single wind farm is high. For each operation, the result of up and down variation exceeds 90%. The variation is better for the aggregate wind farm in Ethiopia resulting in 53.4% of the wind farm being up and -65.74% being

Table 3.1: The correlation coefficient of Ethiopian wind farms

Farms	Correlation result
Between Adama-II and Adama-I	0.9987
Between Ashegoda and Adama-I	0.2658
Between Ashegoda and Adama-II	0.2651

Table 3.2: The largest hourly changes (%) and proportion of time that the variations exceed 5% of capacity of Ethiopian wind farms.

Farms	Max-up variation	Max-down variation	Above 5%	Below -5%
Adama-I	100	-100	23.49	22.97
Adama-II	99.20	-96.71	21.69	21.35
Ashegoda	93.22	-90.84	9.26	8.41
Ethiopia	53.40	-65.74	15.33	14.47

Table 3.3: Correlation of Ethiopian wind farms.

Farms	Correlation result
Between Adama-II and Adam-I	0.5498
Between Ashegoda and Adama-I	0.0152
Between Ashegoda and Adama-II	0.0651

down. Due to the lower installed power compared to other wind farms, the production fluctuation of Adama-I corresponds to the nominal power. This illustrates how aggregation can minimize the variability of wind energy generation.

The proportion of time when the variation is larger than 5% and less than -5% was examined and is displayed on Table 3.2 to assess how long a wind farm is in a calm state and when it is at its peak. Additionally, the table reassures that most of the time, an extreme magnitude of fluctuation occurs when the installed capacity is small.

Table 3.3 shows the correlation of hourly fluctuations in farms' wind energy production. The table shows that there is a weak relationship between Adama-I and Ashegoda and between Adama-II and Ashegoda. There is a strong correlation between Adama-I and Adama-II. This is because of the geographical location of wind farms, as seen in Figure 2.3. The figure illustrates how the correlation between wind farms decreases as the distance between them increases.

Figure 3.2 depicts the variance of wind power generation in Ethiopia over one and four hours. From the figure, it can be concluded that the longer the duration of change, the greater the production variance.

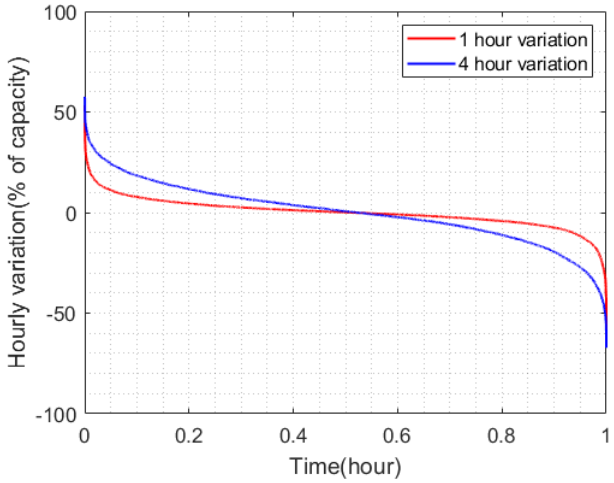

Figure 3.2: Wind power generation step change for 1 hour and 4-hour duration

Chapter 4

Ethiopian Wind Power Generation Modelling and Simulation Studies

4.1 Introduction

Global warming is a consequence of the cumulative impact of human life on Earth during the past few decades, especially the industrial revolution, which led to a steady rise in greenhouse gas (GHG) emissions from the combustion of fossil fuels. Deforestation, urbanization, increased agricultural production, transportation, manufacturing and thermal power plants based on fossil fuels are responsible for this problem [59, 60, 61].

Furthermore, the food-energy-water nexus is an important cross-sectoral and interdisciplinary factor that impacts emissions and contributes to climate change if not managed effectively. As a result, problems with water supply, energy production, universal access, food production and its frequent shortages, and other population-related problems are now widespread in many countries [61]. These problems are caused by several factors, including an increase in population, urbanization, increasing incomes, changes in consumer behavior, and climate change. For example, to produce food we need energy in the form of electricity, fertilizers, and water for irrigation. We need energy for purification to produce clean water, and we also need food if we want to use biofuels and water for cooling.

According to an assessment by the US Environmental Protection Agency, heat and electricity production is responsible for a significant portion of total CO2 emissions, approximately 25% [62]. Fossil fuels (coal, oil, etc.), which are non-renewable, are currently the main sources of energy.

As consumption increases, global fossil fuel supplies continue to deplete and may no longer be sufficient for future production. As a result, globally, the focus is on renewable energy sources, which currently represent around 13.5% of the world energy mix, to create a sustainable and clean energy supply [63].

4.2 Literature review

The cost of electricity produced by all commercially available renewable energy production technologies has decreased in recent decades and is approaching the cost of well-developed hydropower production. The report from [64] showed that new hydropower projects had global weighted average electricity costs of 0.05/kWh, while onshore wind and bioenergy projects had costs of 0.06/kWh and 0.07 USD/kWh.

Therefore, there is an interest worldwide in generating significant amounts of electrical energy from renewable energy sources due to factors such as global warming, fossil fuel depletion, and the attractively decreasing costs of renewable energy. Especially recently, advances in wind energy technology have resulted in wind power accounting for over 5.1% of global electricity production [63]. Therefore, wind energy production is constantly changing around the world and has become essential to grid operations in most countries that have made significant investments in this area.

As already mentioned in the previous chapter, Ethiopian electricity mix consists of less than 5.2% wind power, 94.7% hydropower, and the rest from diesel and geothermal energy [58]. The country suffers from electricity shortages and is forced to carry out scheduled load shading during drought periods due to the climate sensitivity of hydropower, which is the driving factor behind the development of wind power as the next choice for the future.

According to preliminary studies, Ethiopia has a wind power potential of 1350 GW with wind speeds of more than 7 m/s (see table 2.1) [58]. However, with only 324 MW of installed capacity, it accounts for just 5.2% of the country's total electricity production. Numerous scientific research have been studied to assess Ethiopia's wind energy potential for various locations [65, 66]. All studies were conducted using mast data collected by the National Meteorological Services Agency (NMSA).

To increase power production from wind power, the country is planning to build more wind

farms. However, since wind energy is a variable and intermittent energy source, system operation and planning become more challenging [57, 67, 68]. It is incredible to study its features because it affects load following costs, the amount of transmission infrastructure to invest in, CO2 and other pollutant emissions, and electricity costs [57, 19, 68]. Therefore, an acceptable model of hourly wind power generation is critical both to integrate large amounts of wind power into the grid and to make informed decisions about the location and timing of wind farm installation [69, 19].

It is possible to model wind power generation using statistical methods [70, 71, 72] or physical methods [19, 73]. One can develop physical models using meteorological models or based on meteorological measurements. To estimate the wind field more accurately, physical models simply take into account factors such as topography, terrain, local temperature, and pressure; In contrast, statistical methods use statistical models to establish the relationship between historical and predicted power [70]. It is possible to use the meteorological models directly or by increasing its resolution through statistical or dynamic down-scaling [19].

Installed masts could be used to collect on-site meteorological measurements. However, this approach is expensive, time-consuming, and often incomplete. The mast may not be at the correct height above the ground (usually around 10 m) or at a wind production location, which could result in distortion of the production profile [69]. In developing countries such as Ethiopia, where resources are extremely limited, it is particularly difficult to estimate wind direction and speed at the necessary altitude and location.

The meteorological model data, on the other hand, is readily available, complete in terms of location and time, and was collected at high altitudes. Reanalysis data is one of the available meteorological models. Data reanalysis combines historical observations from multiple sources with a state-of-the-art numerical model to provide consistent data over an extended period of time [69]. It is a crucial resource for the study of historical atmospheric conditions in many research areas [74, 75, 76, 77, 78, 79]. Reanalysis data includes, but is not limited to, NASA's MERRA-2, ECMWF's ERA-5 and ERA-Interim. Table 4.1 displays the features of each reanalysis dataset [19, 80, 81, 77, 82, 83, 84, 85, 86, 87].

Table 4.1: Details of freely accessible reanalysis data. One degree is equivalent to 111 kilometers near the equator.

Dataset	Spatial Resolution	Temporal Resolution	Time Coverage	Height
ERA5	0.28°× 0.28°	1 hour	1979 – present	100m
MERRA-2	0.5°× 0.625°	6 hour	1957 – present	50m
MERRA	1/2°× 2/3 °	1 hour	1979 – 2016	50m
ERA-Interim	79 km	6 hour	1979 – 2019	50m
ERA-40	1.125°	6 hour	1957 – 2002	50m

However, as Table 4.1 shows, reanalysis data hardly takes the local effect into account due to their low resolution, especially in the spatial domain. Therefore, without proper processing, especially for onshore wind energy production, they cannot be directly used for investment decisions and planning [19]. The role of reanalysis data in simulating regional wind production variability was examined in the study conducted by [69]. The MERRA reanalysis data was used to estimate wind power generation in Sweden, several parameters were used to reduce uncertainty, and bias correction was performed [19]. The author [88] simulated European wind energy production using statistical down-scaling applied to reanalysis data. The study showed the significance of statistical down-scaling to extract wind speed from the reanalysis data and improve its resolution.

The main objective of this work is to use the ERA5 dataset to model wind power production and to assess how well this dataset works for the Ethiopian energy sector. The model should take into account the wake losses of wind farms and systematic bias in the underlying meteorological model. The model was trained with data from 2016 and validated with data from 2017.

4.3 Methodology

This section describes the methods used to model wind power generation using the ERA5 dataset. It begins with a brief description of the research area, data collection, and modeling of wind power production time series.

Figure 4.1 illustrates the paper's workflow, which begins with extracting wind speed from the ERA5 reanalysis dataset and applying horizontal interpolation, also known as bilinear interpolation, to find wind speed on the site. To find the actual wind speed at the site, spatial statistical down-scaling can be used to improve the spatial resolution and then finally extrapolate it to the turbine hub-height.

After obtaining the wind speed at the necessary hub-height, it can be converted to power using a farm-specific power curve by applying wake loss. Finally, the task may be completed by validating the model against the measurement.

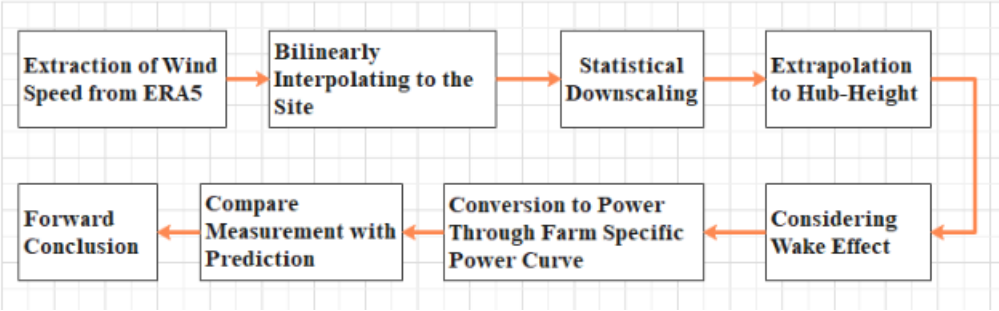

Figure 4.1: The workflow diagram.

Accordingly, the fundamental steps of the modelling are:

1. Extract the hourly time series of ERA5 wind speed and gather data on wind farms, such as installed capacity and coordinates (location).

2. ERA5 hourly wind speed is bilinearly (horizontally) interpolated from geographic grid points to the actual location of wind farms.

3. The bilinearly interpolated ERA5 wind speed was statistically down-scaled spatially to improve resolution.

4. Using the power law, get the true wind speed at the farm's hub height from the down-scaled wind speed.

5. Determine the hourly wind energy for each farm based on the true wind speed and the farm's specific power curve, taking into account wake, internal, and external losses.

6. To account for the underlying meteorological model uncertainty based on the observed bias in wind energy computed at step 5 in comparison to the historical energy gathered from farms, apply bias correction. By removing the inaccuracy and uncertainty from the meteorological model, the goal is to get the same simulated result as the real data.

All of the above steps will be covered in the following sections with the respective data used. This particular investigation was conducted at two Ethiopian wind farms (see Figure 2.3), namely

Ashegoda and Adama-II. Data on wind speed was gathered from the European Centre for Medium-Range Weather Forecasting (ECMWF), and measurement data was gathered from Ethiopian Electric Power (EEP) over two years (January 2016 to December 2017). The next sections will cover both data sources.

ERA5

Reanalysis is the process of providing a consistent reprocessing of meteorological observations over an extended portion of the historical data record using an unchanging data assimilation system [89]. Numerous robust reanalysis datasets, such as MERRA (Modern Era Retrospective Analysis for Research and Applications) from NASA and ERA5 from ECMWF, are frequently used to model the production of wind energy.

Table 4.1 shows that ERA5, the most recent version, was chosen for this research since it offers better resolution compared to the others. It can be found in the Climate Data Store with a spatial resolution of 0.28° (31 km) and a temporal resolution of one hour on standard latitude-longitude grids. Since ERA5 covers the years 1979 to the present and its wind speed data is found at a height of 100 meters, it is relevant to modern wind turbines. Of course, there are still uncertainties, even if the ERA5 reanalysis data has a smaller error than the forecasts.

Wind power measurement data

Ethiopian Electric Power (EEP) provided historical production output data for wind farms over the specified period. To effectively model and assess the generation output power, the following information has been gathered.

- The farms' location (coordinates) and installed capacity.
- Mean hourly wind farm production measurements.

The EEP measurement data contains numerous errors, such as negative values and occasionally higher-than-rated power readings, which have been eliminated beforehand. A further issue is that the measurement is typically zero. This could be the result of a measurement error or turbine downtime. These data points have been eliminated once more. Table 4.2 lists the wind farm's data.

Table 4.2: Wind farm turbine data.

Farms	Type of turbine	Power rating (MW)	Installed capacity (MW)	Number of turbine	Hub-height (m)
Ashegoda	Ecotecnia 74	1.67	120	84	70
Adama-II	Sany SE7715	1.5	153	102	80

Next, using equation (4.1), the capacity factor of the power for each farm is determined for comparison.

$$CF = \frac{P_{MW}}{P_{inst}} \tag{4.1}$$

where:

CF is capacity factor, P_{MW} is the actual production and P_{inst} is the installed capacity.

4.4 Modelling of wind power generation

Standard method for transforming wind speed into electricity involves utilizing a power curve specific to a farm to transform wind speed data from meteorological models or observations. The power curve provides the power output value at turbine hub height as a function of wind speed. Since the data were released, other researchers have used the reanalysis data to convert wind speed time series to their equivalent power time series. Nonetheless, the degree of complexity associated with conversion varies among researchers in the possible use of parameters that are to be optimized. Table 4.3 shows a list of the parameters utilized in this paper.

Table 4.3: The model optimisation parameters.

Parameter name	Range	Description
Losses_S	[0.0, 0.25]	Loss taken into account when determining the wind speed scaling constant; this is covered in section 4.4
PLoss_{int}	[0.00, 0.30] $\times 12$	Internal power losses at incoming wind speed for each wind sector; they are discussed in the section 4.4
Bias correction	12×24 matrices	For every farm, a matrix that accounts for seasonal and diurnal bias and is presented in this section 4.4

Accordingly, the means of modeling hourly wind power output in this work begins with a mathematical computation to find wind speed at the necessary site and hub height from reanalysis data and then uses a farm-specific power curve to convert the obtained wind speed to power. Lastly,

it talks about systematic errors in the meteorological model and losses that should be taken into account.

Interpolation and spatial statistical down-scaling of ERA5 wind speed

Bilinear interpolation is used to get the extracted ERA5 wind speed to the desired location. Even though ERA5 wind speed is derived from reanalysis and should, therefore, have fewer errors than forecasts, there are still uncertainties because of the meteorological model's uncertainty and its limited spatial resolution. Figure 4.2 qualitatively illustrates the spatial resolutions of ERA5 and the global wind atlas (GWA), with the colors denoting various ranges of the site's mean wind speeds at a height of 100 meters. Therefore, as the graphic illustrates, GWA provides a clearer pattern than ERA5. This is due to the ERA5 dataset having a low spatial resolution.

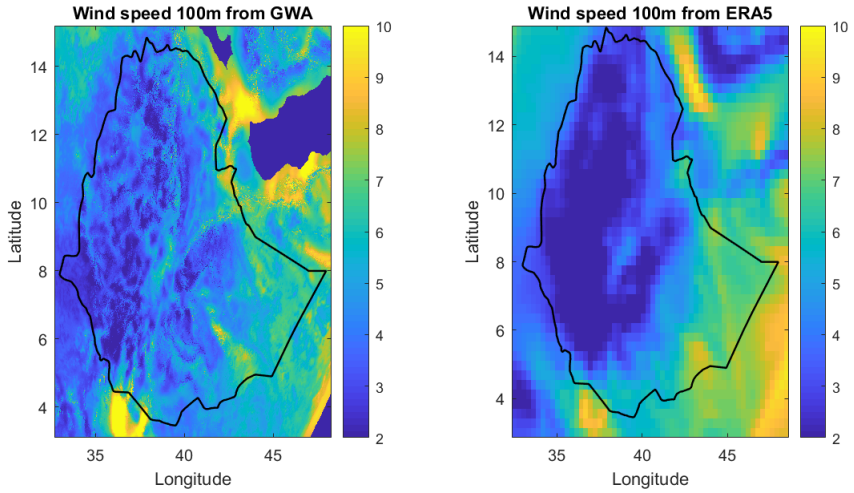

Figure 4.2: The Ethiopian mean wind speed of ERA5 reanalysis and Global Wind Atlas.

To improve the resolution and decrease systematic bias in the reanalysis data, many researchers have used different approaches. A few have applied the spatial statistical down-scaling method [88, 90], while others have employed the bias correction method [91, 19, 92].

The present study employs a statistical down-scaling technique on ERA5 wind speed to enhance its spatial resolution and account for the local effect around wind farms. The spatial statistical down-scaling method is applied to reanalysis wind speed data [88] by using the Global Wind Atlas (GWA) data, which takes into account local orography and surface roughness features at a 250 $\times$ 250 m spatial resolution.

Equation (4.4) illustrates how each low-resolution wind speed value collected from the ERA5 hourly time series is correlated with the high-resolution wind speed value, resulting in equivalent values for the cumulative distribution function [88]. To capture the local effect, the method was applied to hourly wind speeds at a specified site. To best fit the wind speed distribution of the site, the Wei-bull parameters, shape factor (k), and scale factor (c) of the reanalysis data are calculated empirically using equations (4.2-4.3). The micro-scale values of the same parameters are derived from the global wind atlas.

$$k = \left(\frac{\delta}{V}\right)^{-1.086} \tag{4.2}$$

$$c = \frac{V}{gamma\left(1+\frac{1}{k}\right)} \tag{4.3}$$

$$F_{hr}(v_{hr}) = F_{lr}(v_{lr}) \tag{4.4}$$

$$1 - e^{-(\frac{v_{hr}}{c_{hr}})^{k_{hr}}} = 1 - e^{-(\frac{v_{lr}}{c_{lr}})^{k_{lr}}} \tag{4.5}$$

Where:

k is the Weibull distribution shape factor ,

c is the Weibull distribution scale factor ,

V is the mean wind speed,

δ is the standard deviation of the wind speed,

F_{lr} is the cumulative distribution function of low resolution,

F_{hr} is the cumulative distribution function of high resolution,

v_{lr} is the low resolution wind speed time series &

v_{hr} is the high resolution wind speed time series to be calculated.

Solving for v_{hr} from equation (4.5), it becomes:

$$v_{hr} = c_{hr}\left(\frac{v_{lr}}{c_{lr}}\right)^{\frac{k_{lr}}{k_{hr}}} \tag{4.6}$$

Extrapolation

It is necessary to vertically extrapolate the statistically down-scaled hourly wind speed to hub height. The power law is utilized to perform vertical extrapolation, and the formula is given

by (4.7).

$$v_{hrtur} = v_{hr}\left(\frac{h_{tur}}{h_{100m}}\right)^{\alpha} \tag{4.7}$$

Where:

v_{hrtur} is wind speed at turbine hub-height,

v_{hr} is ERA5 wind speed at 100m,

h_{tur} is turbine hub-height ,

h_{100m} is the height of ERA5 wind speed and

α is the shear exponent.

The shear exponent α was calculated from the two height of global wind atlas (between 100 and 50m) and is given by equation (4.8).

$$\alpha = \frac{ln\left(\frac{v_{100m}}{v_{50m}}\right)}{ln\left(\frac{100m}{50m}\right)} \tag{4.8}$$

It is assumed that the shear exponent remains constant; however, the mean annual energy production (AEP) derived from reanalysis needs to match the measurement. An equation (4.7) needs to be multiplied by a constant in order to meet this equality condition. The parameter $Losses_S$ governs losses in the AEP computation.

Power curve and output power

A manufacturer's power curve associates wind power with wind speed. The specific power of the turbine (P_A), which is the ratio of rated power to rotor area, is the most significant component influencing the shape of the power curve. To account for wake loss in the model, it is most effective to convert the power curves into functions of power in the incoming wind (P_u) (watts per square meter swept rotor area). Thus, the wind turbine output power is a function of the power in the incoming wind (P_u) and P_A and it is given by equation (4.9).

$$P_{tur} = f(P_u, P_A) \tag{4.9}$$

Various types of losses in wind farms, such as wakes, availability, blade deterioration, high wind hysteresis, and losses in the transformer and internal electric grid, can affect the amount of elec-

tricity generated and delivered to the end user. The wake impact from upstream turbines causes the wind farm's significant loss. These losses are represented using a variety of techniques [93, 94], such as the Katic/ Jensen model given by equation (4.10).

$$V = U\left(1 - \frac{1-\sqrt{1-C_t}}{(1+2k\frac{X}{D})^2}\right) \tag{4.10}$$

Where: C_t is the thrust coefficient, k is the wake decay constant, X is the distance between two turbines, D is the turbine diameter, and V and U are the disturbed and undisturbed wind speeds.

Since the thrust coefficient is greatest at low wind speeds, a decrease in wind speed using the equation (4.10) is also greatest at low winds. However, due to the shape of the power curve, the losses are zero for undisturbed winds below the cut-in speed, rise to a peak in the steepest part of the power curve, and finally reduce back to zero in undisturbed wind speeds slightly above the nominal speed. A similar form of wind speed-dependent losses is achieved by reducing incoming wind power by a fixed amount (governed by $Ploss_{int}$) in equation (4.11) [19].

The relationship between the power output of the turbine and the power in the incoming wind speed yields two distinct power losses: wake effect and loss in the transmission line. Equation (4.11) can therefore be used to calculate the power at the grid or at the point of common coupling.

$$P_{pcc} = (1 - Ploss_{tr}) f\left((1 - Ploss_{int})\frac{1}{2}\rho u^3, P_A\right) \tag{4.11}$$

Where:

$Ploss_{tr}$ is loss on the transmission line. $Ploss_{int}$ is wake loss or internal loss. P_{tur} is output power of turbine,

P_{pcc} is power at point of common coupling of the grid and

ρ is air density which is constant (1.225kg/m^3).

To account for the seasonal and diurnal bias of reanalysis uncertainty, a meteorological model bias correction is carried out [95]. It is triggered by an observed ERA5 systematic error that varies with the time of day and month of the year (see Figure 4.3). The figure illustrates how this error depends on the hour of the day and the month of the year. The observed discrepancies could result from ERA5's inability to accurately represent the seasonal and diurnal variations in wind shear and speed.

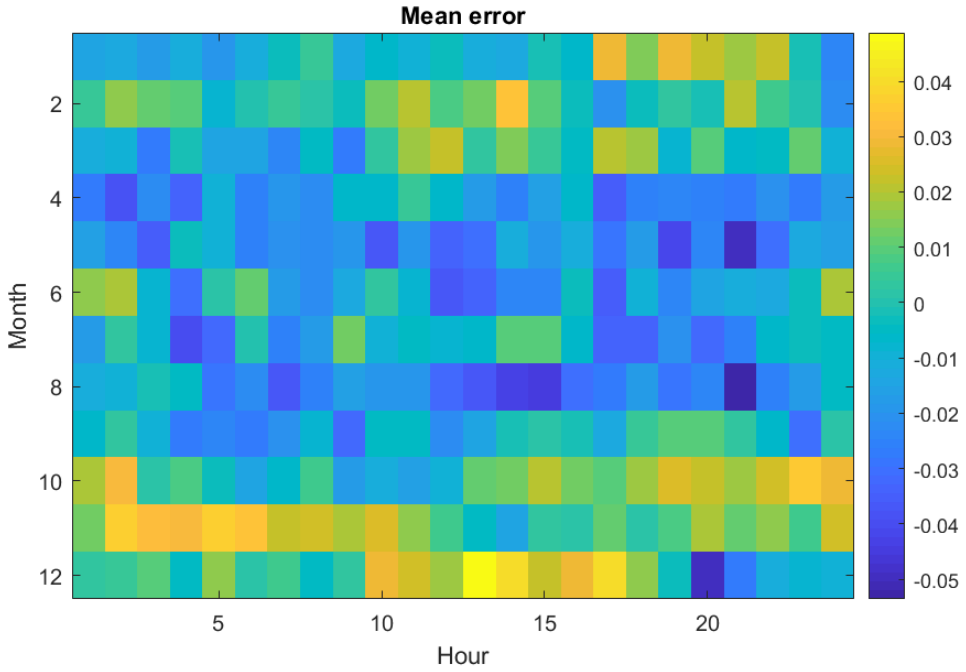

Figure 4.3: The mean error for Adama-II depends on the day and month of the year prior to bias correction.

Performance metrics

For any model, several statistical performance error metrics can be applied as performance indicators. Because of their widespread use, hourly mean absolute error (MAE) and hourly root mean squared error (RMSE) are utilized in this work [96]. Equations (4.12) and (4.13) provide the mathematical expressions for the two performance indicators.

$$MAE = \frac{1}{n}\sum_{t=1}^{n}\left(\left|P_{mt} - P_{cc,t}\right|\right) \tag{4.12}$$

$$RMSE = \sqrt{\frac{1}{n}\sum_{t=1}^{n}\left(P_{mt} - P_{cc,t}\right)^2} \tag{4.13}$$

where:

P_{mt} is the measured power at time t,

$P_{cc,t}$ is the modeled power at the point of common coupling during time t and

n is the total number of hours in a year.

Parameters optimization

Proper optimization technique is required to determine the optimal value of the parameter indicated in Table 4.3. The goal was to reduce the root mean square error (RMSE), which is provided by equation (4.13). Accordingly, the main goal of wind power modeling is to minimize the model error compared to measurement. As a result, equation (4.14) formulates and provides the objective function (OF).

$$OF = min\Big(RMSE\Big) \tag{4.14}$$

The nonlinear "Patternsearch Optimization" technique in Matlab was selected to tune the parameters to be optimized.

4.5 Simulation results and discussion

The following results have been obtained through a simulation of the wind power generation using ERA5. The study has two goals: to predict wind power production and verify the outcome using measurements. Concurrently, the research attempted to test whether the ERA5 reanalysis data was suitable for the country. As a first attempt, the two topographically unique and remote locations of Ethiopian wind farms are chosen as the case study to examine the appropriateness of the ERA5 data for Ethiopia.

The historical hourly wind power data from EEP is used to validate the simulated wind power generation. Table 4.4 shows the performance error metrics result for each wind farm. The results cover the two-year modeling period ranging from January 1, 2016, to December 31, 2017, in Gregorian calendar time (G.C.). A year is dedicated to training the model and another year is dedicated to validating the model. Each result is expressed in units (p.u.), where a p.u. shows the installed capacity of the corresponding farm. The mean absolute error (MAE) and root mean square error (RMSE) of hourly power are 2.32% and 5.29%, respectively, for Ashegoda and 2.5% and 4.54%, for Adama-II.

Table 4.4: Performance error metric.

Metrics	Ashegoda	Adama-II
MAE	2.32%	2.5%
RMSE	5.29 %	4.54%

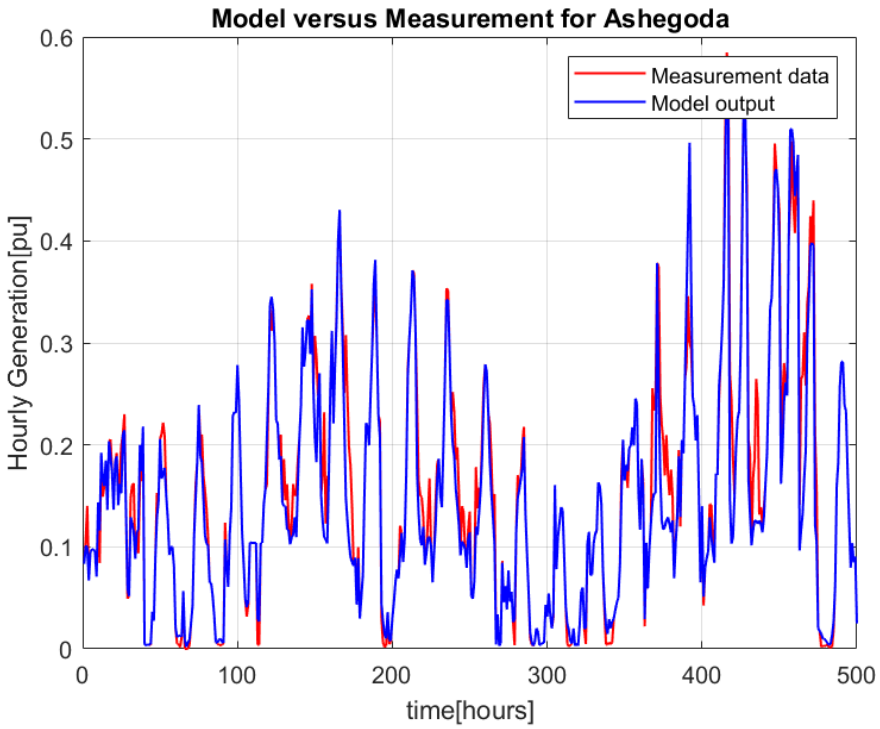

Figure 4.4: Model output and validation data from Ashegoda.

The measured data and model output for 500 hours from Ashegoda and Adama-II are shown in Figures 4.4 and 4.5, respectively. For Ashegoda and Adama-II, MAE and RMSE are 2.8 and 5.1% and 3 and 4.8%, respectively. For the entire year of the validation period, the results are almost identical to the MAE and RMSE of this period. The figures indicate that the model accurately reflects the fluctuations in measured.

Comparing the study to former research, the discrepancy is not significant because this research was conducted on individual wind farms and not at a regional or national level, where plant distribution compensates for fluctuations in wind power. Using the MERRA dataset, J. Olauson and M. Bergkvist modeled hourly wind power generation in Sweden at regional and national levels; the RMS errors were 3.8% [19]. Using the MERRA dataset, Kubik [69] simulated for Northern Ireland and obtained an RMS error of 11.9%, which is larger than the finding we obtained in this research.

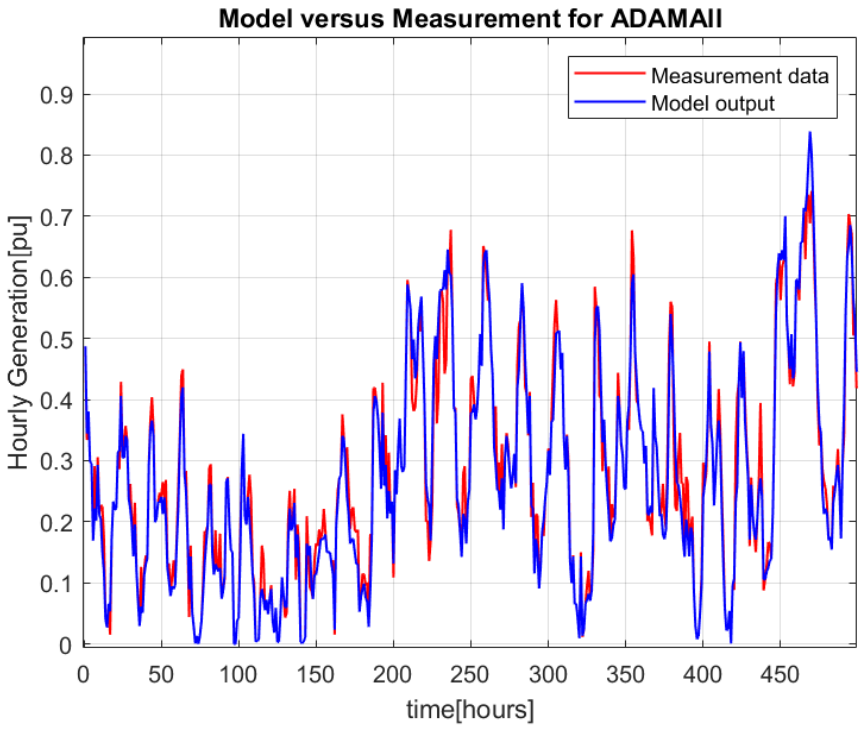

Figure 4.5: Model output and validation data from Adama-II.

Thus, the result indicates that the proposed model and measurements for the two wind farms agree well. It will be interesting to see whether simple models produce comparable results. As a result, we present the following simple modeling steps for comparison with the proposed model. A simple model does not take into account bias correction, wake loss, or statistical down-scaling.

1. The ERA5 hourly wind speed at 100 m level was bilinearly interpolated to the turbine location.

2. Power law-based wind speed extrapolation to turbine hub height.

3. To give the annual energy production determined by measurement, the mean wind speed for each site was modified.

4. Each farm's hourly power production was determined using the power curve of the farm.

Influence of parameters and discussion of the result

This part discusses the effect of the parameters on the suggested model and the respective result. The result is achieved by adjusting the parameters of the suggested model and applying spatial

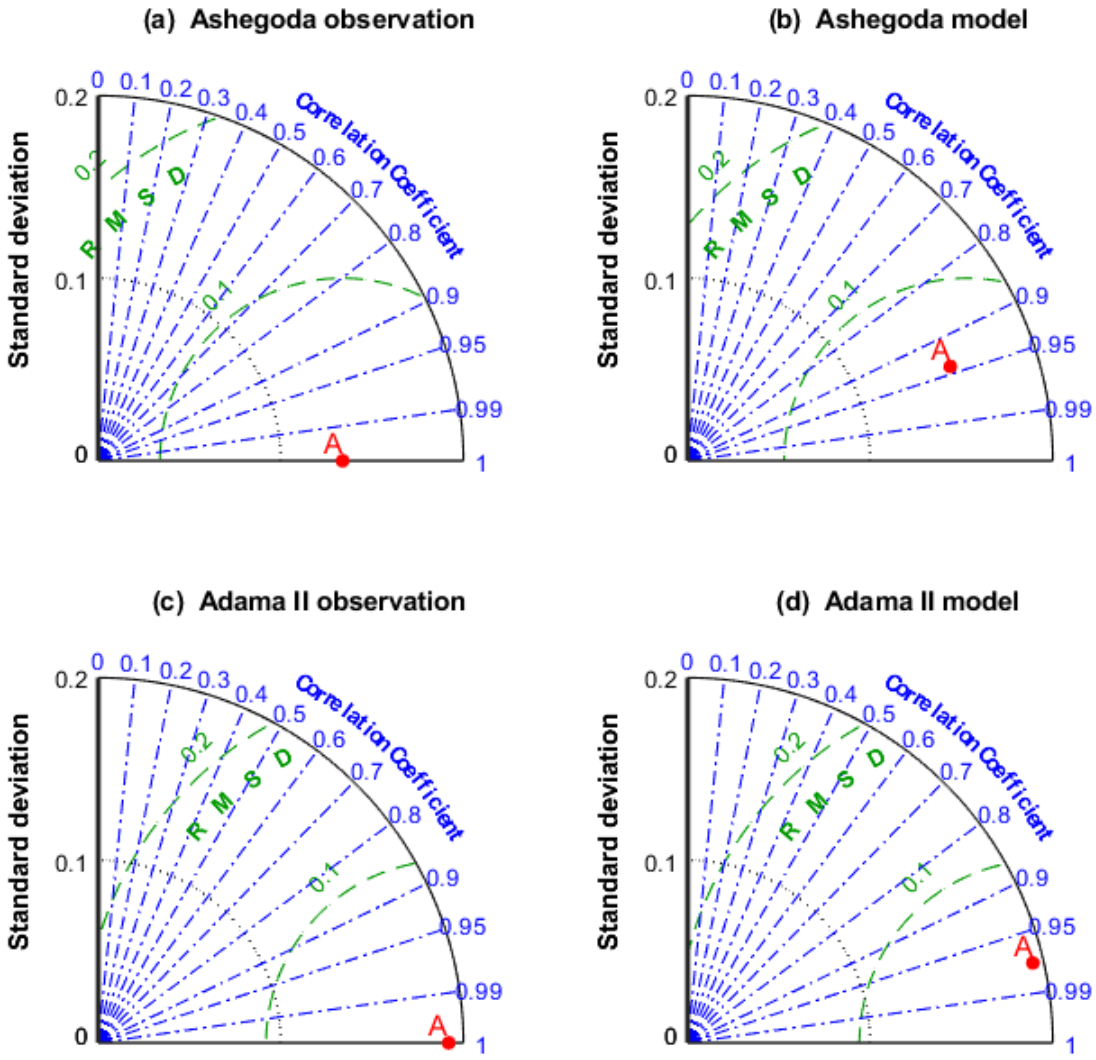

Figure 4.6: Taylor diagram of the model and measurement for Ashegoda and Adama-II wind farms.

statistical down-scaling. Three parameters have been taken into consideration, including seasonal and diurnal corrections, as shown in Table 4.2.

Applying spatial statistical down-scaling to reanalysis data through the use of a high-resolution global wind atlas (GWA) improved Ashegoda's result somewhat and Adama-II's result greatly. The root mean square error (RMSE) of the simple model without spatial statistical down-scaling is 11.51% for Adama-II and 10.38% for Ashegoda. The results are corrected by 42.4% for Adama-II and by 7% for Ashegoda using spatial statistical down-scaling. This demonstrates that, compared

to the suggested model, the simple model overestimates the output power. As a result, the RMSE value for Adama-II and Ashegoda has been reduced by approximately 42.4% and 7%, respectively, due to down-scaling. Thus, it is clear that spatial statistical down-scaling is an essential factor in the modeling of Ethiopian wind power generation and needs to be taken into account.

Even though the wake effect cannot be calculated at the level of individual wind turbines, attempts have been made to enhance results by taking into account a global loss factor in the incoming wind power for each wind sector (bin of 30°). For Ashegoda, however, this has resulted in a considerable improvement over Adama-II. Using the "pattern-search" algorithm included in Matlab, a loss of 0–30% has been applied and optimized for each distinct wind sector. For Ashegoda, the result of the objective function has been decreased by 17%. Due to the upstream turbines mentioned before, we recommend that future wind power output simulations should take into account a wake effect of about 25%.

The observed bias caused by inaccuracy and uncertainty in the reanalysis was corrected by the introduction of seasonal and diurnal bias, which greatly improved the RMSE value for both wind farms. The objective function values for Adama-II and Ashegoda, without bias correction, were 6.63% and 8.16%, respectively. After accounting for bias, the RMSE for Adama-II became 4.54%, while Ashegoda's became 5.29%. This indicates that there is a 28.05% and 45% decrease in the RMSE value for Adama-II and Ashegoda, respectively. This suggests that there is bias in the ERA5 data, which should be considered while calculating Ethiopian wind power output. For any Ethiopian wind power production, we therefore advise $\pm 3\%$ seasonal and diurnal correction.

Moreover, the model has nearly perfectly reproduced the measurement, as shown by the simulation results in Figures 4.4 and Figure 4.5. Thus, it can be concluded that prior to the installation of a wind turbine, it is possible to choose good wind locations around the country using ERA5.

Additionally, a Taylor diagram has been utilized to reflect the relationship of the model with measurement. Three parameters (standard deviation, root mean square deviation (RMSD), and correlation coefficient) are used to show the relationship between the model with measurement. The model's variation from the observation is shown by the standard deviation. The model's performance and how much it deviates from the observation are shown using the RMSD. The correlation coefficient is the final and most interesting variable that is used to show the relation. The degree to which two-time series follow one another is indicated by this variable.

The result of the three variables (standard deviation, RMSD, and correlation coefficient) for

each farm's observation and model is depicted in Figure 4.6, where the variables are marked by red dots under the letter A. Every farm has a corresponding diagram for modeling and observation. The measurement diagram is used as a reference to evaluate the model. The Taylor diagrams for Ashegoda wind farm's measurement and model are indicated in Figures 4.6 (a) and (b), respectively. Since the three parameters for measurement are calculated against themselves, the result becomes a unity correlation coefficient and a zero RMSD. The Taylor diagrams for the Adama-II wind farm for measurement and model are displayed in Figures 4.6 (c) and (d), respectively. Figures illustrate that the model's standard deviations for Adama-II and Ashegoda are 18.80% and 15.44% respectively. This result is nearly identical to the measurement's standard deviation, which for Adama-II is 13.38% and for Ashegoda is 19.19 %. Likewise, the model's RMSD for Ashegoda and Adama-II is 5.37% and 4.54%, respectively. This demonstrates that there is little discrepancy between the model and the measurement.

Furthermore, the model's correlation coefficient is given in the same figure. For Adama-II and Ashegoda, it becomes 97.47% and 94.03%, respectively. This shows that the model follows the measurement. Therefore, the three-parameter generally indicates that the model functions well and reflects the features of the measurement time series.

Therefore, to sum up, the suggested model has attempted to examine the applicability of ERA5 to the Ethiopian wind farm industry as well as simulate current wind power production. The obtained findings demonstrated that it is possible to model wind power generation time series and choose potential wind speed areas in the country by using ERA5. However, ERA5 has to be seriously processed first to represent the site.

Moreover, to the best of our knowledge, this is the first work on simulating wind power generation using reanalysis data and validating the result with an Ethiopian measurement. The outcome is encouraging and demonstrates that, with reanalysis data, wind power output can be accurately modeled in a chosen location in the country by appropriately extracting and processing wind speed using the previously mentioned parameters.

Chapter 5

Estimation of Maximum Variable Renewable Energy Integration with High Share of Hydropower

5.1 Introduction

Electricity generation from renewable resources is becoming a future issue for every country's energy system. The crucial reason to focus on generating electrical energy by using renewable resources is the world's high dependence on fossil fuels for all purposes including transportation, power generation, heat generation, global warming due to the use of these fuels, their price increase, uncertainty and a limited amount of world reserves [97]. However, shifting from fossil fuels to carbon-free renewable energy resources will pose technical and economic challenges and require smart decisions. Furthermore, renewable energies, particularly variable renewable energies (VREs) such as wind and solar sources, bring an additional challenge for electric grid operators because of the inherent variability and unpredictability.

To make the right decision about how much wind and solar energy can be reliably integrated into a national grid, various countries have conducted a grid integration study of VREs [18, 12, 13, 14, 15, 16, 17]. The grid integration study focuses on the system level to analyze the technical and/or economic influence of accomplishing a significant percentage of variable renewable energy in the electricity mix. It adjusts generation expansion planning (GEP) to find the type, quantity,

timing, and geographical placement of solar and wind production capacity.

GEP helps to jointly assess the optimal integration or portfolio study of various energy sources. This means determining an optimal result for the planning problem in which the integration of new production units meets all physical, technical, and financial constraints. However, the detailed methods used in the GEP varied between countries, depending on their particular energy system. Therefore, traditional long-term generation expansion planning models have been used for years, based primarily on operational cost simplifications and ignoring detailed operational aspects such as ramp rates, operating reserves, and decisions related to start-up and shutdown. To determine how many VREs can be reliably integrated into a national grid, it is better to conduct a grid integration study that takes short-term operational constraints into account.

5.2 Literature review

Several authors have studied generation expansion planning using different methods [97, 11, 98, 99, 100, 101]. In [97], the author developed a long-term mathematical model for Argentina to decide on investment planning for the period 2010-2030. In [101], the author developed an investment planning model to minimize total annual costs while meeting different CO2 emission constraints and annual electricity demand forecasts. The developed model is a single-period mixed integer linear programming (MILP). Article [102] has developed a MILP model for the Greek electricity sector to achieve an optimal determination of the electricity mix. The optimal electricity mix focuses on connecting autonomous island systems to the Greek mainland power grid via undersea electric cables. In [103], the author developed a model for studying the planning of an energy system to find the optimal energy road map of a grid.

The major problem with all of the above articles is that demand was only represented in a limited time slice and was also unable to reflect the variability of renewable energy resources and their impact on the electricity grid. They also did not consider the short-term operational constraints such as the ramp rate and reserves for uncertainty. The power plants considered for expansion planning were primarily thermal power plants, so the impact of significant variable renewable energy scenarios was not apparent. This means that the operational challenge of 100% renewable combinations, particularly VREs, is not clear from the documents listed.

Article [104] has developed a power system planning model that takes life cycle costs and

environmental impacts into account. However, operational constraints were not taken into account. Therefore, the inherent variability of variable renewable energy sources may not be observed in the study.

In [105], the author presented a traditional GEP modeling including some features of renewable energy sources. However, this work does not take into account the chronological duration curve of the load and neglects the hourly and monthly fluctuations that characterize the contribution of renewable energy resources. Therefore, the stability of the system is questionable. Furthermore, its main focus is on thermal energy and has not seen the 100% renewable energy sources and their impact on system operations. Article [106] examines the reliability of limited GEP in the presence of wind uncertainty in the deregulated electricity market.

Therefore, none of the above studies consider planning a 100% expansion of renewable energy production, but their goal was to reduce greenhouse gas (GHG) emissions. However, to accomplish a significant reduction in greenhouse gas emissions, a significant deployment of renewable energy sources is required which might be changing the power system to 100% renewable resources. This brings new challenges as the output of renewable technologies cannot be easily predicted and adjusted to demand. This leads to a paradigm shift towards long-term generation and short-term operational planning of the energy system.

Author [107] examined the steps of designing energy systems with the flexibility required to keep stability and reliability, mainly utilizing variable energy sources through flexibility assessment. Literature [108] discussed the implications of interconnecting power grids versus isolating power grids in Western European countries when each country's only energy source is sunlight, water, and wind. To address the unpredictability and uncertainty associated with intermittent renewable energy, the study used demand response and hydrogen storage. The stability of the system without storage was not tested in this study.

Studies on 100% renewable energy systems have been carried out for countries such as Denmark [109], Portugal [110], Ireland [111], New Zealand [112] and Macedonia [113]. In the majority of the studies, biomass is utilized as the primary source for achieving 100% renewable energy systems. In addition, pumped storage power plants, together with wind, biomass, and heat pumps, were selected in various studies as a remedy for the 100% renewable energy system. The question, however, is what happens when hydropower is the dominant renewable energy source, as in the Ethiopian power grid. Authors such as Luca [45], [114] and [115] examined the integration

of variable renewable energies using Ethiopia as an example. However, all of the above works do not necessarily consider all future hydropower as a done deal, whereas the present work does (only the VRE amount is optimized while forcing future hydropower into the model).

In general, all the above-mentioned works have not investigated the technical evaluation of the integration of variable renewable energy with the aim of 100% renewable energy and a high share of hydropower. In addition, the authors did not consider the detailed short-term operational planning of hydropower. Additionally, the papers did not consider reserves for system balancing due to the variability and uncertainty of variable renewable energy and loads.

The goal of this study is therefore to study the estimation of maximum variable renewable energy integration with the goal of 100% renewable energy and a high share of hydropower using a modified GenX tool with corresponding detailed short-term operational constraints to assess its impact on the system operation considering eight scenarios for the horizon year of 2030.

GenX is a highly configurable, open-source power resource capacity expansion model that incorporates multiple state-of-the-art power system planning practices to provide enhanced decision support for a changing power landscape. The GenX model was developed at MIT and used in various MIT publications for a variety of analyses including long-term production and transmission expansion planning and short-term operational simulations and optimization, and has been used in many energy system decarbonization studies [116]. This planning software has been used by various authors, including the Nuclear Energy Agency (NEA), to simulate the operation and planning of energy systems. [117, 118, 119, 120, 121, 122, 123, 124] are some of the articles published with GenX.

GenX has some shortcomings in operating the system under detailed operational constraints. The original version of GenX did not take into account cascaded hydropower, which could have a large impact on model performance. In addition, the individual reservoirs were not considered. Furthermore, the curtailment of variable renewable energy was not taken into account in the objective function. Therefore, in this article, the original GenX has been modified to include all cascaded hydropower and also consider individual reservoirs. Then the new GenX is called modified GenX.

Thus, the novel contributions of the research are summarized as given below:

- We presented a novel model of cascaded hydropower model rather than considering all as one reservoir for a country during the evaluation of maximum VRE integration study (section 5.3 Model Formulation).

- We include short-term operational constraints in the VRE integration evaluation problem such as ramp rate and reserve consideration which were not considered by other papers to see their impact on integration (section 5.3 Model Formulation).
- We study a VRE integration evaluation with 100% renewable energy in which hydropower is a dominating resource and identify the challenge of variable renewable integration.
- We have considered a full-year hourly load and VRE time series rather than a time slice.
- We included minimization of VRE curtailment in the objective function which was not considered by GenX (section 5.3 Model Formulation).

In this paper some assumptions have been considered such as no financial constraints and no transmission limits in the Ethiopian power system as the study focuses on the technical evaluation of the VRE integration.

5.3 Methodology

To evaluate the maximum amount of VRE that can be integrated into the Ethiopian power grid, the appropriate methodology has been followed. The work started with data collection and adapting an existing simulation model. Both of them are briefly discussed in the subsequent sections.

The data used in this study is based on extensive data collection, mainly from the Ethiopian Electricity Sector (EEP). The following sections discuss generation, demand, and inflow data.

Generation and transmission capacities The installed capacity and average annual energy generation capacity of each generation type used in the model was based primarily on data from the Ethiopian Electricity Master Plan (EEP) [2]. In addition, the master plan also identified potential power plant candidates for integration into the national grid for the year 2030. The technologies included in the master plan are hydropower, wind power, solar power, and must-run (biomass and geothermal plants).

For each technology, the installed capacity in the year 2020 and the planned capacity for year 2030 are shown in Table 5.1. The question mark in the table for wind and solar in the planning year is that we do not know how much of their capacity can be integrated and the model is going to answer it by optimally solving the problem. In this model, hydropower is selected for ramping

and reserve provision purposes due to its high flexibility. Table 5.2 shows a list of all installed, expected average annual generating capacity of hydropower for the year 2030. The annual average inflow or average annual generating capacity of hydropower plant is shown in Table 5.2 and it is assumed as a maximum annual energy generation in this model.

Table 5.1: Total installed capacity and annual energy generation capacity of resources [2].

Technology	2020 [MW]	2030 [MW]	Annual energy [TWh] for 2030
Hydropower	4077	17628	64.67
Wind	324	?	?
Solar	0	?	?
Must run	32.3	1441	9.37

Load profile

For the horizon year of 2019, the hourly load has been collected from EEP and this load is scaled up for the planning year of 2030 using business as usual methods which is given by equation (5.1) and it is taken from [125]. Annual domestic demand is expected to increase from 16.7 TWh in the year 2020 to 58.5 TWh in the year 2030 [2], representing an annual growth rate of 13.7%. To reflect the load growth for the anticipated year, the load is subsequently scaled up by a factor of 3.5. Load profile is also given in Figure 5.1.

$$Load_{t,2030} = Load_{t,2020} x \frac{Load_{2030}}{Load_{2020}} \qquad \forall\, t \in \mathscr{T} \tag{5.1}$$

where:

$Load_{t,2030}$: it is the hourly load during time t for the year 2030.

$Load_{t,2020}$: it is the hourly load during time t for the year 2020.

$Load_{2030}$: it is peak load of the year 2030.

$Load_{2020}$: it is peak load of the year 2020.

Wind power production

The model in [126] was used to create the wind energy production time series. The chosen wind sites are used to compute wind power generation depending on the ERA5 meteorological wind

Table 5.2: Existing and prospective or candidate hydro power plants [2].

Hydropower plant	Installed capacity [MW]	Commissioning year	status	Annual generating capacity [MWh]	capacity factor [%]
Koka	43	1960	Existing	133470	36
Awash2	32	1966	Existing	183480	65
Awash3	32	1971	Existing	184220	65
Gilgel gibe2	420	2010	Existing	2030170	55
Tisabay1	11	1964/2000	Existing	1700	1.7
Tisabay2	67	2001	Existing	10100	1.7
Koisha	2160	2022	Existing	6460000	34
Tana Beles	460	2010	Existing	2748740	68
Fincha	128	1974	Existing	614670	55
Genale Dawa 3	254	2018	Existing	1690560	76
Gilgel gibe1	210	2004	Existing	882130	48
Gilgel gibe3	1870	2010	Existing	5348270	33
Melkawakena	153	1988/2014	Existing	555490	42
Amertineshe	97	2013	Existing	245000	29
Tekeze	300	2009	Existing	1399480	53
GERD	5150	2024	UC	14684100	26
Baro1	166	2023	candidate	651710	45
Baro2	507	2023	candidate	1573186	44
Birbir	467	2023	candidate	2716650	66
Dabus	304	2023	candidate	2626082	49
Geba1	214	2023	candidate	951970	51
Geba2	157	2023	candidate	753490	55
Genale5	100	2023	candidate	572990	65
Genale6	246	2023	candidate	1528460	71
Genji	214	2023	candidate	814100	71
Halele	96	2024	candidate	449770	54
Karadobi	1600	2029	candidate	7830780	56
Tams	1700	2025	candidate	5714000	38
Warabesa	340	2024	candidate	224885	51
Yeda1	162	2023	candidate	627110	44
Yeda2	118	2023	candidate	460450	45
Total				64667213	

speed. The selected parameters in the model are adjusted to historical wind production. Therefore, a realistic time series of wind energy generation can be created for individual wind farms. The wind power production profile is also shown in Figure 5.2.

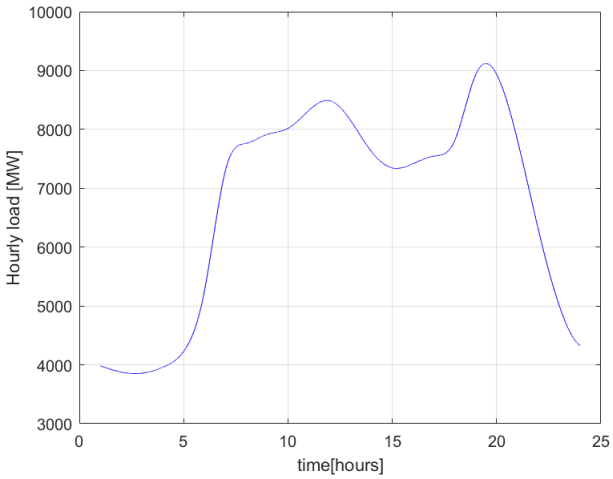

Figure 5.1: Daily average load profile.

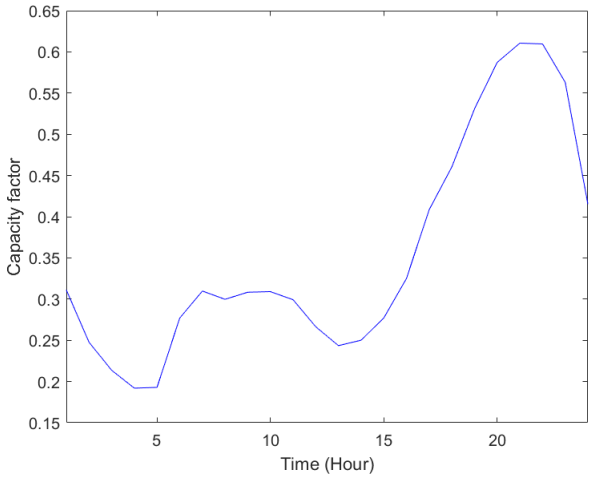

Figure 5.2: Daily average profile of wind power production.

Table 5.3: Existing wind power plants [2].

Farms	Installed capacity (MW)	Year of commissioning	Status
Adama-I	51	2011	Existing
Adama-II	153	2015	Existing
Ashegoda	120	2010	Existing
Sum	324		

Solar power production

The System Advisory Model (SAM) [127] is used to create time series of solar power production for simulation purposes. It was developed by the National Renewable Energy Laboratory (NREL). It is a free technical-economic software model that makes decision-making easier for people in the

renewable energy industry. The solar power production profile is also displayed in Figure 5.3.

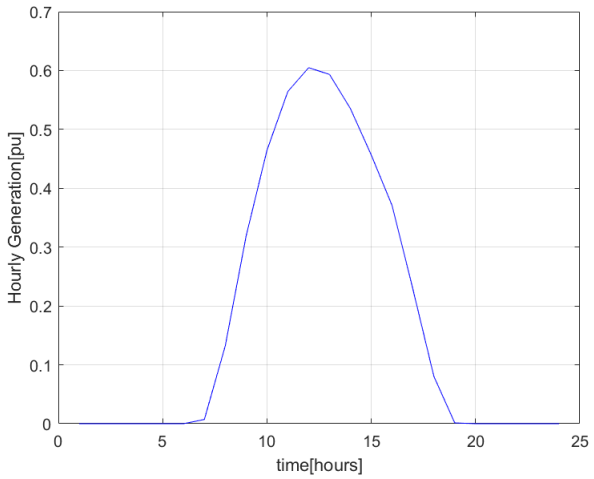

Figure 5.3: Daily average profile of PV power production.

Reservoir inflow

The storage capacity of each reservoir was collected from the EEP master plan. The monthly average reservoir inflow was collected from the same document and is available from 1961 to 2005. To obtain a more realistic inflow, cubic spline interpolation was used to interpolate the monthly inflow to obtain an hourly inflow. For instance, Figure 5.4 depicts the interpolated inflow of the Beles hydropower plant.

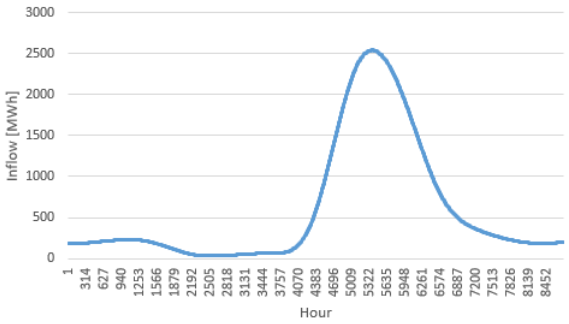

Figure 5.4: Interpolated inflow for Beles hydropower plants.

Formulation of the Model

The existing model was adapted for the power grid of Ethiopia to estimate the maximum amount of variable renewable energy that can be integrated during the planning year. The model consists

of two parts, namely: objective function and constraints. Both parts are briefly explained below.

Objective function

As already explained above, the general objective function of the problem is defined as minimizing the total system costs (capital costs, fixed operation and maintenance costs, variable operation and maintenance costs, unserved load penalty, curtailment penalty, etc.) and is given by equation (5.2).

$$
\begin{aligned}
min \sum_{g \in \mathscr{W}} \left(c_g^{inv} \times cap_g^{new} \right) + \sum_{g \in \mathscr{PV}} \left(c_g^{inv} \times cap_g^{new} \right) + \sum_{g \in \mathscr{W}} \left(c_g^{fom} \times cap_g^{tot} \right) + \\
\sum_{g \in \mathscr{PV}} \left(c_g^{fom} \times cap_g^{tot} \right) + \sum_{g \in \mathscr{MR}} \left(c_g^{fom} \times cap_g^{tot} \right) + \sum_{g \in \mathscr{H}} \left(c_g^{fom} \times cap_g^{tot} \right) + \\
\sum_{t \in \mathscr{T}} \left(\sum_{g \in \mathscr{W}} \left(c_g^{vom} \times p_{g,t} \right) + \sum_{g \in \mathscr{PV}} \left(c_g^{vom} \times p_{g,t} \right) + \sum_{g \in \mathscr{MR}} \left(c_g^{vom} \times p_{g,t} \right) + \right. \\
\left. \sum_{g \in \mathscr{H}} \left(c_g^{vom} \times p_{g,t} \right) + \left(c^{ns} \times \Lambda_t \right) + \left(c^{curt} \times \left(w_t^{curt} + pv_t^{curt} \right) \right) - \sum_{l \in \mathscr{L}} \left(c_{exp} \times exp_{l,t} \right) \right)
\end{aligned} \tag{5.2}
$$

However, the objective of this chapter is to estimate the technically feasible VRE that can be integrated to Ethiopian grid, then it has ignored all the economic part of the objective function by assuming zero investment cost c_g^{inv}, zero fixed operational and maintenance cost c_g^{fom} and zero variable operational and maintenance cost c_g^{vom} of all technology g. Then, simplifying the above equation, the objective function to be solved in this chapter is given by equation (5.3). Therefore, the final objective function is aimed to increase the flexibility of the system thereby increasing the amount of VREs to be integrated.

The insufficient system flexibility will reduce the system's ability to integrate the required amounts of VRE production and as a result, the system operator may need to curtail a part of the available VRE production. On the other hand, if the available VRE production drops below the forecasted levels and the system lacks flexible production units to quickly recover this VRE output reduction, the system operator may need to curtail a part of the system load to keep the supply/demand balance. To penalize the insufficient system flexibility in the optimization problem, the penalty costs of curtailed VRE production given by cost of curtailment (c^{curt}) times the amount of energy curtailed from wind (w_t^{curt}) and PV (pv_t^{curt}) during each time step and curtailed system load given by cost of load shedding (c^{ns}) times the amount load shed (Λ_t) are added to the

objective function to reflect the additional costs paid by the utility due to the lack of sufficient system flexibility. Moreover, to increase the penetration level and system flexibility, the extra energy is to be exported to neighboring countries. This concept is included to the objective function as an income from selling energy to neighboring countries and it is obtained by multiplying the cost of selling energy (c_{exp}) and the amount of hourly energy exported per hour over each line ($exp_{l,t}$). Thus, the objective function to be optimized is given by equation (5.3). Furthermore, for clarity, subscripts g, t, and l represent the technology representing a type of power plant, the time step in an hour, and the transmission line to neighboring countries respectively. Thus, the system cost or objective function to be minimized is given by:

$$min \sum_{t \in \mathscr{T}} \left((c^{ns} \times \Lambda_t) + \left(c^{curt} \times \left(w_t^{curt} + pv_t^{curt}\right)\right) - \sum_{l \in \mathscr{Z}} \left(c_{exp} \times exp_{l,t}\right) \right) \tag{5.3}$$

Thus, the terms in order are the cost for load shedding, cost of variable renewable energy curtailment and net income from export to neighboring countries respectively. In this model, the cost for variable renewable energy curtailment is set as low compared with the cost of load shedding. This means VRE is curtailed before load shedding. All the power parameters and variables are in the unit of MWh as the model uses hourly average values.

The objective function described above is subjected to power balance, VRE production, hydropower, unserved load, reserve requirement, transmission line, and must-run constraints. Each of these constraints is clearly described below.

Power balance

The power balance constraint of the model ensures that electricity demand is met at every time in the year. As given by equation (5.4), electricity demand (D_t), at each time step must be strictly equal to the sum of production ($p_{g,t}$) from variable renewable energy resources ($\mathscr{VRE}$), must run resources ($\mathscr{MR}$), and hydropower resources ($\mathscr{H}$). At the same time demand curtailment (Λ_t) also decreases the total demand. Finally, power flows ($exp_{l,t}$) on each line out of Ethiopia are considered in the demand balance equation. Thus, the power balance constraint defines that the sum of power production from all technologies plus the non-served demand minus the export to

the neighboring countries must be equal to the anticipated domestic consumption.

$$\sum_{g\in\mathscr{W}} p_{g,t} + \sum_{g\in\mathscr{PV}} p_{g,t} + \sum_{g\in\mathscr{MR}} p_{g,t} + \sum_{g\in\mathscr{H}} p_{g,t} + \Lambda_t - \sum_{l\in\mathscr{L}} exp_{l,t} = D_t \tag{5.4}$$

Thus, the terms in order are energy production from VRE (wind and PV), must-run units, hydropower, the possible load shedding, and the sixth term shows the export to neighboring countries. Therefore, the sum of all energy production plus demand curtailed minus export to neighboring countries must be equal to domestic demand.

Variable renewable energy (VRE)

The operational constraints for wind ($\mathscr{W}$) and solar ($\mathscr{PV}$) resources are a function of each technology's time-dependent hourly capacity factor ($\rho^{max}_{g,t}$) in per unit terms, and the total available capacity (cap^{tot}_g) and are given by equations (5.5 - 5.6). The equations state that the power generation ($p_{g,t}$) from the VRE must be less than or equal to the maximum power generation capacity of the resources. The inequality constraint indicates that the production can be curtailed for flexibility purposes.

$$p_{g,t} \leq \rho^{max}_{g,t} \times cap^{tot}_g \qquad \forall g \in \mathscr{W}, t \in \mathscr{T} \tag{5.5}$$

$$p_{g,t} \leq \rho^{max}_{g,t} \times cap^{tot}_g \qquad \forall g \in \mathscr{PV}, t \in \mathscr{T} \tag{5.6}$$

On the other hand, the equations can be modified as the power production ($p_{g,t}$) plus the curtailment of energy due to over production should be equal to the maximum power production capacity of wind and solar as given by equations (5.7 - 5.8) respectively.

$$p_{g,t} + w^{curt}_t = \rho^{max}_{g,t} \times cap^{tot}_g \qquad \forall g \in \mathscr{W}, t \in \mathscr{T} \tag{5.7}$$

$$p_{g,t} + pv^{curt}_t = \rho^{max}_{g,t} \times cap^{tot}_g \qquad \forall g \in \mathscr{PV}, t \in \mathscr{T} \tag{5.8}$$

Finally, the total capacity (cap^{tot}_g) of each resources is the sum of existing capacity (cap^{exist}_g) and new capacity (cap^{new}_g) and is given by equation (5.9).

$$cap^{tot}_g = cap^{exist}_g + cap^{new}_g \qquad \forall g \in (\mathscr{PV}, \mathscr{W}) \tag{5.9}$$

Hydropower constraint This constraint enforces that energy level of the hydropower reservoir g in time step t ($m_{g,t}$) is defined as the sum of the reservoir level in the previous time step, less the amount of electricity generated ($p_{g,t}$) minus any spillage ($s_{g,t}$) plus the hourly inflows into the reservoir equal to the installed reservoir discharged capacity times the normalized hourly inflow parameter ($\rho_{g,t}^{max} \times cap_g^{tot}$) plus the sum of the power discharged ($p_{k,t-\tau_g^q}$) from all upstream power plants k during time ($t-\tau_g^q$) plus the sum of spilled energy ($s_{k,t-\tau_g^s}$) from all upstream power plants k during time ($t-\tau_g^s$) plus annual average energy inflow per hour (Q_k^{avg}) from all upstream power plants k when the time to reach downstream power plant (τ_g^q) is greater than the planning time t. Thus, the constraint is given by equation (5.10) and it indicates the energy balance of reservoir hydropower. The modified hydropower plant modeling can be seen from [128].

Certainly, equation (5.10) shows a practical way of modeling the energy flow delays between succeeding power plants. τ_g^q is assumed to be a constant time delay for discharge from each upstream power plant k to reach the downstream power plant g. The quantity τ_g^q can be expressed in hours (h_g^q) and minutes (m_g^q). Equation (5.11) provides then the delayed upstream flow as a weighted average of the discharge between the hours (h_g^q and h_g^q+1), as described in [129]. For the spillage delays, a similar expression can be used.

Electricity production ($p_{g,t}$) from hydro resources, is constrained to always be above a minimum output power which is given by a parameter (ρ_g^{min}) times the total installed capacity (cap_g^{tot}) to represent operational constraints related to minimum stream flows or other demands for water from hydro reservoirs and it is given by equation (5.12). Equation (5.13) shows that the total annual electricity production from each hydropower plant should be less or equal to the maximum energy level m_g^{max} of each reservoir. Equation (5.14) brings an additional constraint that the total stored energy in each time step is less than or equal to the maximum. Equation (5.15) depicts the end reservoir content constraint. It represents that at the end of planning period T, reservoir content m_T should be equal to end reservoir content m^{end}. Equation (5.16) shows the spillage constraint. It represents that the spillage $s_{g,t}$ for each hydropower plant and at each time step should be greater than or equal to zero.

$$m_{g,t} = m_{g,t-1} - p_{g,t} - s_{g,t} + \rho_{g,t}^{max} \times cap_g^{tot} + \sum_{k \in F_g^{\mathscr{D}}} p_{k,t-\tau_g^q} + \sum_{k \in F_g^{\mathscr{S}}} s_{k,t-\tau_g^s} + \sum_{k \in F_g^{\mathscr{D}}} Q_k^{avg} \Big|_{t \leq \tau_g^q} +$$

$$\sum_{k \in F_g^{\mathscr{Q}}} \frac{60 - m_k^q}{60} Q_k^{avg} \Big|_{t=\tau_g^q+1} \qquad \forall g \in \mathscr{H}, t \in \mathscr{T} \quad (5.10)$$

$$p_{k,t-\tau_g^q} = \frac{m_g^q}{60} p_{k,t-h_g^q} + \frac{60 - m_g^q}{60} p_{k,t-h_g^q-1} \qquad \forall k \in \mathscr{F}^{\mathscr{Q}}, t \in \mathscr{T} \quad (5.11)$$

$$\rho_g^{min} \times cap_g^{tot} \leq p_{g,t} \leq cap_g^{tot} \qquad \forall g \in \mathscr{H}, t \in \mathscr{T} \quad (5.12)$$

$$\sum_{t \in \mathscr{T}} p_{g,t} \leq m_g^{max} \qquad \forall g \in \mathscr{H} \quad (5.13)$$

$$0 \leq m_{g,t} \leq m_g^{max} \qquad \forall g \in \mathscr{H}, t \in \mathscr{T} \quad (5.14)$$

$$m_T = m^{end} \quad (5.15)$$

$$0 \leq s_{g,t} \qquad \forall g \in \mathscr{H}, t \in \mathscr{T} \quad (5.16)$$

The constraints given by equations (5.17) and (5.18) enforce hourly changes in power output (ramps up and ramps down respectively) to be less than the maximum ramp rates (δ_g^{up} and δ_g^{down}) in per unit terms times the total installed capacity of technology g (cap_g^{tot}).

$$p_{g,t} - p_{g,t-1} \leq \delta_g^{up} \times cap_g^{tot} \qquad \forall g \in \mathscr{H}, t \in \mathscr{T} \quad (5.17)$$

$$p_{g,t-1} - p_{g,t} \leq \delta_g^{down} \times cap_g^{tot} \qquad \forall g \in \mathscr{H}, t \in \mathscr{T} \quad (5.18)$$

Non served demand

Equation (5.19) represents an additional constraint that enforces the total demand curtailed Λ_t during each time step cannot exceed available demand D_t.

$$\Lambda_t \quad \leq \quad D_t \qquad\qquad \forall t \quad \in \quad \mathscr{T} \quad (5.19)$$

Frequency regulation requirements

Total requirements for frequency regulation also known as primary reserves in each time step t are specified as fractions of hourly demand (to reflect demand forecast errors) and variable renewable availability in the time step (to reflect wind and solar forecast errors) and it is given by equation (5.20).

$$\sum_{g \in \mathscr{H}} f_{g,t} \quad \geq \quad x_{reg}^{load} \times D_t + x_{reg}^{vre} \times \rho_{g,t}^{max} \times cap_g^{\text{tot}} \qquad \forall t \quad \in \quad \mathscr{T} \quad (5.20)$$

Where D_t is the forecasted electricity demand at time t ; $\rho_{g,t}^{max}$ is the forecasted capacity factor for variable renewable resource $g \in \mathscr{VRE}$ in time step t; cap_g^{tot} is the total installed capacity of variable renewable resources $g \in \mathscr{VRE}$; and x_{reg}^{load} and x_{reg}^{vre} are parameters specifying the required frequency regulation as a fraction of forecasted demand and variable renewable production respectively.

Operating reserve requirements

Total requirements for operating or balancing reserves in the upward direction in each time step t are specified as fractions of time step demand (to reflect demand forecast errors) and variable renewable availability in the time step (to reflect wind and solar forecast errors) and it is given by equation (5.21).

$$\sum_{g \in \mathscr{H}} r_{g,t} \quad \geq \quad x_{blc}^{load} \times D_t + x_{blc}^{vre} \times \rho_{g,t}^{max} \times cap_g^{\text{tot}} \qquad \forall t \quad \in \quad \mathscr{T} \quad (5.21)$$

Where D_t is the forecasted electricity demand at time t ; $\rho_{g,t}^{max}$ is the forecasted capacity factor for variable renewable resource $g \in \mathscr{VRE}$ in time step t; cap_g^{tot} is the total installed capacity of variable renewable resources $g \in \mathscr{VRE}$; and x_{blc}^{load} and x_{blc}^{vre} are parameters specifying the required balancing

reserve as a fraction of forecasted demand and variable renewable production respectively.

Equation (5.22) defines the modified constraints on power production capacity when modeling operating reserves. The modifications when operating reserves are modeled regarding maximum power production limits and it is modified to account for procuring some of the available capacity for frequency regulation ($f_{g,t}$) and upward operating (or balancing) reserves ($r_{g,t}$). It indicates the sum of power production $p_{g,t}$, operating reserve $r_{g,t}$ and frequency regulation reserve $f_{g,t}$ should be less than the total capacity cap_g^{tot} of the power plant dedicated for reserve.

$$p_{g,t} + r_{g,t} + f_{g,t} \leq cap_g^{tot} \qquad \forall g \in \mathscr{H}, t \in \mathscr{T} \tag{5.22}$$

The modified constraint regarding the amount of downward frequency regulation reserves is shown in equation (5.23). It shows the difference between the power production $p_{g,t}$ and frequency regulation reserve $f_{g,t}$ cannot be less than the minimum power output which is minimum capacity factor ρ_g^{min} times total installed capacity cap_g^{tot}.

$$p_{g,t} - f_{g,t} \geq \rho_g^{min} \times cap_g^{tot} \qquad \forall g \in \mathscr{H}, t \in \mathscr{T} \tag{5.23}$$

Transmission line constraint

Equation (5.24) depicts that the power flow constraint from Ethiopia to neighboring countries. The equation represents that the power flow ($exp_{l,t}$) over the line l during time step t should be less than or equal to the maximum capacity of the transmission line exp_l^{max}.

$$exp_{l,t} \leq exp_l^{max} \qquad \forall l \in \mathscr{L}, \quad t \in \mathscr{T} \tag{5.24}$$

Must run constraint

For must-run resources ($g \in \mathscr{MR}$) output in each time period t must exactly equal to the available capacity factor, $\rho_{g,t}^{max}$, times the installed capacity, cap_g^{tot}, not allowing for curtailment and it is given by equation (5.25). These resources are also not eligible for contributing to frequency regulation or operating reserve requirements.

$$p_{g,t} = \rho_{g,t}^{max} \times cap_g^{tot} \quad \forall g \in \mathscr{MR}, t \in \mathscr{T} \quad (5.25)$$

Summary of the problems

The summary of the optimization problem is depicted by:

minimize (5.3), subjected to:

Constraint for power balance by equation (5.4)

VRE constraints by equations (5.5 - 5.7)

Hydro power constraints by equations (5.10 - 5.18)

Nonserved load constraint by equation (5.19)

Reserve requirement constraints by equations(5.20 - 5.23)

Transmission line constraint by equation (5.24)

Must run constraint by equation (5.25)

5.4 Scenario setup and key assumptions

Scenarios setup

In order to evaluate the maximum feasible VRE integration and their effect on system operation, different scenarios have been considered. These different scenarios and their respective descriptions are given below.

1. Integrated variable renewable energy (IVR).
   This represents the reference scenario required to assess the influence of additional wind and photovoltaic capacity in the Ethiopian electric grid. In this case, the average weather year data has been assumed. The basic characteristics of the IVR scenario are described below.
   - Business as usual method has been used for demand growth as given by equation (5.1).
   - Average weather year availability of hydropower inflow as per EEP master plan given in Table 5.2.
   - VRE capacity is with only existing wind farm and no photovoltaic power plant is given in Table 5.3.

- Geothermal and biomass production is also taken from EEP master plan for the planning year and it is given in Table 5.1.
- Transmission capacity is based on the one in the year 2020 and power purchase agreements with other countries and it is given in Table 5.5.

2. National Generation Expansion Plan (NGEP).

   This scenario is the same as with IVR scenario except for VRE and the transmission line planned for the year 2030 is used as per the EEP master plan.

3. Expansion scenario [ES].

   In this scenario, a lot of combinations of wind, hydro, and PV (W-H-PV) with and without reserve provision for different weather years have been used to see how load shedding and VRE curtailment behaves and at the same time it evaluates how much wind and PV can be integrated to the grid. This scenario consists of 8 cases as shown in Table 5.4. For example, low wind, low hydro, and average PV with the reserve are abbreviated as LW-LH-APV-R1 respectively.

   Average hydro is the one planned by EEP for the year 2030 as 64.67 TWh/year inflow and the low weather year hydro is assumed that the average weather year hydro is reduced by 20%. In the case of wind, average year wind is the one obtained from the Ethiopian wind production model having a capacity factor of 35%, and low year wind is assumed to have a 32% capacity factor. The average year PV is with 22% capacity factor obtained from the system advisory model. Finally, the simulation has been made with and without reserve. With reserve (R1) means to consider reserve for load and VRE uncertainty whereas R0 is when reserve is not considered for the uncertainty.

Key assumptions

The study has been conducted using data of the year 2020 as base or initial point and taking into consideration the basic changes expected until the year 2030 such as expansion in transmission capacity from Ethiopia to neighbouring countries, expansion in hydropower production, increase of load, and some expansion in must run production. Using the developed model, the capacity of

Table 5.4: Expansion scenario cases

Scenario	Wind (W)	PV	Hydro (H)	Reserve (R)
1	L	A	A	R1
2	L	A	A	R0
3	L	A	L	R1
4	L	A	L	R0
5	A	A	A	R1
6	A	A	A	R0
7	A	A	L	R1
8	A	A	L	R0

wind and solar to be added is estimated. The sections that follow go over the main presumptions about each of these aspects of the case study.

Minimum production level

In case of high wind and PV power generation, production from hydropower plant can be reduced to its minimum level based on the constraint given by equation (5.12). In this paper, geothermal and biomass power plants are treated as a must-run and some percentage of hydropower is treated as a must-run. From the EEP master plan, it has been given that irrigation is assumed as load and is anticipated to reach 3 TWh/year in the year 2030. Therefore, for this case study around 1000 MWh/h of hydropower is considered as a minimum flow. This minimum flow is not spillage rather it is water going through a turbine for irrigation.

Transmission capacity

There are fundamental changes in transmission capacity from Ethiopia to neighboring countries for the year 2030 and it is depicted in Table 5.5. For the planning year, a transmission capacity of 4100 MW was planned. During the planning year, it is assumed that there will be some uncertainty in the transmission line and taking into account the market agreement between the countries, 3955 MW was assumed as a maximum transmission capacity governed by equation (5.24). Thus, this transmission capacity yields a maximum annual energy export of 34.6 TWh/year to neighbouring countries if fully utilised.

Table 5.5: Transmission capacity [1]

Year	From	To	Export [MW]
2020	Ethiopia	Djibouti	100
	Ethiopia	Kenya	0
	Ethiopia	Tanzania	0
	Ethiopia	Sudan	200
2030	Ethiopia	Djibouti	100
	Ethiopia	Kenya	2000
	Ethiopia	Tanzania	400
	Ethiopia	Sudan	1600

.

Annual energy production and domestic demand assumptions

It was reported by the EEP master plan that annual domestic demand is 58.5 TWh/year and the export to neighbouring countries is assumed to be 34.67 TWh/year. Furthermore, an average annual inflow of hydropower was given as 64.6 TWh/year and 9.37 TWh/year from must-run power plants for the year 2030.

Reserve assumptions

Table 5.6 depicts the assumed minimum level of reserves during the study. Furthermore, it indicates the load shedding and VRE curtailment penalty cost parameters. Table 5.7 depicts the amount of reserves contributed by each technology. Additionally, each technology's ramp rate is displayed.

Table 5.6: Reserve requirement, penalty of load shedding and VRE curtailment cost.

Type of reliability requirement	Minimum level required	Penalty cost
Load shedding (c^{ns})	-	2000 $/MWh
Selling energy (c^{exp})	-	2000 $/MWh
VRE curtailment (c^{curt})	-	160 $/MWh
Regulating reserve $(x_{reg}^{load} and x_{reg}^{vre})$	1% Load + 1% VRE	binding
Balancing reserve $(x_{blc}^{load} and x_{blc}^{vre})$	5% Load + 15% VRE	binding

Model implementation

The Ethiopian power system is chosen as a study area in which the model is to be implemented taking into account the total transmission capacity to neighboring countries such as Djibouti, Kenya,

Table 5.7: Maximum reserve contribution of each generating resources

Technology	Contribution to regulating reserve $f_{g,t}$[% of max output]	Contribution to balancing reserve $r_{g,t}$[% of max output]	Ramp rate δ [% of maximum output/hour]
. Hydropower	5	20	100
Wind	0	0	-
Solar	0	0	-
Must run	0	0	-

Sudan, and Tanzania. In the year 2020, the total transmission capacity was 100 MW, 200 MW, 0 MW, and 0 MW to Djibouti, Sudan, Kenya, and Tanzania, respectively. Some literature suggests that Sudan's electricity supply in the year 2030 will come largely from fossil fuels, which are more expensive compared to renewable energy in Ethiopia. Thus, to make money, Ethiopia can export more energy to Sudan during excess generation.

The model is implemented in Julia software using a planning tool known as GenX with Gurobi 9.14 solver for solving the optimization problem. For a whole year, solving the model took around 20 minutes on a computer with Intel Core i7-4790 CPU @ 3.6 GHz and 32 GB of RAM.

5.5 Simulation results and discussion

In this part, the result of the maximum possible combination of wind and solar photovoltaic (PV) integration in the Ethiopian power grid for the year 2030 is presented and discussed. In the study, eight different cases were considered to determine the maximum technically feasible combination of wind and solar energy and their impact on system operation such as load shedding and curtailment of VREs. In this way, the model has identified the optimal combination of the two energy sources in the grid that could lead to minimal load shedding and curtailment of renewables. Detailed comparisons were also made between the scenarios.

The expansion scenario (ES) consists of 8 additional cases to determine the technically feasible combination of wind and PV. For each case, the model assumes two extreme points, wind only (without PV) and PV only (with existing wind), to know the maximum possible integration of each resource and determine its impact on system operation.

Figure 5.5 shows the energy balance of the IVR scenario, in which total production (75 TWh/year) exceeds domestic demand (58.5 TWh/year). Ethiopia can therefore export the remaining energy to

neighboring countries. Accordingly, 3 TWh to Kenya, 3 TWh to Tanzania, 0.56 TWh to Djibouti in accordance with the market agreement, and the remaining 9.94 TWh to Sudan.

Figure 5.6 shows an example of an hourly time series simulation of system operation in the first week of January. The figure shows that hydropower is highly flexible and can easily be ramped up and down to follow the net load, i.e. the difference between load and VREs. In this scenario, there is no domestic load shedding and no curtailment of VRE.

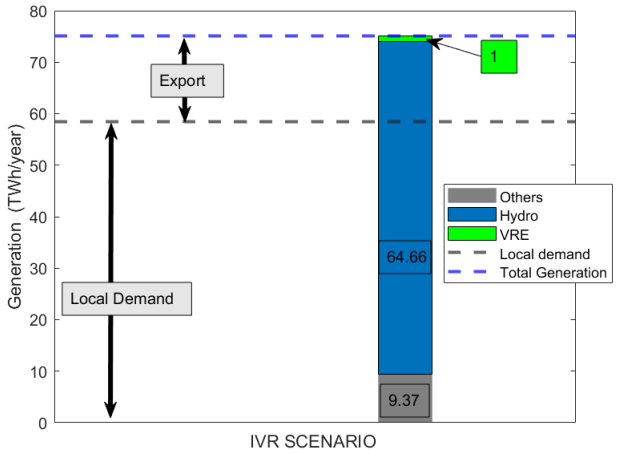

Figure 5.5: IVR scenario energy balance.

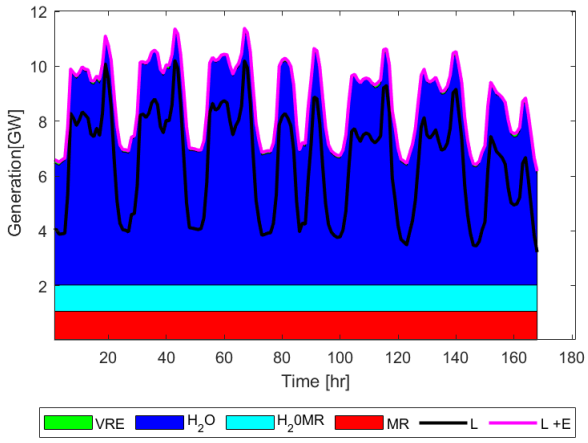

Figure 5.6: IVR scenario hourly simulation during the first week of January.

During the ES, various cases have been examined to assess the feasible combination of wind and PV. Initially, load shedding (unmet export) and VRE curtailment were analyzed with existing wind power and varying PV penetrations to evaluate the impact of penalty costs on integration.

As indicated in Figure 5.7, VRE curtailment decreases and unmet export increases with rising VRE curtailment costs, based on the assumption of a base load curtailment cost. Concurrently, PV penetration capacity decreases as curtailment cost increases. However, the fundamental principle is that customers' demands should be met to avoid penalties at the same time the export should be maximized to minimize the objective function. To compromise, the VRE curtailment cost should be kept at a reasonable level to prevent excessive domestic load shedding and maximize exports. The goal can be accomplished by increasing the cost of domestic load-shedding and cost of energy selling to neighboring countries beyond the cost of VRE curtailment.

Figure 5.8 illustrates the impact of varying load shedding costs on both domestic load shedding or export and VRE curtailment while using the base case VRE curtailment cost. Furthermore, the figure shows that as the cost of load shedding rises, the occurrence of load shedding decreases rapidly, while VRE curtailment increases. Consequently, higher load-shedding costs lead to greater integration of VRE, as minimal load-shedding prompts greater reliance on VRE to meet domestic demand or export.

In general, as the cost of curtailment increases, VRE curtailment decreases. Similarly, as load shedding cost increases, domestic load shedding or unmet export decreases. It is important to note in this paper that load shedding is more sensitive than VRE curtailment. Therefore, for further analysis, the domestic load shedding cost and energy selling cost are set to 2000 $/MWh, and the VRE curtailment cost is set at 160 $/MWh. This cost selection prioritizes VRE curtailment over load shedding. Thus, the following analysis utilizes the mentioned costs.

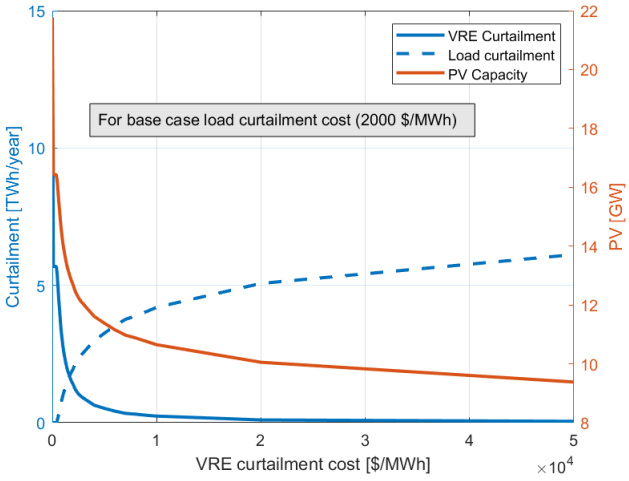

Figure 5.7: PV curtailment for different VRE curtailment cost with base case load shedding cost.

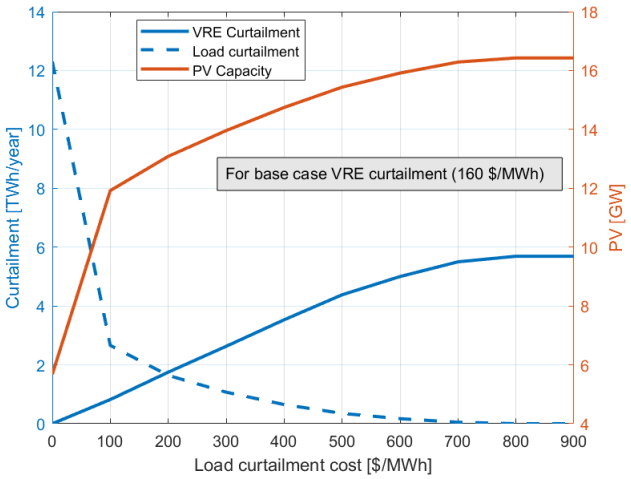

Figure 5.8: Load shedding for different load shedding cost with base case VRE curtailment cost.

Table 5.8: Sample result of the simulation for all scenarios considering 1324 MW of wind.

Scenarios	Wind	PV
1	1324	12601
2	1324	7706
3	1324	18508
4	1324	19195
5	1324	12280
6	1324	7530
7	1324	18436
8	1324	18600

The maximum possible combinations of wind and PV are illustrated in Figure 5.9, demonstrating the ability to supply planned energy while minimizing load shedding, VRE curtailment and unmet export for each expansion scenario. Additionally, yellow and pink dots represent the IVR and NGEP scenarios, respectively, in addition to the possible wind and PV combinations.

Furthermore, the analysis examined the effects of reserve on the integration of variable renewable energy (VRE) and curtailment, as well as the impact on unmet exports. In Figure 5.9, it is evident that reserve plays a significant role in enhancing the integration capacity of VRE. When reserve is taken into account, the capacity of VRE increases. This increase is due to a portion of hydropower being allocated for reserve, allowing VRE to meet the demand and expected export. However, during periods of low weather conditions with low hydropower and a small capacity of wind power, the integration of VRE is reduced compared to scenarios without reserve. This reduction is due to insufficient hydropower to provide reserve during the daytime and meet the

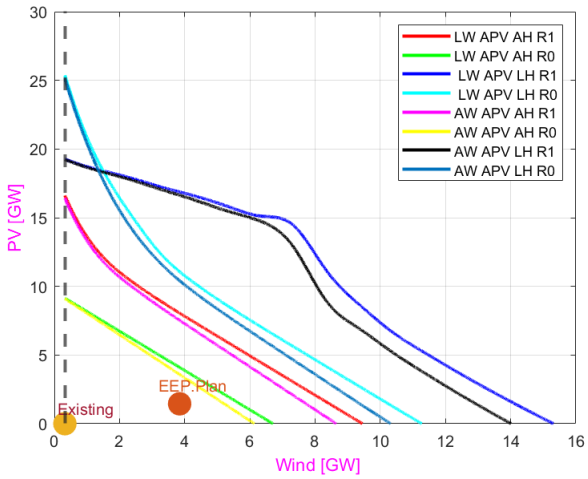

Figure 5.9: Possible combination of wind and PV.

demand during the nighttime. On the other hand, as the penetration of wind power increases, the integration capacity of VRE also increases when a reserve is considered compared to scenarios without a reserve in all cases. This is because wind power is available throughout the day and night, complementing the availability of hydropower. Consequently, with reserve, the maximum integration capacity of photovoltaic (PV) with existing wind power is 19 GW, while the maximum integration capacity of wind power without PV is 15 GW. It is important to note that the integration capacity cannot exceed these values due to the limited availability of hydropower for reserve and meeting the demand. In contrast, without reserve, the system can integrate 25 GW of PV with existing wind power and 11 GW of wind power without PV.

Moreover, the inadequate hydropower supply for reserve provision is the main cause of the irregular shape of the black and blue color lines depicted in Figure 5.9 which limits PV integration and this leads to an increase in unmet export. Consequently, in those lines, when wind power begins to increase, PV resists decreasing rapidly, unlike the scenario without reserve, which is due to the insufficient hydropower supply.

There are no technical constraints when it comes to incorporating wind power into the grid. In every scenario where a reserve is present, the capacity of wind power increases compared to scenarios without a reserve. As a result, the maximum amount of wind power that can be integrated is 15 GW, without any need for domestic load shedding or unmet export and with minimal curtailment of variable renewable energy (VRE). This is due to the complementary nature of wind power during both daytime and nighttime, which works in cooperation with hydropower to meet

the demand. Therefore, when considering reserve capacity, the integration of wind power without photovoltaic (PV) energy increases and is greater than the scenario without reserve.

Furthermore, based on the information presented in Figure 5.9, a comparison of the three scenarios (IVR, NGEP, and ES) reveals that the Ethiopian power system still has the potential to incorporate additional VRE during the ES cases. It is evident that the VRE capacity mix outlined in the EEP master plan for the year 2030 (indicated by the pink point representing NGEP) falls significantly short of the simulation result. Consequently, the simulation outcome indicates that, from a technical point of view, Ethiopia can integrate a greater VRE capacity than what was initially projected in the EEP generation expansion plan. This higher integration of VRE could be increased mainly by exploiting the interconnections with neighboring countries willing to buy cheaper energy from Ethiopia.

Figure 5.10 illustrates the curtailment of VRE in all assumed ES cases. Significant curtailments are observed when there is no reserve consideration, as a result of the high penetration of VRE to meet the domestic demand and export. This increased integration of VRE is due to a low hydro scenario, leading to excess production of VRE and consequently higher curtailment. However, as the penetration of photovoltaic (PV) decreases and wind penetration increases, the curtailment of VRE gradually decreases until it approaches zero.

Figure 5.11 shows the unmet export. The scenarios of LW-APV-LH-R1 and AW-APV-LH-R1 exhibit higher unmet export. This is primarily attributed to limited water availability, which restricts the maximum integration of PV. On the other hand, scenarios LW-APV-AH-R1 and AW-APV-AH-R1 demonstrate a smaller unmet export. The increase in hydropower from a low to an average weather year significantly reduces the unmet export.

The findings of our study are compared to three previous research works conducted in Ethiopia. These works include Luca Marena [45], Sebastian Ste [114], and A.A. Solomon [115]. Despite variations in research methodologies and scenarios among these studies, they can serve as a reference point for our own study's results.

Furthermore, none of the aforementioned papers took into account the possibility of future hydropower as necessarily a done deal, whereas the present paper does (only the VRE amount is optimized, whereas the future hydropower is forced into the model).

Figure 5.12 and 5.13 display the energy production from each resources during the scenarios of LW-APV-AH-R1. The figures clearly illustrate variables such as the curtailment of VRE, hy-

dropower reservoir management, and ramping capability of hydropower. In the case of high PV and low wind capacity (refer Figure 5.12), there is a significant amount of curtailment due to PV only being available in the daytime. Additionally, as depicted in the same figure, hydropower adjusts its operation to match the VRE production and manages the reservoir by shifting its operation from daytime to nighttime. On the other hand, Figure 5.13 showcases the production when high wind is integrated. It is evident from this figure that there is no curtailment as wind is available throughout both day and night.

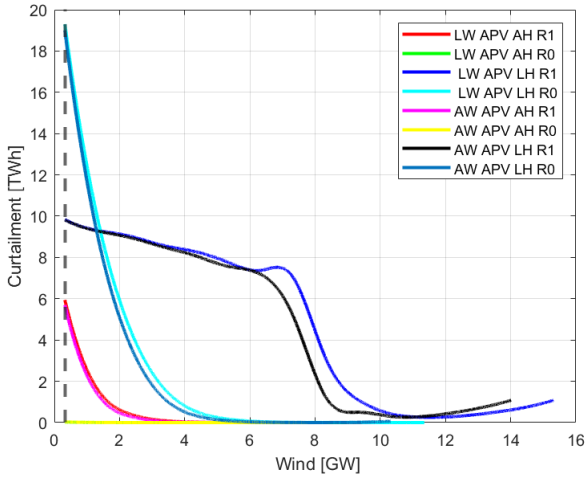

Figure 5.10: Wind and PV curtailment during each scenario.

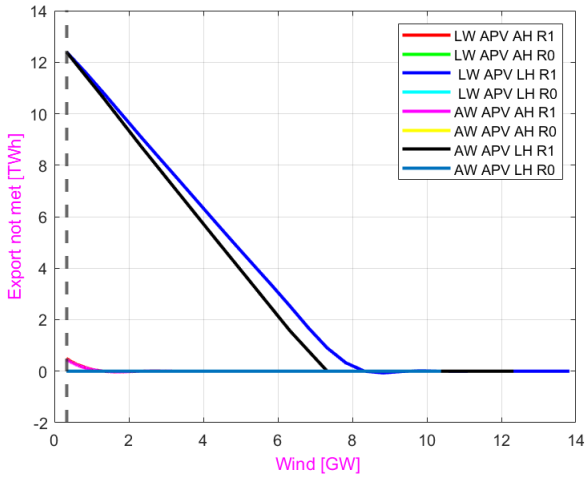

Figure 5.11: Load shedding for different scenarios.

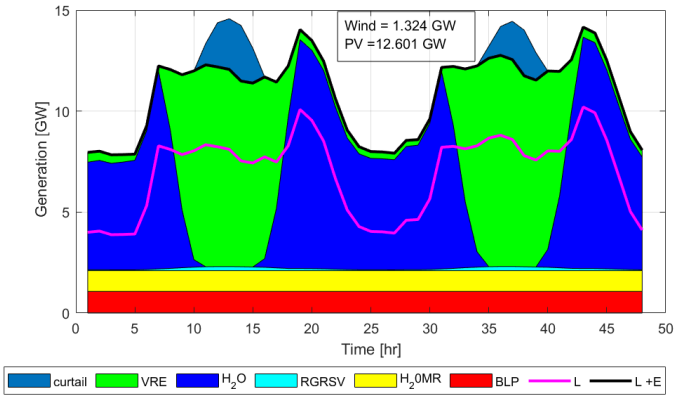

Figure 5.12: Production of electricity from each resources during the scenarios of LW-APV-AH-R1.

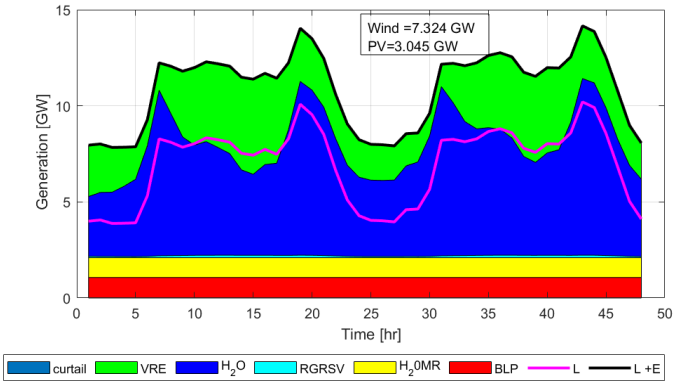

Figure 5.13: Production of electricity from each technology during the scenarios of LW-APV-AH-R1.

Chapter 6

Analysis of Wind Power Curtailment and System Balancing Challenges

6.1 Introduction

It is crucial for any power grid to ensure that the gross production and consumption of electricity are always equal [130]. Achieving a perfect balance between generation and demand , while accounting for losses, is naturally challenging [131]. One of the most significant challenges that electrical systems face is the abrupt disconnection of a large power plant and loss of a transmission line [20, 21]. This scenario brings a great problem to stability of the grid. Furthermore, the integration of VREs into grid adds another layer of complexity to maintaining equilibrium [132, 133]. Researchers have identified three main balancing challenges: low generation of wind and solar power coupled with huge electricity demand, managing continuous balancing, and high generation of wind and solar power with low electricity consumption.

6.2 Literature review

Balancing the electricity system is becoming increasingly difficult as the amount of electricity generated by VREs increases. If significantly more electricity is available from fluctuating renewable sources than the power grid can handle, this poses challenges for grid operators. Under these circumstances, extra electricity can be stored, exported to neighboring countries, or curtailed meaning production falls below available capacity [134].

System balancing issues include transmission line bottlenecks, reserve requirements, minimum production requirements of conventional power plants, the limited flexibility of the power system, and the level of integration of VREs, which are aggravating factors that can lead to curtailment. However, the degree of curtailment and difficulty of system balancing varied across systems based on the features and operating policies of the power grid.

Curtailment in Sweden was projected to be less than 1.7% for a 33 GW wind penetration and less than 0.3% for a 26 GW wind scenario in 2025 [135]. The thermal power plant's limited flexibility and the transmission line's reduced capacity as a result of failures were the causes of the curtailment.

Operators of the Ethiopian electricity system, which relies heavily on hydropower (exceeding 94% of total capacity in the year 2020), have not had to worry about wind power curtailment so far because of the relatively low penetration level. But the country's wind power capacity is increasing so quickly that future curtailments will be agitated. By the planning year 2030, Ethiopian Electric Power plans to add 1450 MW of solar and 3844 MW of wind power to its current plants.

The necessity of curtailing renewable production in future power grids has been the subject of many researches. Article [136] has conducted research on the amount of wind that the Irish power grid would curtail in 2020. Another article [137] examined the curtailment of wind power in China in 2016 and found a significant annual curtailment of about 49.7 TWh.

Significant penetrations of VREs on the grids are resulting in curtailment, according to research conducted by Task 25 of the IEA wind [138]. The amount of curtailment, how it happens, why it happens, and steps being taken to lessen curtailment have all been covered in this study.

Article [139] analyzes the relationship between curtailing renewable energy and operational flexibility through the use of a unit commitment and economic dispatch model that incorporates system constraints for a power system as well as operational features of conventional power plants in Great Britain. The outcome illustrates that as wind deployment increases, an increase in curtailment is largely anticipated. According to the report, the curtailment amounts to 17% of the yearly available variable renewable power production.

Numerous works of literature have also been written about the balancing of wind power. Demand-side management has been studied in Article [140] to balance wind power under high wind penetration. Different studies [141, 142, 143, 144, 145] have examined wind power balancing for different countries using various techniques.

Nevertheless, no single study of this kind has been conducted for the Ethiopian electricity system. Most likely, this is because integrated wind power capacity is still quite small. According to the national electrification program document, even though there is significant potential of energy sources, especially wind power [1], only about 40% of the population—with an annual per capita consumption of 143 kWh—is connected to the grid in 2022 G.C. Ethiopian government (GoE) has set an ambitious goal to raise energy generation, especially from renewable resources, to increase per capita energy consumption and access to electricity [35]. Consequently, the country has set an ambitious goal of enhancing the integration of renewable energy resources in the upcoming years. As a consequence, it is more essential and desirable to conduct a research on the anticipated future system balancing difficulty and wind power curtailment in Ethiopian power systems.

To achieve this, an hourly dispatch model was developed for Ethiopian electricity grid. It takes into account the average hourly generation of different generators. This means that the model incorporates the hourly production capacities of several kinds of generators and employs a cascaded hydropower. As already described in chapter five, a meteorological model known as (SAM) [127] was used to obtain time series data for solar power output, and ERA-5 and currently operating wind farms were used to obtain wind power production time series.

Wind power curtailment in this work happens when hydropower production reaches its minimum production limits, the available transmission capacity for exporting the extra wind power has been fully used up, and the reserve requirement increases. Configuring these parameters together give the magnitude of system balancing and wind power curtailment challenge. Consequently, the model is employed to evaluate the difficulty of system balancing and the degree of wind curtailment under the case of a future power grid, taking into account the anticipated changes in wind power, load, hydropower production, and transmission capacity until the year 2030.

Thus, the influence of various system configurations and wind power penetration levels on wind power curtailment and system balancing challenges are examined considering a total of twenty-four scenarios. The results show that increasing some transmission capacity and, if practical, reducing scheduled irrigation are the most crucial steps toward reducing curtailment and system balancing challenges; regulating reserve requirements has less effect.

As a result, the study has brought the following contribution to the researcher. We have developed a dispatch model to simulate the Ethiopian electric grid operation, which has never been done before. Moreover, we used the model to analyze the wind power curtailment and system balanc-

ing challenges in future situations for the Ethiopian electric grid, taking into account transmission capacity, regulation reserve needs, and minimum hydropower production. This can also be seen in (Section 6.5).

6.3 Methodology

The work have started with data collection , model formulation and finally simulating the result which will be discussed in the subsequent sections.

Data collection

The simulation has been done in Ethiopian electric grid, taking into account the capacity of the transmission line to neighboring countries. The optimization problem was solved by implementing the model in Julia using the Gurobi 9.14 solver. A 3.6 GHz Intel Core i7-4790 CPU with 32GB of RAM was able to solve the model for each scenario for an entire year in about 20 minutes.

The entire information related to data used in this chapter was taken from Chapter 5 and Section 3.3 provides a brief explanation of it. The production capacities of each technology, load statistics, and solar, and wind data of the Ethiopian power system are all provided in the same section.

Model Formulation

To analyze the VRE curtailment and system balancing challenges for the planning year, a model has been developed for the Ethiopian electric grid. There are two main elements of the model: the objective function and the constraints. Below is a quick explanation of each element.

Objective function

The system operator might be forced to curtail some of the available VRE production because of the low system flexibility, which will hinder the system's capacity to integrate the necessary level of VRE. On the other side, the system operator might have to reduce some of the system load to maintain the supply-demand balance if the available VRE production drops below planned levels and the system lacks flexible generating units to quickly recover this VRE output reduction.

The penalty costs of curtailed system load, given by the cost of load shedding (c_{ns}) times the amount load shed ($\Lambda_{a,t}$) for each day a of the year and during each time step t of the day, and to enhance the flexibility of the system, the objective function has been supplemented with the income from selling energy to neighboring countries, which is computed by multiplying the cost of selling energy c_{exp} by the quantity of energy exported hourly over each line ($exp_{l,a,t}$). As a result, equation (6.1) provides an objective function to be optimized. Additionally, for the purpose of clarification, subscripts w, v, a, t, g, i, and l stand for wind power, solar power, every day of the year, time step in an hour, must run power plant, hydroelectric power plant, and transmission line capacity, respectively. Consequently, equation (6.1) represents the system cost or objective function that needs to be minimized.

$$min \sum_{a \in \mathscr{A}} \sum_{t \in \mathscr{T}} \left((c_{ns} \times \Lambda_{a,t}) - \sum_{l \in \mathscr{L}} (c_{exp} \times exp_{l,a,t}) \right) \tag{6.1}$$

The quantities in order are therefore the cost of load shedding, and the net income from exports of energy. All power quantities are in MWh because the model uses hourly averages.

The aforementioned objective function is subjected to the following constraints: power balance, hydropower, VRE production, nonserved load, reserve requirement, transmission line, and must run. The descriptions of each of these constraints are provided below.

Wind power generation cost

The cost of wind power production per hour (c_w) times the amount of wind power production ($p_{w,a,t}$) during each day of the year and time step of the day and it is given by equation (6.2). Note that the low cost of wind power is merely placed on the model to encourage curtailing wind power over solar or hydropower as necessary. As a result, curtailing wind power will always happen before curtailing solar power or spilling water.

$$c_w \times p_{w,a,t} \tag{6.2}$$

Power balance constraint

The model's power balance constraint makes sure that the electricity demand is always met throughout the year. Equation (6.3) shows that the sum of power production $p_{w,a,t}$ from wind power ($\mathscr{W}$), $p_{v,a,t}$ from solar power ($\mathscr{PV}$), $p_{g,a,t}$ from must run resources ($\mathscr{MR}$), and $p_{i,a,t}$ from hydropower resources ($\mathscr{H}$) for each day of the year and at each time step of the day the load shedding ($\Lambda_{a,t}$) during each day of the year and each time step t in an hour minus the export ($exp_{l,a,t}$) must be strictly equal to electricity demand ($D_{a,t}$). Concurrently, curtailment of demand ($\Lambda_{a,t}$) lowers the total demand. Lastly, the demand balance equation takes into account power flows ($exp_{l,a,t}$), on each line out of Ethiopia.

$$p_{w,a,t} + p_{v,a,t} + \sum_{g \in \mathscr{G}} p_{g,a,t} + \sum_{i \in \mathscr{H}} p_{i,a,t} + \Lambda_{a,t} - \sum_{l \in \mathscr{L}} exp_{l,a,t} = D_{a,t} \qquad \forall a \in \mathscr{A}, t \in \mathscr{T} \tag{6.3}$$

Consequently, the quantities in order are wind, photovoltaic, must-run, hydropower, and potential load shedding. The last term indicates the potential exports to neighboring countries.

Variable renewable energy (VRE) constraint

The operational constraints associated with wind ($\mathscr{W}$) and solar ($\mathscr{PV}$) resources are the time-dependent hourly capacity factor (ρ^{max}), expressed as per unit, and the total available capacity (cap^{tot}), and these are given by the equations: (6.4 - 6.5) for PV and wind, respectively. According to this equation, the electricity production ($p_{v,a,t}$) from photovoltaics and ($p_{w,a,t}$) from wind energy must be less than or equal to the maximum electricity production capacity of the resources. The inequality condition shows that production can be curtailed for reasons of flexibility.

$$p_{v,a,t} \leq \rho^{max}_{v,a,t} \times cap^{tot}_{v} \qquad \forall v \in \mathscr{PV}, \forall a \in \mathscr{A}, t \in \mathscr{T} \tag{6.4}$$

$$p_{w,a,t} \leq \rho^{max}_{w,a,t} \times cap^{tot}_{w} \qquad \forall w \in \mathscr{W}, \forall a \in \mathscr{A}, t \in \mathscr{T} \tag{6.5}$$

On the other hand the equations can be modified as the power production ($p_{v,a,t}$) from PV or ($p_{w,a,t}$) from wind plus the curtailment of energy due to over production should be equal to the maximum

power production capacity of wind and solar as given by equations (6.6 - 6.7) respectively.

$$p_{w,a,t} + w^{curt}_{a,t} = \rho^{max}_{w,a,t} \times cap^{tot}_{w} \qquad \forall w \in \mathscr{W}, \forall a \in \mathscr{A}, t \in \mathscr{T} \tag{6.6}$$

$$p_{v,a,t} + pv^{curt}_{a,t} = \rho^{max}_{v,a,t} \times cap^{tot}_{v} \qquad \forall v \in \mathscr{PV}, \forall a \in \mathscr{A}, t \in \mathscr{T} \tag{6.7}$$

Hydro constraints

It enforces that energy level of the hydropower reservoir i during the day a in time step t ($m_{i,a,t}$) is defined as the sum of the reservoir level in the previous time step, minus the amount of electricity generated ($p_{i,a,t}$), minus any spillage ($s_{i,a,t}$), plus the hourly inflows into the reservoir ($\rho^{max}_{i,a,t} \times cap^{tot}_{i}$) plus the sum of the power discharged ($p_{k,a,t-\tau^q_i}$), from all upstream power plants k during a time ($t - \tau^q_i$) plus the sum of spilled energy ($s_{k,a,t-\tau^s_i}$), from all upstream power plants k during the time ($t - \tau^s_i$) plus annual average energy inflow per hour (Q^{avg}_k) from all upstream power plants k when the time to reach downstream power plant (τ^q_i) is greater than the planning time t. Thus, the constraint is given by equation (6.8) and it indicates the energy balance of reservoir hydropower. The modified hydropower plant modeling can be seen from [128].

In fact, equation (6.8) depicts a realistic way to model the energy flow delays between successive power plants. τ^q_i is assumed to be a constant time delay for discharge from each upstream power plant k to arrive at the downstream power plant i. The quantity τ^q_i can be expressed in hours (h^q_i) and minutes (mn^q_i). Equation (6.9) then yields the delayed upstream inflow as a weighted average of the discharge between the hours (h^q_i and $h^q_i + 1$), as discussed in [129]. The same expression can be used for the spillage delays.

Electricity production ($p_{i,a,t}$) from hydro resources is constrained to always be above a minimum output parameter (ρ^{min}_i) times the total installed capacity (cap^{tot}_i) to represent operational constraints related to minimum stream flows or other demands for water from hydro reservoirs and it is given by equation (6.10). Equation (6.11) shows that the total annual electricity production from each hydropower plant should be less or equal to the maximum energy level (m^{max}_i) of each reservoir. Equation (6.12) brings an additional constraint that the total stored energy in each time step is less than or equal to the maximum. Equation (6.13) depicts the end reservoir content constraint. It represents that at the end of planning period T, reservoir content m_T should be equal to end reservoir content m^{end}. Equation (6.14) shows the spillage constraint. It represents that the

spillage $s_{i,a,t}$ for each hydropower plant i, during each day a of the year and at each time step t of the day must be larger than or equal to zero.

$$m_{i,a,t} = m_{i,a,t-1} - h_{i,a,t} - s_{i,a,t} + v_{i,a,t} + \sum_{k \in F_i^{\mathscr{Q}}} h_{k,a,t-\tau_i^q} + \sum_{k \in F_i^{\mathscr{S}}} s_{k,a,t-\tau_i^s} - \sum_{k \in F_i^{\mathscr{Q}}} \rho_k^{min} \times cap_k^{total} + \sum_{k \in F_i^{\mathscr{Q}}} Q_k^{avg} \Big|_{t \leq \tau_i^q} + \sum_{k \in F_i^{\mathscr{Q}}} \frac{60 - mn_k^q}{60} Q_k^{avg} \Big|_{t \leq \tau_i^q + 1} \quad \forall i \in \mathscr{H}, a \in \mathscr{A}, t \in \mathscr{T} \tag{6.8}$$

$$p_{k,a,t-\tau_i^q} = \frac{mn_i^q}{60} p_{k,a,t-h_i^q} + \frac{60 - mn_i^q}{60} p_{k,a,t-p_i^q-1} \qquad \forall k \in \mathscr{F}^{\mathscr{Q}}, a \in \mathscr{A}, t \in \mathscr{T} \tag{6.9}$$

$$\rho_i^{min} \times cap_i^{tot} \leq p_{i,a,t} \leq cap_i^{tot} \qquad \forall i \in \mathscr{H}, a \in \mathscr{A}, t \in \mathscr{T} \tag{6.10}$$

$$\sum_{a \in \mathscr{A}} \sum_{t \in \mathscr{T}} p_{i,a,t} \leq m_i^{max} \qquad \forall i \in \mathscr{H} \tag{6.11}$$

$$0 \leq m_{i,a,t} \leq m_i^{max} \qquad \forall i \in \mathscr{H}, a \in \mathscr{A}, t \in \mathscr{T} \tag{6.12}$$

$$m_T = m^{end} \tag{6.13}$$

$$0 \leq s_{i,a,t} \qquad \forall i \in \mathscr{H}, a \in \mathscr{A}, t \in \mathscr{T} \tag{6.14}$$

The constraints given by equations (6.15) and (6.16) enforce hourly changes in power output (ramps up and ramps down respectively) to be less than the maximum ramp rates (δ_i^{up} and δ_i^{down}) in per unit terms times the total installed capacity of technology i (cap_i^{tot}).

$$p_{i,a,t} - p_{i,a,t-1} \leq \delta_i^{up} \times cap_i^{tot} \qquad \forall i \in \mathscr{H}, a \in \mathscr{A}, t \in \mathscr{T} \tag{6.15}$$

$$p_{i,a,t-1} - p_{i,a,t} \leq \delta_i^{down} \times cap_i^{tot} \quad \forall i \in \mathscr{H}, t \in \mathscr{T} \quad (6.16)$$

Non-served load

Equation (6.17) shows an additional constraint that enforces the total demand curtailed $\Lambda_{a,t}$ during during each day of the year and each time step of the day cannot exceed available demand $D_{a,t}$.

$$0 \leq \Lambda_{a,t} \leq D_{a,t} \quad \forall a \in \mathscr{A}, t \in \mathscr{T} \quad (6.17)$$

Frequency regulation requirements

Total requirements for frequency regulation $f_{i,a,t}$ also known as primary reserves during day of a year and in each time step of the day are specified as fractions of hourly demand (to reflect demand forecast errors) and variable renewable availability in the time step (to reflect wind and solar forecast errors) and it is given by equation (6.18).

$$\sum_{i \in \mathscr{H}} f_{i,a,t} \geq x_{reg}^{load} \times D_{a,t} + x_{reg}^{vre} \times \rho_{v,a,t}^{max} \times cap_v^{\text{tot}} + x_{reg}^{vre} \times \rho_{w,a,t}^{max} \times cap_w^{\text{tot}} \ \forall a \in \mathscr{A}, t \in \mathscr{T} \quad (6.18)$$

Where $D_{a,t}$ is the forecasted electricity demand during day a at time t; $\rho_{v,a,t}^{max}$ is the forecasted capacity factor for PV during each day of the year a in time step t; $\rho_{w,a,t}^{max}$ is the forecasted capacity factor for wind during each day of the year a in time step t; cap^{tot} is the total installed capacity of wind or PV; and x_{reg}^{load} and x_{reg}^{vre} are parameters specifying the required frequency regulation as a percentage of forecasted demand and variable renewable production (wind or PV) respectively.

Operating reserve requirements

Total requirements for operating or balancing reserves $r_{i,a,t}$ in the upward direction during each day of the year a in each time step t are specified as fractions of time step demand (to reflect demand forecast errors) and variable renewable availability in the time step (to reflect wind and solar forecast errors) and it is given by equation (6.19).

$$\sum_{i \in \mathscr{H},} r_{i,a,t} \geq x_{blc}^{load} \times D_{a,t} + x_{blc}^{vre} \times \rho_{v,a,t}^{max} \times cap_v^{\text{tot}} + x_{blc}^{vre} \times \rho_{w,a,t}^{max} \times cap_w^{\text{tot}} \ \forall a \in \mathscr{A}, t \in \mathscr{T} \quad (6.19)$$

Where $D_{a,t}$ is the forecasted electricity demand during day a at time t ; $\rho^{max}_{v,a,t}$ is the forecasted capacity factor for PV during each day of the year a in time step t; $\rho^{max}_{w,a,t}$ is the forecasted capacity factor for wind during each day of the year a in time step t; cap^{tot} is the total installed capacity of wind or PV; and x^{load}_{blc} and x^{vre}_{blc} are parameters specifying the required operating reserve requirements as a percentage of forecasted demand and variable renewable production (wind or PV) respectively.

Equation (6.20) defines the modified constraints on power production capacity when modeling operating reserves. The modifications when operating reserves are modeled regarding maximum power production limits and it is modified to account for procuring some of the available capacity for frequency regulation ($f_{i,a,t}$) and upward operating (or balancing) reserves ($r_{i,a,t}$). It indicates the sum of power production $p_{i,a,t}$, operating reserve $r_{i,a,t}$ and frequency regulation reserve $f_{i,a,t}$ should be less than the total capacity cap^{tot}_{i} of the power plant dedicated for reserve.

$$p_{i,a,t} + r_{i,a,t} + f_{i,a,t} \leq cap^{tot}_{i} \qquad \forall i \in \mathscr{H}, a \in \mathscr{A}, t \in \mathscr{T} \quad (6.20)$$

The modified constraint regarding the amount of downward frequency regulation reserves is shown in equation (6.21). It shows the difference between the power generation $p_{i,a,t}$ and frequency regulation reserve $f_{i,a,t}$ cannot be less than the minimum power output which is the minimum capacity factor ρ^{min}_{i} times total installed capacity cap^{tot}_{g}.

$$p_{i,a,t} - f_{i,a,t} \geq \rho^{min}_{i} \times cap^{tot}_{i} \qquad \forall i \in \mathscr{H}, a \in \mathscr{A}, t \in \mathscr{T} \quad (6.21)$$

Transmission line constraint

Equation (6.22) indicates that the power flow constraint from Ethiopia to neighboring countries. The equation represents that the power flow, $exp_{l,a,t}$, over the line l during day of the year a, in each time step t should be less than or equal to the maximum capacity of the transmission line exp^{max}_{l}.

$$exp_{l,a,t} \leq exp^{max}_{l} \qquad \forall l \in \mathscr{L}, a \in \mathscr{A}, t \in \mathscr{T} \quad (6.22)$$

Must run constraint

For must-run resources ($g \in \mathscr{MR}$) output during each day a of the year, in each time period t must exactly equal to the available capacity factor, $\rho^{max}_{g,a,t}$, times the installed capacity, cap^{tot}_{g}, not allowing for curtailment and it is given by equation (6.23). These resources are also not eligible for contributing to frequency regulation or operating reserve requirements.

$$p_{g,a,t} = \rho^{max}_{g,a,t} \times cap^{tot}_{g} \qquad \forall g \in \mathscr{G}, a \in \mathscr{A}, t \in \mathscr{T} \quad (6.23)$$

Summary of the problem

The summary of the optimization problem is depicted by:

minimize (6.1), subjected to:

Constraint for power balance by equation (6.3)

VRE constraints by equations (6.4 - 6.7)

Hydro power constraints by equations (6.8 - 6.16)

Nonserved load constraint by equation (6.17)

Reserve requirement constraints by equations(6.18 - 6.21)

Transmission line constraint by equation (6.22)

Must run constraint by equation (6.23)

6.4 Scenario setup and key assumptions

Scenarios setup

To investigate the influence of operational constraints on curtailment of wind power and issue of system balancing with varying wind levels, different scenarios were considered. Table 6.1 shows the various configurations of wind penetration levels and operational constraints which were set up as scenarios. The table includes 24 scenarios consisting of three levels of wind penetration and operational constraints such as transmission capacity to neighboring countries, minimum daily hydropower production, and regulation reserve requirement. For instance, the model configuration W5000-MP0-R1-TL0 in the table corresponds to scenario 9. Below you will find an explanation of the model configurations.

1. Wind power scenario

    - W3844: 3844 MW scenario (14.5% production share).
    - W5000: 5000 MW scenario (17.8% production share).
    - W8000: 8000 MW scenario (25.2% production share).

2. Minimum power production (see section 6.4)

    - MP0: Planned minimum power production (24000 MWh/day).
    - MP1: Increased minimum power production (129200 MWh/day) .

3. Net transmission line capacity (see section 6.4)

    - TL0: The full nominal NTC capacity is used.
    - TL1: Reduced transmission line capacity is used.

4. Regulation reserve (see section 6.4)

    - R0: Planned regulating reserve is used.
    - R1: Increased regulating reserve is used.

Table 6.1: Scenario table for wind power curtailment analysis.

Wind scenario		W3844		W5000		W8000	
Minimum power		MP0	MP1	MP0	MP1	MP0	MP1
Transmission capacity	Regulating reserve						
TL0	R0	1	2	3	4	5	6
	R1	7	8	9	10	11	12
TL1	R0	13	14	15	16	17	18
	R1	19	20	21	22	23	24

Key assumptions

The case study was undertaken considering the significant changes expected in Ethiopia's power system by the year 2030, using data from the year 2020 as a starting point. These changes encompass an increment in hydropower production, an increment in demand, an increment in must run

production, and an increment in transmission capacity from Ethiopia to neighboring countries. The following sections also present and examine the assumptions underlying these and other aspects of the case study.

Minimum production levels

To minimize the challenge of balancing and wind power curtailment, the production of other power plants could be reduced to a minimum, based on the constraints imposed on them during wind and photovoltaic production. In this model, biomass and geothermal power plants are treated as must-run power plants, and part of the hydropower plants are also treated as must-run power plants for minimum production because of the requirement for irrigation and other stability issues. Irrigation was considered as a type of load in the EEP Master Plan and is anticipated to reach 3 TWh/year in 2030. This minimum amount of hydropower that EEP plans is estimated to be around 24000 MWh per day. We have assumed that the minimum production is increased to 129200 MWh per day to see how this minimum production influences wind power curtailment and system balancing. This minimum flow is the water that passes through a turbine, not overflows.

Transmission line capacity assumption

Table 5.5 shows that significant changes in transmission capacity from Ethiopia to neighboring countries are expected by 2030. The total transmission capacity in the year 2030 will be 4100 MW [1]. This corresponds to the nominal value of the total transmission capacity. However, the nominal value of the transmission line may not be fully utilized due to scheduled maintenance or due to stability issues such as voltage and rotor angle stability. To investigate the impact on wind curtailment and system balancing, we have assumed an average hourly line interruption of 5% in our case study.

Annual energy production and assumption

As per the report from the EEP master plan, the annual domestic demand is 58.5 TWh, and assuming that the assumed transmission line capacity is fully utilized, the maximum annual export is equivalent to 35,916 TWh. The EEP Master Plan states that the average annual hydropower inflow is 64.67 TWh, which is obtained from a multi-year simulation of each hydroelectric power plant,

while the average annual energy production from must-run power plants for the year 2030 is 9.37 TWh.

Reserve assumptions

Table 6.2 depicts the assumed various types of reserve needed in this investigation, together with their minimum level. It also shows the parameters for the penalty costs for load shedding. The same table also assumes the minimum level of balancing and regulating reserve requirements. In this case study, we have increased the regulating reserve for VREs from 1% to 3% to observe how this affects system balancing and curtailment of wind energy. The required reserves from each technology are shown in Table 6.3. A table also shows the ramp rate of each technology.

Table 6.2: Required reserves and the cost of load shedding.

Type of requirement	**Minimum level**	**Penalty cost**
Load shedding	-	2000 $/MWh
Cost of selling energy	-	2000 $/MWh
Regulating reserve	1% Load + 1% VRE	binding
Balancing reserve	5% Load + 15% VRE	binding

Table 6.3: Reserve contribution of the production resources.

Technology	**Contribution to regulating reserves[% of max output]**	**Contribution to balancing reserves[% of max output]**	**Ramp rate [% of maximum output]**
Hydropower	5	20	100
Wind	0	0	-
Solar	0	0	-
Must run	0	0	-

Model validation

By calculating the difference between the model result and the observed values for the year 2020, the model was validated against historical data. Total hydropower production in Ethiopia is presented in Figure 6.1 using historical data and a model. Ethiopia's main energy source is hydropower, indicating that there is a strong agreement between the two datasets and the root mean square error (RMSE) is 6%.

The result of the model for energy export to neighboring countries was validated against observations. Figure 6.2 shows the result of the export. The figure shows that the agreement between the model and the measurement data is not good. This is because the historical data was simulated using the result produced based on market or load demand in neighboring countries, while the model was simulated based on transmission capacity.

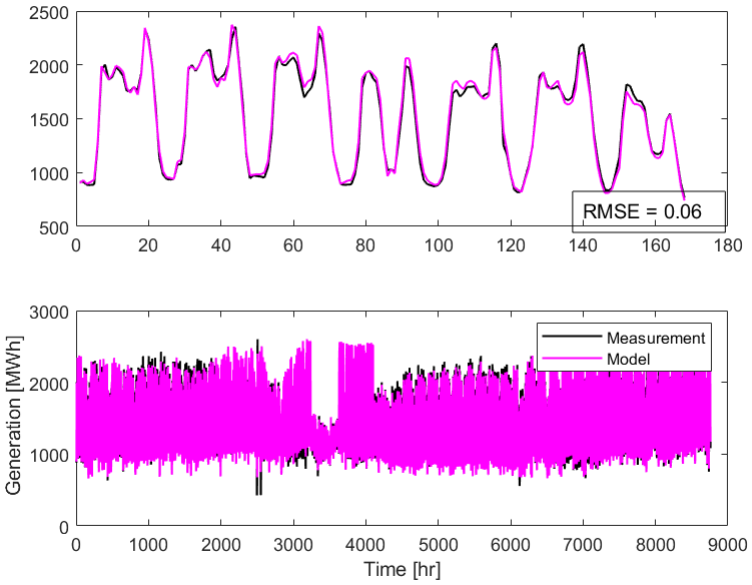

Figure 6.1: A hydropower simulation validation for the year 2020.

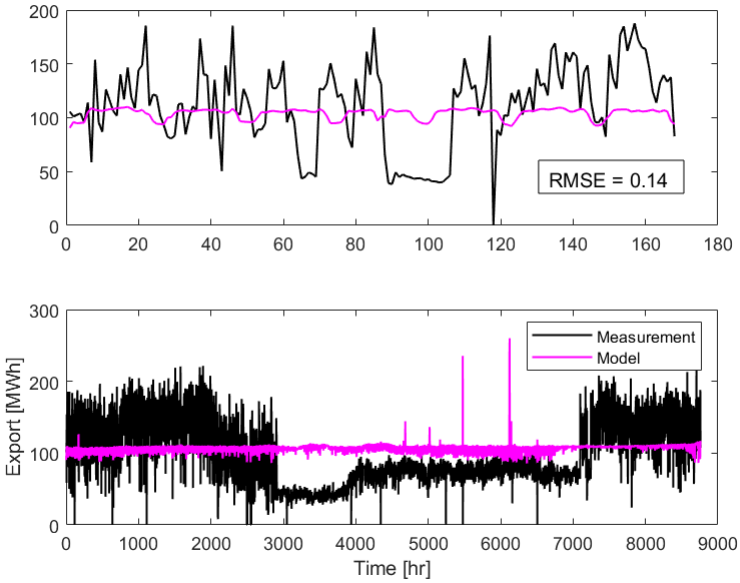

Figure 6.2: The model result is validated using historical data for the year 2020.

6.5 Simulation results and discussion

This part presents and discusses the case study's findings. Different wind penetration levels with specific operational constraints are taken into consideration to examine the maximum curtailment of wind energy and its influence on system balancing.

To better explain the result, the scenario configurations are shortened as code. For instance, the configuration code W5000–MP0-R0-TL1 shows a scenario where there is 5000 MW of wind penetration, 24000 MWh minimum daily hydropower production for irrigation, a regulating reserve of 1%, and 5% decrease in transmission line capacity. MP illustrates how daily minimum hydropower production influences wind power curtailment and system balancing. In addition, R illustrates how the regulating reserve requirement influences the above objective, and TL depicts how transmission line capacity influences system balancing and wind power curtailment.

The wind power curtailment simulation result is presented in Table 6.4 as a percentage of the annual production capacity of wind power for different configurations of operation constraints and wind power scenarios. It implies that an aggregation of wind penetration, net transmission line potential, minimum daily hydropower production, and regulation reserve constraints were implemented to achieve the simulation results. The maximum curtailment is recorded when W8000-MP1-TL1-R1 is configured. The major causes of this maximum curtailment are a decrease in

transmission line capacity and an increasing minimum daily production of hydropower for irrigation.

The curtailment of wind power is significantly influenced by the net transmission capacity. Reducing transmission capacities from their maximum values to their historical values leads to a huge increase in curtailment, regardless of the other configurations. For instance, configuration W8000-MP1-R0-TL0 shows that curtailment rises from 5.76% to 8.12% due to transmission line congestion.

Table 6.4 further suggests that the regulating reserve restrict the curtailment of wind power to some extent. The influence of the regulating reserve is noticed from two directions, namely from up and down-regulation based on the daily minimum electricity production from hydropower. When daily minimum hydropower production is high and at the same time the down-regulation reserve held by the hydropower increases to the maximum then this reserve increases the minimum hydropower production. Increasing the minimum hydropower production in turn decreases the hydropower flexibility finally resulting in an increment of the wind curtailment. On the other way, when minimum daily hydropower production is low, the curtailment decreases because of the up-regulation reserve that has been withheld from hydropower, thus reducing its production capacity and high flexibility of hydropower. Subsequently, reducing the hydropower production capacity allows the use of wind power, thereby reducing the curtailment.

Moreover, the flexibility of hydropower is not significantly influenced by low minimum daily hydropower production. This means that if we increase the regulating reserve, the maximum production capacity of hydropower decreases, allowing more wind power to be generated, which reduces the wind curtailment. The opposite is true for high daily minimum power. To sum up, the regulating reserve has a smaller influence on curtailment than the other two constraints.

Table 6.4: Curtailment of wind power as a percentage of total production.

Wind scenario		W3844		W5000		W8000	
Minimum power		MP0	MP1	MP0	MP1	MP0	MP1
Transmission capacity	Regulating reserve						
TL0	R0	0	0	0	0.36	1.18	5.76
	R1	0	0.03	0	0.62	0	7.51
TL1	R0	0	0.05	0	0.68	2.12	8.12
	R1	0	0.2	0	1.1	1.37	9.8

For the case of MP, the minimum daily hydropower production required for irrigation results in a curtailment as certain portions of the hydroelectric plant are forced to operate as baseload generators. This minimum electricity production reduces the flexibility of hydropower not to accommodate more wind power. According to Table 6.4, during the configuration W8000-MP0-TL1-R1, the curtailment increased from 1.37% to 9.8% as a result of an increment in the daily minimum production of hydropower, irrespective of other constraints. It is therefore possible to conclude that increasing the daily minimum power production significantly reduces hydropower's flexibility, leading to increased curtailment and a greater balancing challenge.

Ultimately, the curtailment is influenced by the amount of wind power in the grid, based on the level of penetration. According to the simulation result shown in Table 6.4, regardless of other operational constraints, the maximum curtailment becomes 0.2%, 1.1%, and 9.8% of wind power annual production capacity for the penetration level of 3844 MW, 5000 MW, and 8000 MW, respectively. These findings suggest that wind power curtailment will increase in line with its penetration level. The largest curtailment of wind power and frequency with which curtailment occurs in a year are also shown on the duration curve given by Figure 6.3.

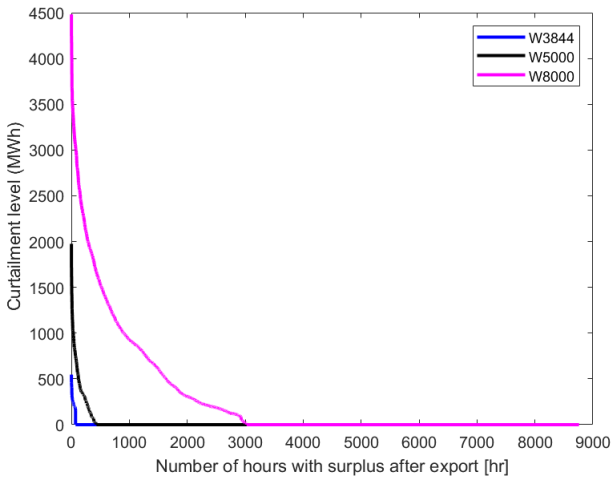

Figure 6.3: Wind power curtailment duration curves for different penetration levels.

This section addresses the challenges of maintaining system balance during periods of high wind and low consumption. The most difficult balancing problem occurs during high curtailment, when consumption is at its lowest and wind is at its peak. The result is shown in Figure 6.4 and is noticeable in the W8000-MP1-TL1-R1 setup. This figure shows an unbalanced situation where extra production occurs over several hours, especially in the first two days. Since such a state is

physically impossible, the problem must be handled by exporting, storing, or curtailing to restore balance in the system. In this study, excess wind energy is curtailed and exported to bring the system into balance. After wind power is curtailed, the result is shown in Figure 6.5 and indicates that the system is balanced.

Figure 6.6 shows that in the case of W8000-MP0-TL1-R1, there is no curtailment of wind power. This is a result of the significant flexibility of hydropower due to the low daily minimum power production constraint

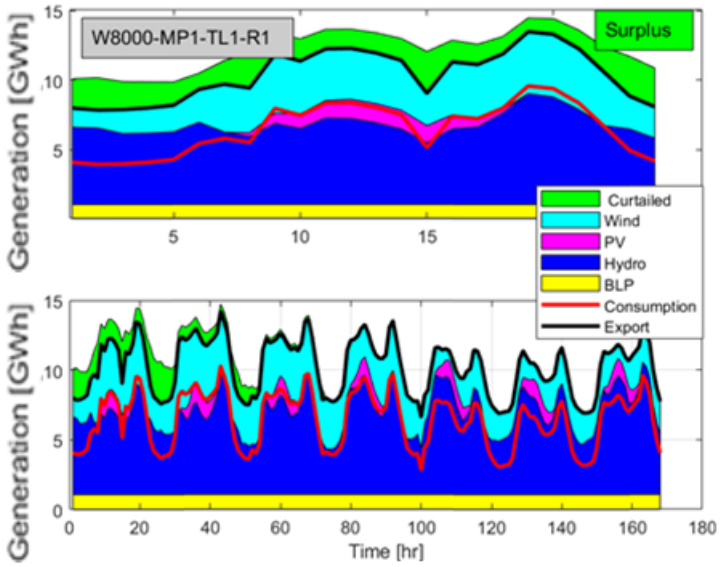

Figure 6.4: Energy generation during third week of January. The bottom figure depicts the full week, while the top figure displays the first day of the week.

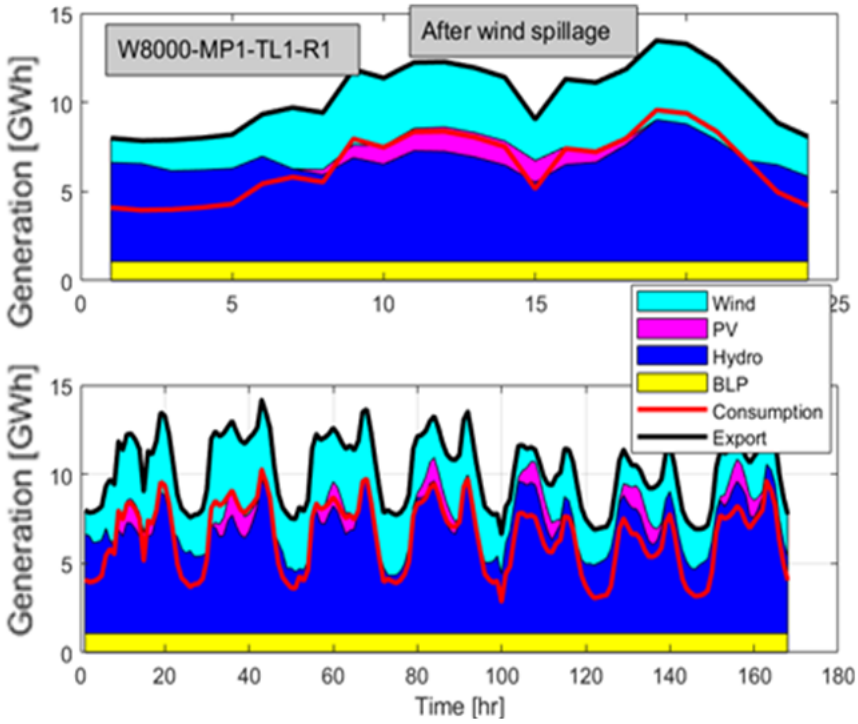

Figure 6.5: Energy generation during third first of January. The first day of the week is represented by the figure at the top, and the entire week is represented by the figure at the bottom.

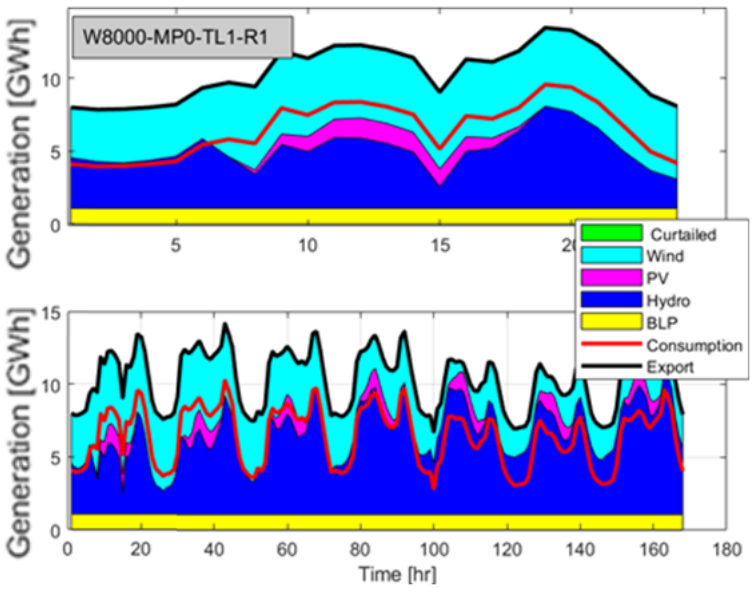

Figure 6.6: Eenergy generation during third week of January. The first day of the week is represented by the figure at the top, and the entire week is represented by the figure at the bottom.

Figure 6.7 shows that in the W8000-MP1-TL1-R1 configuration, there are 3024 hours of curtailment per year, with the total curtailed energy being 2.52 TWh/year. In other words: 9.8% of

all wind energy is lost. Economically, this indicates that wind energy costs increase by 9.8% since all of the production is not used. The energy can also be used for other purposes; For example, charging electric cars, which Ethiopia is planning, or exporting if there are enough transmission lines available.

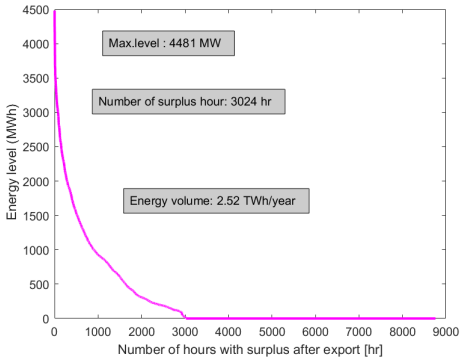

Figure 6.7: The wind curtailment duration curve for the worst case scenario.

Exporting excess energy to neighboring countries is one way to mitigate the problem of wind power curtailment and system balancing. The export duration curve for each wind scenario is given in Figure 6.8. As integration increases, exports also increase, provided there is sufficient transmission capacity, as the figure illustrates.

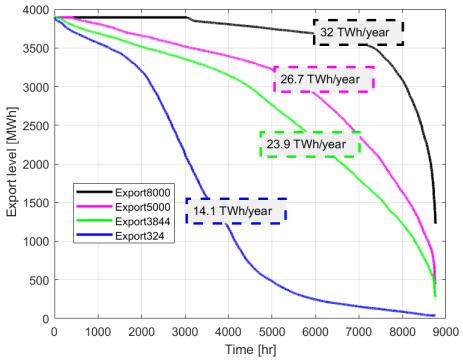

Figure 6.8: Duration curve of energy exporting for every wind penetration.

Chapter 7

Conclusions and Future Work

This chapter brings the main contributions and conclusions of this Ph.D. dissertation and provides suggestions for further research.

7.1 Conclusions

Because of the unpredictable and variable characteristics of VREs, integration of the resources to the grid becomes more difficult as its percentage increases. Consequently, VRE production variability must be assessed using suitable techniques before its integration into the national grid.

To determine how frequently a given production level occurs, several techniques are employed, including the correlation between farms and step change. After evaluating the evaluation result, the maximum up and down variation value was determined. This result indicates that Adama-I, which has a 100% up and down variation, experienced extreme variation. As was mentioned in the introduction, this is a result of the farm's small capacity.

Since there is now very little penetration of wind power in Ethiopia, fluctuation in wind power is not a major issue. The analysis of the geographical distribution of wind farms and their individual variability accompanied by correlation becomes necessary as penetration levels rise. Therefore, it is essential to assess the variability of wind power generation on the grid due to its intermittent nature.

Second, modeling of wind power generation was done for Ethiopia, and measurements were used to assess performance error metrics. No researcher has yet verified the generation output based on measurements, nor has the model created for wind power production using reanalysis

data been tried. Because of this, the study is original and unique in the country.

First, wind speed data were extracted from the ERA5 meteorological model and statistically down-scaled to the location. Statistical down-scaling was utilized to enhance output performance and boost spatial resolution, as ERA5 fails to account for the local impact of location. The RMSE of the simple model without spatial statistical down-scaling is 11.51% for Adama-II and 10.38% for Ashegoda. With spatial statistical downscaling, the results for Ashegoda and Adama-II were enhanced by 7% and 42.4%, respectively. Wake loss was defined as the power loss of the incoming wind speed in each wind sector (between 30^o and 40^o), which increased output power. The outcome demonstrated that while this parameter did not greatly improve the Ashegoda result, it did significantly improve the Adama-II result.

The objective function value for both wind farms was greatly increased by adding the seasonal and diurnal biases from the observed bias. For Adama-II and Ashegoda, the objective function values without bias correction were 6.63% and 8.16%, respectively. After applying the bias adjustment, the RMSE for Ashegoda and Adama-II was 5.29% and 4.54%, respectively. This demonstrates that Ashegoda's and Adama-II's RMSE values dropped by 45% and 28.05%, respectively.

It was also shown that the ERA5 reanalysis wind speed data was a suitable resource for locating favorable wind speed regions. The simulation results demonstrated that, when the ERA5 wind speed was appropriately taken into account, the model nearly replicated the observation.

Thus, the outcome shown that, if wind speed is appropriately considered, the ERA5 reanalysis wind speed data may be utilized to both identify prospective sites for further locations across the nation and simulate the production of wind power.

Moreover, The technical assessment of the integration of variable renewable into the national grid is important due to their variability and uncertainty. In this paper, an existing model was adapted to determine the maximum VRE that can be integrated into the Ethiopian grid with minimum load shedding and VRE curtailment.

The model solved the problem with the help of GenX, a planning tool. The goal of the model is to minimize the cost of load shedding and the cost of curtailing renewable power generation. The problem is subject to hydrological balance, power balance, reserve requirements, power plant flexibility, and VRE constraints. In this way, and considering different scenarios, the maximum integration of VRE for the year 2030 was determined.

Of the eight scenarios, one of the cases was considered the worst-case scenario, where unful-

filled exports and VRE curtailments were very high. This case occurs in a year with little wind, a year with little hydropower (drought), and the model with reserve. During this case, Ethiopia could integrate 19 GW of photovoltaics or 15 GW of wind power to harness the required energy production at a high cost. This maximum integration was limited by the reserve requirement, must-run units, VRE constraint, and hydropower flexibility.

In order to assess the degree of wind power curtailment and identify the system balancing problem for the future Ethiopian power grid with wind penetration levels of 3844 MW, 5000 MW, and 8000 MW, we lastly created and employed an hourly dispatch model for the Ethiopian power grid.

When you take into account the high minimum daily hydropower generation, regulation reserve, and reduced transmission capacity, wind curtailment and system balance become even more difficult. The wind curtailment in this setup is 9.8% of the yearly wind power generation capacity that is available. When weighed against the other limitations, the regulatory reserve requirement has minimal effect on curtailment and the system balancing problem.

The transmission capacity and the minimal daily hydropower generation were the main contributing elements for the curtailment. The flexibility of hydropower is restricted by the minimum daily generation, which exacerbates the difficulty of system balance and causes more curtailment.

Another significant factor influencing wind power curtailment is the grid's wind power capacity. Regardless of other factors, curtailment increases as wind power capacity grows. The system's operation and the cost of wind energy are both impacted by the curtailment. This means that because not all of the wind energy is used, the costs of wind power grow as curtailment increases. In this article, the configuration of W8000-MP1-T1-R1 resulted in a 9.8% rise in wind energy costs.

Therefore, it is necessary to consider the curtailment and balancing difficulties as well as identify the worst-case situations when integrating wind power into a national grid. In this article, the reserve requirement had little effect and the biggest difficulties happened when the daily minimum power was high and transmission capacity to neighboring nations were reduced. Furthermore, with the same amount of curtailment, the cost of wind energy also rises.

7.2 Future work

The following are the suggested future works. Modelling of VRE production time series considering parameter like power curve smoothing for GIS study. Conducting GIS considering financial and power flow constraint. Study about expansion of Ethiopian network to area where good wind and PV resources are available.

Bibliography

[1] , "National Electrification Program 2.0," 2019.

[2] V. Ii, "Ethiopin Electric Power System Development," vol. II, no. February, 2022.

[3] C. Zou, "Energy revolution: From a fossil energy era to a new energy era," *Natural Gas Industry B*, vol. 3, no. 1, pp. 1–11, 2016.

[4] Irena, "International renewable energy agency," 2019.

[5] T. Ackermann, *Wind Power in Power Systems*. 2005.

[6] U.S. Energy Information Administration, "Levelized Cost of New Generation Resources in the Annual Energy Outlook 2022," *US Energy Information Administration*, no. March, pp. 1–26, 2022.

[7] "Net Zero by 2050: A Roadmap for the Global Energy Sector," 2021.

[8] K. Eber and D. Corbus, "Hawaii Solar Integration Study," *NREL Technical Report*, pp. 1–40, 2013.

[9] GE-Energy, *New England Wind Integration Study Executive Summary*. 2010.

[10] E. Corporation, "Eastern Wind Integration and Transmission Study," *Energy*, vol. SR-550-470, no. February, pp. 1–242, 2010.

[11] J. Katz and I. Chernyakhovskiy, "Variable Renewable Energy Grid Integration Studies," *Greening the Grid*, p. 73, 2020.

[12] J. Olauson, *Modelling Wind Power for Grid Integration Studies*. 2016.

[13] GE Energy, "Analysis of Wind Generation Impact on ERCOT Ancillary Services Requirements Electric Reliability Council of Texas," *GE Report for Electric Reliability Council of Texas*, 2008.

[14] S. D. Ahmed, "Grid Integration Challenges of Wind Energy: A Review," *IEEE Access*, vol. 8, pp. 10857–10878, 2020.

[15] A. Gupta, "Integration Challenges of Wind Power on Power System Grid A Review," *2018 International Conference on Advanced Computation and Telecommunication, ICACAT 2018*, vol. 2, no. 4, 2018.

[16] G. M. Shafiullah, "Potential challenges of integrating large-scale wind energy into the power grid-A review," *Renewable and Sustainable Energy Reviews*, vol. 20, pp. 306–321, 2013.

[17] H. Holttinen, "Variability of load and net load in case of large scale distributed wind power," *Proceedings of the 10th International Workshop on Large-Scale Integration of Wind Power into Power Systems as well as on Transmission Networks for Offshore Wind Farms*, no. September 2014, pp. 177–182, 2011.

[18] M. J. Patterson, "Greening the grid," *Alternatives Journal*, vol. 27, no. 4, pp. 30–35, 2001.

[19] J. Olauson and M. Bergkvist, "Modelling the Swedish wind power production using MERRA reanalysis data," *Renewable Energy*, vol. 76, pp. 717–725, 2015.

[20] L. Soder, "Simplified analysis of balancing challenges in sustainable and smart energy systems with 100 % renewable power supply," vol. 5, no. August, pp. 401–412, 2016.

[21] L. Soder, "Possibilities for Balancing Wind Power Variations," no. February, pp. 1–16, 2010.

[22] J. Olauson, *Modelling Wind Power for Grid Integration Studies*. No. November, 2016.

[23] E. Muljadi, "Understanding inertial and frequency response of wind power plants," *PEMWA 2012 - 2012 IEEE Power Electronics and Machines in Wind Applications*, no. July, 2012.

[24] M. Persson, *Frequency Response by Wind Farms in Power Systems with High Wind Power Penetration*. 2017.

[25] F. Democratic and R. Of, "Ethiopia's Climate-Resilient Green Economy,"

[26] C. M. Tiebout, "UC Santa Barbara," *Journal of political economy*, vol. 64(5), pp. 416–424, 1956.

[27] A. Burtin, "TECHNICAL AND ECONOMIC ANALYSIS OF THE EUROPEAN ELECTRICITY SYSTEM WITH 60% RES TECHNICAL AND ECONOMIC ANALYSIS OF THE EUROPEAN ELECTRICITY SYSTEM WITH 60% RES EDF R&D," no. June, 2015.

[28] A. D. Hailu, "Ethiopia renewable energy potentials and current state," *AIMS Energy*, vol. 9, no. 1, pp. 1–14, 2020.

[29] M. Teferra, "Power sector reforms in Ethiopia: Options for promoting local investments in rural electrification," *Energy Policy*, vol. 30, no. 11-12, pp. 967–975, 2002.

[30] M. H. A. Mondal, "Ethiopian universal electrification development strategies," *Intl Food Policy Res Inst.*, p. 4 pages, 2018.

[31] U.-e. Trade, "Ethiopian Electric Power the Ethiopian Energy Sector – Investment Opport," 2015.

[32] D. A. Senshaw, "Modeling and Analysis of Long-Term Energy Scenarios for Sustainable Strategies of Ethiopia," 2014.

[33] *Water Resources and Irrigation Development in Ethiopia*. 2007.

[34] D. Diarra, *Inclusive green growth in Ethiopia : selected case studies*. 2015.

[35] GTP-2, "Federal Democratic Republic of Ethiopia, Second Growth and Transformation National Plan for the Water Supply and Sanitation Sub-Sector.," 2016.

[36] IEA, "Africa Energy Outlook 2019 Africa Energy Outlook 2019," *Iea*, no. November, p. 288, 2019.

[37] M. H. A. Mondal, "Ethiopian universal electrification development strategies," *Intl Food Policy Res Inst.*, p. 4 pages, 2018.

[38] M. Shanko, "Ethiopia ' s Solar Energy Market Target Market Analysis," no. November 2009, 2015.

[39] B. Khan, "The current and future states of Ethiopia's energy sector and potential for green energy: A comprehensive study," *International Journal of Engineering Research in Africa*, vol. 33, no. November, pp. 115–119, 2017.

[40] S. Tesema, "Resource Assessment and Optimization Study of Efficient Type Hybrid Power System for Electrification of Rural District in Ethiopia," *International Journal of Energy and Power Engineering*, vol. 3, no. 6, p. 331, 2014.

[41] I. The, S. Development, E. Poverty, S.-s. Africa, E. Electric, P. Corporation, and S.-s. African, "Study on the Energy Sector in Ethiopia," *Project Appraisal*, pp. 1–16, 2008.

[42] Z. Tessama, "Mainstreaming Sustainable Energy Access into National Development Planning: the Case of Ethiopia," *Stockholm Environment Institute, Working Papaer*, no. February, 2013.

[43] "REPORT ON THE ETHIOPIAN Volume IV 2004 / 05 Transformation of the Ethiopian Agriculture: Potentials , Constraints and Suggested Intervention Measures Ethiopian Economic Association," *Constraints*, vol. IV, 2004.

[44] W. Wolde-Ghiorgis, "Renewable energy for rural development in Ethiopia: The case for new energy policies and institutional reform," *Energy Policy*, vol. 30, no. 11-12, pp. 1095–1105, 2002.

[45] EEP, "Integration of Variable Renewable Energy in the National Electric System of Ethiopia," *Renewable Energy Solutions for Africa*, no. February 2019, p. 18, 2019.

[46] M. M. Alemu, "Household Energy Demand and Its Impact on the Ecological Capital of Nech Sar National Park, Ethiopia," *Journal of Environmental Protection*, vol. 07, no. 10, pp. 1273–1282, 2016.

[47] A. Ababa, "Table of Contents," 2013.

[48] N. Blair, "Electricity Capacity Expansion Modeling, Analysis , and Visualization: A Summary of Selected High-Renewable Modeling Experiences," no. October, 2015.

[49] B. P. Evergreen, "Renewable Electricity Grid Integration Roadmap for Mexico: Supplement to the IEA Expert Group Report on Recommended Practices for Wind Integration Studies," 2015.

[50] K. Poncelet, "Optimization Models for Descriptive Scenario Analyses," no. January, 2018.

[51] P. M. Haugan and I. M. Solbrekke, "A review of modeling tools for energy and electricity systems with large shares of variable renewables," *Renewable and Sustainable Energy Reviews*, vol. 96, no. July, pp. 440–459, 2018.

[52] N. Van Beeck, "Classification of energy models," 1999.

[53] J. Johnston, "Switch 2.0: A modern platform for planning high-renewable power systems," *SoftwareX*, vol. 10, p. 100251, 2019.

[54] I. E. Agency, "Electricity information: Overview (2020 edition)," 2020.

[55] I. Denmark, "Nordic Countries," no. November 2004, pp. 173–195, 2005.

[56] *Wind and load variability in the Nordic countries*. 2013.

[57] J. Olsson, "Future wind power production variations in the Swedish power system," *IEEE PES Innovative Smart Grid Technologies Conference Europe, ISGT Europe*, 2010.

[58] C. Report, "Federal Democratic Republic of Ethiopia," 2017.

[59] S. I. Zandalinas, "Global Warming, Climate Change, and Environmental Pollution: Recipe for a Multifactorial Stress Combination Disaster," *Trends in Plant Science*, vol. xx, no. xx, pp. 1–12, 2021.

[60] E. M. Biggs, "Sustainable development and the water-energy-food nexus: A perspective on livelihoods," *Environmental Science and Policy*, vol. 54, pp. 389–397, 2015.

[61] P. F. Borowski, "Nexus between water, energy, food and climate change as challenges facing the modern global, European and Polish economy," *AIMS Geosciences*, vol. 6, no. 4, pp. 397–421, 2020.

[62] United States Environmental Protection Agency, "Global Greenhouse Gas Emissions Data — Greenhouse Gas (GHG) Emissions — US EPA," 2019.

[63] IEA, "IEA webstore," 2017.

[64] IRENA, *Renewable Power Generation Costs in 2017 ACKNOWLEDGEMENTS*. 2018.

[65] G. Bekele, "Wind energy potential assessment at four typical locations in Ethiopia," *Applied Energy*, vol. 86, no. 3, pp. 388–396, 2009.

[66] K. T. Megra, "WIND RESOURCE ASSESSMENT AT ADAMA II WIND FARM USING WAsP ," no. June, 2014.

[67] J. Kiviluoma, "Variability in large-scale wind power generation," *Wind Energy*, vol. 19, no. 9, pp. 1649–1665, 2016.

[68] L. Hirth, "Balancing power and variable renewables: Three links," *Renewable and Sustainable Energy Reviews*, vol. 50, pp. 1035–1051, 2015.

[69] M. L. Kubik, "Exploring the role of reanalysis data in simulating regional wind generation variability over Northern Ireland," *Renewable Energy*, vol. 57, pp. 558–561, 2013.

[70] C. Stathopoulos, "Wind power prediction based on numerical and statistical models," *Journal of Wind Engineering and Industrial Aerodynamics*, vol. 112, pp. 25–38, 2013.

[71] V. Katinas, G. Gecevicius, and M. Marciukaitis, "An investigation of wind power density distribution at a location with low and high wind speeds using statistical model," *Applied Energy*, vol. 218, no. February, pp. 442–451, 2018.

[72] L. Cornejo-Bueno, "Wind Power Ramp Events prediction with hybrid machine learning regression techniques and reanalysis data," *Energies*, vol. 10, no. 11, 2017.

[73] D. J. Cannon, "Using reanalysis data to quantify extreme wind power generation statistics: A 33 year case study in Great Britain," *Renewable Energy*, vol. 75, pp. 767–778, 2015.

[74] W. L. Henson, "Utilizing reanalysis and synthesis datasets in wind resource characterization for large-scale wind integration," *Wind Engineering*, vol. 36, no. 1, pp. 97–110, 2012.

[75] S. Kobayashi, "The JRA-55 reanalysis: General specifications and basic characteristics," *Journal of the Meteorological Society of Japan*, vol. 93, no. 1, pp. 5–48, 2015.

[76] X. G. Lars and A. Kruger, "Application of the spectral correction method to reanalysis data in south Africa," *Journal of Wind Engineering and Industrial Aerodynamics*, vol. 133, pp. 110–122, 2014.

[77] D. Laslett, C. Creagh, and P. Jennings, "A simple hourly wind power simulation for the South-West region of Western Australia using MERRA data," *Renewable Energy*, vol. 96, pp. 1003–1014, 2016.

[78] M. McPherson, T. Sotiropoulos-Michalakakos, D. Harvey, and B. Karney, "An open-access web-based tool to access global, hourly wind and solar PV generation time-series derived from the MERRA reanalysis dataset," *Energies*, vol. 10, no. 7, 2017.

[79] S. Rose, "What can reanalysis data tell us about wind power?," *Renewable Energy*, vol. 83, pp. 963–969, 2015.

[80] H. Hersbach, "The ERA5 global reanalysis," *Quarterly Journal of the Royal Meteorological Society*, vol. 146, no. 730, pp. 1999–2049, 2020.

[81] D. P. Dee, "The ERA-Interim reanalysis: Configuration and performance of the data assimilation system," *Quarterly Journal of the Royal Meteorological Society*, vol. 137, no. 656, pp. 553–597, 2011.

[82] S. M. Uppala, , and A. J. Simmons, "The ERA-40 re-analysis," *Quarterly Journal of the Royal Meteorological Society*, vol. 131, no. 612, pp. 2961–3012, 2005.

[83] M. M. Rienecker and Suarez, "MERRA: NASA's modern-era retrospective analysis for research and applications," *Journal of Climate*, vol. 24, no. 14, pp. 3624–3648, 2011.

[84] R. Gelaro, "The modern-era retrospective analysis for research and applications, version 2 (MERRA-2)," *Journal of Climate*, vol. 30, no. 14, pp. 5419–5454, 2017.

[85] Web, "https://gmao.gsfc.nasa.gov/reanalysis/,"

[86] S. n. Uppala, "https://www.ecmwf.int/en/elibrary/15704-era-15-era-40-and-era-interim,"

[87] S. Uppala, "From ERA-15 to ERA-40 and ERA-Interim,"

[88] F. Monforti, "Simulating European wind power generation applying statistical downscaling to reanalysis data," *Applied Energy*, vol. 199, pp. 155–168, 2017.

[89] J. Olauson, "ERA5: The new champion of wind power modelling?," *Renewable Energy*, vol. 126, pp. 322–331, 2018.

[90] K. Gruber, "Bias-correcting simulated wind power in Austria and in Brazil from the ERA-5 reanalysis data set with the DTU Wind Atlas," pp. 1–15, 2019.

[91] I. Staffell, "Using bias-corrected reanalysis to simulate current and future wind power output," *Energy*, vol. 114, pp. 1224–1239, 2016.

[92] G. Johannes, "Assessing simulation and bias correction methods for wind power generation in Brazil – can global datasets compete with local measurements ?," no. April, pp. 0–25, 2019.

[93] A. Duckworth and R. J. Barthelmie, "Investigation and validation of wind turbine wake models," *Wind Engineering*, vol. 32, no. 5, pp. 459–475, 2008.

[94] C. L. Archer, "Review and evaluation of wake loss models for wind energy applications," *Applied Energy*, vol. 226, no. February 2018, pp. 1187–1207, 2018.

[95] X. Costoya, A. Rocha, and D. Carvalho, "Using bias-correction to improve future projections of offshore wind energy resource," *Applied Energy*, vol. 262, no. October 2019, p. 114562, 2020.

[96] S. Shokrzadeh, "Wind turbine power curve modeling using advanced parametric and nonparametric methods," *IEEE Transactions on Sustainable Energy*, vol. 5, no. 4, pp. 1262–1269, 2014.

[97] J. R. Flores, "An optimization approach for long term investments planning in energy," vol. 122, pp. 162–178, 2014.

[98] M. Ozcan, "Turkey's long-term generation expansion planning with the inclusion of renewable-energy sources," *Computers and Electrical Engineering*, vol. 40, no. 7, pp. 2050–2061, 2014.

[99] N. E. Koltsaklis and A. S. Dagoumas, "State-of-the-art generation expansion planning : A review," vol. 230, no. April, pp. 563–589, 2018.

[100] M. Milligan, "Operating Reserves and Wind Power Integration: An International Comparison," *9th Annual International Workshop on Large-Scale Integration of Wind Power into Power Systems*, no. October 2010, pp. 1–19, 2010.

[101] S. Ahmed, "New technology integration approach for energy planning with carbon emission considerations," vol. 95, pp. 170–180, 2015.

[102] P. N., "A bottom-up optimization model for the long-term energy planning of the Greek power supply sector integrating mainland and insular electric systems," *Computers and Operations Research*, vol. 66, no. March 2015, pp. 292–312, 2016.

[103] N. E. Koltsaklis, "A spatial multi-period long-term energy planning model: A case study of the Greek power system," vol. 115, pp. 456–482, 2014.

[104] C. Barteczko-Hibbert, "A multi-period mixed-integer linear optimization of future electricity supply considering life cycle costs and environmental impacts," *Applied Energy*, vol. 133, pp. 317–334, 2014.

[105] J. H. Wu, "Electricity portfolio planning model incorporating renewable energy characteristics," *Applied Energy*, vol. 119, pp. 278–287, 2014.

[106] R. Hemmati, "Reliability constrained generation expansion planning with consideration of wind farms uncertainties in deregulated electricity market," *Energy Conversion and Management*, vol. 76, pp. 517–526, 2013.

[107] G. Papaefthymiou, "Towards 100% renewable energy systems: Uncapping power system flexibility," *Energy Policy*, vol. 92, pp. 69–82, 2016.

[108] M. Z. Jacobson, "The cost of grid stability with 100 % clean, renewable energy for all purposes when countries are isolated versus interconnected," *Renewable Energy*, vol. 179, pp. 1065–1075, 2021.

[109] H. Lund and B. V. Mathiesen, "Energy system analysis of 100 % renewable energy systems — The case of Denmark in years 2030 and 2050," vol. 34, pp. 524–531, 2009.

[110] K. Goran and Dui, "How to achieve a 100% RES electricity supply for Portugal?," *Applied Energy*, vol. 88, no. 2, pp. 508–517, 2011.

[111] D. Connolly, "The first step towards a 100% renewable energy-system for Ireland," *Applied Energy*, vol. 88, no. 2, pp. 502–507, 2011.

[112] A. G. Williamson, "A 100% renewable electricity generation system for New Zealand utilizing hydro, wind, geothermal and biomass resources," *Energy Policy*, vol. 38, no. 8, pp. 3973–3984, 2010.

[113] Kraja, "A 100% renewable energy system in the year 2050: The case of Macedonia," *Energy*, vol. 48, no. 1, pp. 80–87, 2012.

[114] S. Sterl and Fadly, "Linking solar and wind power in eastern Africa with operation of the Grand Ethiopian Renaissance Dam," *Nature Energy*, vol. 6, no. 4, pp. 407–418, 2021.

[115] Oyewo and A. Solomon, "Just transition towards defossilised energy systems for developing economies: A case study of Ethiopia," *Renewable Energy*, vol. 176, pp. 346–365, 2021.

[116] J. Jenkins, "GenX: a configurable power system capacity expansion model for studying low-carbon energy futures.,"

[117] D. S. Mallapragada and Sepulveda, "Long-run system value of battery energy storage in future grids with increasing wind and solar generation," *Applied Energy*, vol. 275, no. February, p. 115390, 2020.

[118] E. Bompard, A. Botterud, and S. Corgnati, "An electricity triangle for energy transition: Application to Italy," *Applied Energy*, vol. 277, no. January, p. 115525, 2020.

[119] M. Jafari, "Power system decarbonization: Impacts of energy storage duration and interannual renewables variability," *Renewable Energy*, vol. 156, pp. 1171–1185, 2020.

[120] N. A. . Sepulveda, "The Role of Firm Low-Carbon Electricity Resources in Deep Decarbonization of Power Generation," *Joule*, vol. 2, no. 11, pp. 2403–2420, 2018.

[121] E. Baik, "What is different about different net-zero carbon electricity systems?," *Energy and Climate Change*, vol. 2, p. 100046, 2021.

[122] M. Schulthoff, I. Rudnick, A. Bose, and E. Gençer, "Role of Hydrogen in a Low-Carbon Electric Power System: A Case Study," *Frontiers in Energy Research*, vol. 8, no. January, pp. 1–13, 2021.

[123] N. A. Sepulveda, "The design space for long-duration energy storage in decarbonized power systems," *Nature Energy*, vol. 6, no. 5, pp. 506–516, 2021.

[124] "The Costs of Decarbonisation," *The Costs of Decarbonisation*, 2019.

[125] K. L. Nefabas, "Analysis of System Balancing and Wind Power Curtailment Challenges in the Ethiopian Power System under Different Scenarios," 2023.

[126] K. L. Nefabas, "Modeling of Ethiopian Wind Power Production Using ERA5 Reanalysis Data," pp. 1–17, 2021.

[127] NREL, "SYSTEM ADVISORY MODEL,"

[128] Kouveliotis-Lysikatos, "Exploring Multitemporal Hydro Power Models of the Nordic Power System using Spine Toolbox," *UPEC 2020 - 2020 55th International Universities Power Engineering Conference, Proceedings*, 2020.

[129] A. M. Lennart Söder, "Efficient Operation and Planning of Power Systems," 2011.

[130] Florian and H. Holttinen, *Design and operation of power systems with large amounts of wind power*. 2010.

[131] A. Basit, "Balancing modern Power System with large scale of wind power," *China Wind Power (CWP)*, no. Cwp, 2014.

[132] Chandler, *A Guide to the Balancing Challenge*. 2011.

[133] "BALANCING POWER SYSTEMS WITH LARGE SHARE OF WIND POWER task 25 Fact Sheet," no. Figure 2.

[134] L. Bird, "Wind and Solar Energy Curtailment: Experience and Practices in the United States," *National Renewable Energy Laboratory (NREL)*, no. March, p. 58, 2014.

[135] J. Olauson, "Curtailment analysis for the Nordic power system considering transmission capacity , inertia limits and generation fl exibility," vol. 152, pp. 942–960, 2020.

[136] E. V. Mc Garrigle, "How much wind energy will be curtailed on the 2020 Irish power system?," *Renewable Energy*, vol. 55, no. 2013, pp. 544–553, 2013.

[137] Y. Qi and W. Dong, "Fixing Wind Curtailment with Electric Power System Reform in China," 2018.

[138] D. Lew, "Wind and Solar Curtailment," *International Workshop on Large-Scale Integration of Wind Power Into Power Systems*, no. September, 2013.

[139] L. V. Villamor, "Opportunities for reducing curtailment of wind energy in the future electricity systems: Insights from modelling analysis of Great Britain," *Energy*, vol. 195, 2020.

[140] M. H. Alham, M. Elshahed, and D. K. Ibrahim, "Optimal operation of power system incorporating wind energy with demand side management," *Ain Shams Engineering Journal*, vol. 8, no. 1, pp. 1–7, 2017.

[141] J. Sousa and A. Martins, "Optimal renewable generation mix of hydro, wind and photovoltaic for integration into the Portuguese power system," *International Conference on the European Energy Market, EEM*, pp. 1–6, 2013.

[142] H. Farahmand and G. L. Doorman, "Balancing market integration in the Northern European continent," *Applied Energy*, vol. 96, pp. 316–326, 2012.

[143] I. Graabak and H. Svendsen, "Developing a wind and solar power data model for Europe with high spatial-temporal resolution," *Proceedings - 2016 51st International Universities Power Engineering Conference, UPEC 2016*, vol. 2017-Janua, pp. 1–6, 2016.

[144] M. Korpas, "Balancing of wind power variations using norwegian hydro power," *Wind Engineering*, vol. 37, no. 1, pp. 79–96, 2013.

[145] K. Askeland, "Balancing Europe: Can district heating affect the flexibility potential of Norwegian hydropower resources?," *Renewable Energy*, vol. 141, no. 2019, pp. 646–656, 2019.